2002

The effects of fall coldfront passages on the nekton community in a tidal creek in Port Fourchon, LA, as monitored by hydroacoustics

David J. Harmon
Louisiana State University and Agricultural and Mechanical College

THE EFFECTS OF FALL COLDFRONT PASSAGES ON THE NEKTON COMMUNITY IN A TIDAL CREEK IN PORT FOURCHON, LA, AS MONITORED BY HYDROACOUSTICS

A Thesis

Submitted to the Graduate Faculty of the
Louisiana State University and
Agricultural and Mechanical College
in partial fulfillment of the
requirements for the degree of
Master of Science

in

The Department of Oceanography and Coastal Studies

by
David J. Harmon
B.S., University of South Carolina, 1999
August, 2002

Acknowledgements

I wish to thank Dr. Charles Wilson for his endless help and guidance as my major professor, Drs. Conrad Lamon and Richard Shaw for being excellent committee members. Mark Miller for helping design and implement the new deployment system, Wilton Delaune for field assistance, Jim Dawson and John Hedgepeth for hydroacoustic expertise and all the faculty, graduates students and friends who helped along the way. And without my parents and family, none of this would have been possible.

Table of Contents

Abstract

Split-beam hydroacoustic sampling with two, 420 KHz, 2x6 degree elliptical transducers was evaluated as a tool to quantify nekton movements in a Louisiana estuary. I measured the effects of atmospheric cold front passages on nekton in a tidal creek in Port Fourchon, LA during the fall of 2000. Six "fronts" were sampled between October 6 and December 18, 2000. Nekton density ranged from 0 to 24.4 fish/m^3 with an overall mean of 2.44 fish/m^3. Net samples were taken to supplement the acoustic data with species composition data. Species composition changed from October to December. A higher number of smaller targets were found with the acoustic gear than with the nets, evidence of gear bias.

Hydroacoustic based density was generally greater during falling tide (3.17 fish/m^3) than rising tide (1.81 fish/m^3). Fish Energy, a proxy for biomass, ranged from $1.76*10^{-7}$ units to $2.06*10^{-3}$ units, with an overall mean of $5.96*10^{-5}$ units. Fish Energy was higher on rising tides ($6.10*10^{-5}$) than falling tides ($5.79*10^{-5}$). Biomass and density were highly variable and similar to previous studies. Barometric pressure combined with tide affected nekton movement. The range of barometric pressures during a sampled 'front" had a significant effect on biomass. When interacted with tidal stage, the range of barometric pressure significantly affected biomass and nekton density (α=0.05).

Hydroacoustics were valuable, although sampling during high densities confounded data acquisition. Higher biomass on incoming tides and higher density on outgoing tides suggest an emigration of small nekton during fronts. Thus, judging by total biomass measured over the study, a front may not be as significant a cue in moving estuarine biomass to emigrate as had been hypothesized.

1. Introduction

In an age of heightened environmental awareness and greater scientific understanding of the relationships between the environment and its many associated socio-economic benefits, the importance of Louisiana's coastal estuaries has never been clearer. The state boasts three million acres of coastal wetlands with over two million acres in marshes (Raynie and Beasley, 2000). Since 1930, Louisiana has lost approximately 380,000 hectares of wetlands (Turner, 1990). After decades of research providing links between the wetlands and economic and recreational benefits, it is well established that coastal wetlands stand as one of the state's greatest natural resources.

The relationship between coastal wetlands and commercial and recreational fisheries has been best shown to be positive (Gunter, 1967; Boesch and Turner, 1984; Hoss and Thayer, 1993; Houde and Rutherford, 1993) with evidence supporting the nursery value of estuaries in producing harvests. Eighteen million tons, or 16% of the world's fisheries production, is strictly estuarine. Over 50% of the world's commercial landings are estuarine dependent with a much higher percentage found in the Gulf of Mexico (Houde and Rutherford, 1993). Louisiana's 1999 commercial landings totaled over $2.2 billion and recreational fishing brought in an additional $944 million in revenue, most of this production was estuarine-dependent (Raynie and Beasley, 2000). In 1988, Louisiana landings of gulf menhaden accounted for 29% of US commercial fisheries landings at 635,00 tons and $73.3 million. Annual dockside value of shrimp, Louisiana's most important commercial fishery, ranges from $150 to $200 million annually (Herke et al, 1996).

More recently, studies have shown other benevolent effects of coastal wetlands including storm surge abatement, water quality treatment/filtration, eco-tourism, and endangered species

habitat. A socio-economic study conducted on the value of restoring the wetlands of Galveston Bay, Texas showed that although there was a decrease in wetland acreage from 170 to 138.6 thousand acres from 1956 to 1989, the total value of wetland goods and services remained constant due to the increased value of wetlands in hurricane damage protection for recently developed areas surrounding the bay (Whittington et al., 1994). The same study established a direct relationship between declining wetland acreage and declining total recreational catch (pounds landed) of eight economically important species.

Louisiana's estuaries are disappearing at a rate of 66 km^2/year (Dunbar, 1990) and greater. This land loss accounted for 80% of all US wetland losses (Raynie and Beasley 2000). Coastal land loss is accelerated by eustatic sea level rise, which is intensified by compaction of sediments from organic reduction, saltwater intrusion from the creation of canals and levees (Salinas et al., 1986), and starvation of sediments from the levied Mississippi River. Louisiana's estuaries will continue to disappear despite present day restoration efforts. Modest-scale efforts such as the Army Corps of Engineer's $105 million Davis Pond Diversion Project are being implemented to mitigate land loss. This project will divert Mississippi River fresh water and sediment into upper Barataria Bay. This input of fresh water will change salinities, and push isohaline zones seaward, likely affecting the extent and availability of some nursery areas.

Historically smaller, localized projects such as small-scale marsh creation were shown to sustain lower abundances and different species of fish than natural marsh and may be of lesser habitat value (Minello and Webb, 1997). Utilization of weirs, or low crest dams, to stabilize water levels and decrease salt water intrusion into semi-impoundments was reported to have negative effects on the ingress and egress of important estuarine-dependent species including brown and white shrimp (Herke et al, 1992).

The Barataria-Terrebonne National Estuary incorporating the Barataria-Terrebonne watershed covers over 4 million acres, with 49% of the area made up of wetlands (McKenzie et al., 1995). The area is highly productive accounting for 54% of commercial landings by weight and 70% by value from 1982 to 1992 (McKenzie et al., 1995). The Caminada headland around Port Fourchon, Louisiana is experiencing land loss at a rate of 10.2 square miles a year for the nearby Terrebonne Bay, while Barataria Bay to the east is losing land at 11.1 square miles per year (McKenzie et al., 1995). These values are among the highest in the country. From 1982 to 1992 water acreage increased by 2.3%. Over the previous 40 years, 542 miles^2 of wetlands were lost representing one third of the state's total (McKenzie et al., 1995). Loss rates within the watershed increased from less than 1% to 6% per year, triple the statewide rate (McKenzie et al., 1995). There is a desperate need to forecast continued land loss on fisheries and an equally important need for us to understand this critical habitat.

Estuaries are very dynamic, highly variable systems in terms of physical and environmental characteristics, yet many species utilize estuaries for at least part of their life cycles. Few species are hardy enough to be true residents over their complete life cycle; most enter the estuary as larvae or postlarvae and develop into juveniles or adults before leaving. The role of these highly productive coastal habitats as nurseries and feeding grounds includes them in the definition of Essential Fish Habitat (EFH) declared in the 1996 Magnuson-Stevens Fisheries Conservation and Management Act. Essential Fish Habitat was defined as "those waters and substrate necessary to fish for spawning, breeding, feeding, or growth to maturity." The reauthorization brought a new and increased focus upon ecosystem management of commercially and recreationally important species. The concept of ecosystem management involves monitoring the condition of environmental parameters and relevant physical forcing

processes as well as the biological interactions among predator and prey populations, habitat and fisheries populations, and traditional stock estimates. It is therefore important to study processes within estuaries relevant to primary and secondary production, recruitment, growth, and mortality, and seasonal migrations as these processes bare direct effect upon the standing stocks of commercial and recreational fisheries. Seasonal migrations include not only targeted species of interest, but also their predators and prey, and other non-targeted species that may be part of the food web. These migrations dictate which species are utilizing the estuary at different times of the year.

A paradigm amongst scientists suggests that species time their migrations into and out of these productive areas to maximize recruitment, hence survivorship, during times of high prey and low predator abundance and to minimize competition. For that reason, species composition and biomass vary seasonally (Roundtree and Able, 1992; Shenker and Dean, 1979; Subrahmanyam and Drake, 1975; Subrahmanyam and Coultas, 1980). In Chesapeake Bay, biomass peaked in fall and was lowest in January and throughout spring and summer (Luo, 1993) suggesting mass movement out of the system. In north Florida *Juncus* marshes, fish abundances and biomass peak in March and July. (Subrahmanyam and Coultas, 1980). In the spring, the Florida estuary is dominated by spot, *Leiostomus xanthurus*. The summer months were dominated by bay anchovy (*Anchoa mitchilli*), mumichogs (*Fundulus* spp.), with the sheepshead minnow (*Cyprinodon variegates*) being dominant in late summer. In a Louisiana salt marsh, gulf menhaden (*Brevoortia patronus*) comprised 23% of all fish; highest abundances occurred between October and July and menhaden abundance peaked in late April (Salinas et al., 1986). Menhaden were also dominant in South Carolina tidal marshes from late winter to spring (Bozeman and Dean, 1980). In a Texas salt marsh, *L. xanthurus* and *L. rhomboides* were

dominant from March to June and from October to November, Atlantic croaker *Micropogonus undulatus* in February and *B. patronus* and *M. cephalus* in July and August. In a Texas study, *A. mitchilli* and *L. xanthurus* made up 71% of the abundance (Zimmerman and Minello, 1984). These patterns of seasonal dominance and estuary use, with mass immigrations occurring in the spring and mass emigrations occurring in the fall, are typical of many estuarine systems along the Gulf and Southeast Coasts.

Most scientists believe that nekton migration, especially from the fall through the spring, is linked to seasonal and environmental cues with atmospheric processes playing an important role. It has been shown that frontal passage is one of the stronger environmental cues for white shrimp emigration in the fall (Knudsen et al., 1996). Larval brown shrimp, *Penaeus aztecus* recruit into the estuary with the influx of coastal water following the passage of cold fronts in the spring (Rogers et al., 1993).

Along the Gulf of Mexico, cold fronts, or conditions when "a cold air mass displaces a warm air mass all along the frontal zone" are associated with "heavy rains, gusty winds, and thunderstorms" (Hsu, 1988), and begin in late September or early October. Prefrontal conditions are dominated by southerly winds with warm air temperatures, moderate barometric pressure and astronomically dominated tides. As cold fronts approach, winds remain southerly but increase in strength as barometric pressure drops. Increased wind velocity and the Gulf's large fetch can cause "coastal setup" with water levels higher than those caused by normal high tides. With frontal passage, winds intensify and rapidly rotate through the west to out of the north. Barometric pressure increases, air temperature drops, and water levels decrease rapidly due to the strong north wind's effect on these north-south trending estuaries. Intense storms can develop with heavy precipitation during the early stages of frontal events. After passage, the

cold air mass brings clear skies, cooler air temperatures, weakening northerly winds that eventually rotate through the eastern quadrant back out of the south. Once the cold air mass is replaced, conditions rebound rapidly to those of prefrontal (i.e., more normal) patterns. These fronts can have important effects on the hydrology and environmental conditions. During a fall season water levels in Atchafalaya Bay varied by 0.9 m, three times the normal astronomical (tidal) variation, with even greater fluctuations during frontal passage events (Perez et al., 2000). Thus, strong northerly winds associated with frontal passage can significantly lower the water level of an estuary. Offshore or coastal species that have recruited to their estuarine nurseries in the winter and spring will have matured by the following fall to the point of leaving once environmental conditions begin to significantly change.

Proposed models of nekton migrations range from immediate evacuation to long, gradual movements of the older individuals over the course of the season. Gradual emigration, or "bleeding off", of adults over a spring season has been noted in Atlantic croaker, *Micropogonias undulatus*, in western Louisiana estuaries (Yakupzack et al., 1977). This gradual migrational pattern is likely also seen for a number of species during the fall.

Alternatively to a gradual, extended migration, white shrimp have been shown to emigrate en masse coinciding with cold fronts in the fall between September and November (Knudsen et al., 1996). Nekton may react to the changing conditions brought on by fronts and essentially ride the outgoing water offshore. Some of the movement of nekton out of the estuary may be in a temporary effort to seek thermal refuge in deeper water. Once water level and temperature conditions rebound after frontal passage, nekton may then return to the estuary. It is likely that the larger predators within the estuary react to the movements of their prey resulting in secondary waves of migration based on foraging interactions. Whether nekton are reacting to

rapid changes in barometric pressure and water temperature, strong wind-reinforced outgoing tides, or a combination of these effects is unknown. Rapid changes in hydrostatic pressure have been shown to decrease feeding behavior in the guppy, *Poecilia reiculata*, and roach, *Rutilus rutilus* (Zakharcheno et al., 1997). Hydrostatic pressure gradients, and acclimation to high pressures, have been shown to alter the photoreaction of young perch from positive to negative, and affect their vertical distribution (Pavlov et al., 2000). Rapid fluctuations in barometric pressure, such as those associated with cold front passage in the fall, could exhibit similar effects on fish, possibly acting as a cue to emigration from the estuary.

Studies of nekton seasonality have been performed using a variety of traditional techniques including gill nets, traps, trawls and wing nets, and have been performed over varying time frames from tidal to seasonal scale (Knudsen et al., 1996; Yakupzack et al., 1977; Zimmerman and Minello, 1984). Such time-scale differences across studies make it difficult to compare results.

A well-established technology that is gaining momentum in monitoring nekton populations is hydroacoustics. Hydroacoustics has been used in fisheries biology, especially in fresh water and oligotrophic environments such as lakes (Gauthier et al., 1997; Burczynski and Johnson, 1986) and salmon streams in the Pacific Northwest. Hydroacoustics is used to estimate nekton densities, biomass, and sample size distributions (Luo, 1993), with recent advances being made in determining direction and velocity of movement. Hydroacoustics has many advantages over traditional sampling in that it is non-invasive, requires no handling or capture of fish, and provides accurate *in situ* quantifiable measurements. Marine applications around natural reefs and oil and gas platforms have shown acoustics can provide estimates of fish densities and biomass which were well above those previously determined by diver and net surveys (Stanley

and Wilson, 1995; Thorne, 1979). Hydroacoustic systems allow for continuous, nearly autonomous sampling dependent only on a continuous power source and sufficient data storage media. Advances in transducer engineering have led to the development of split beam and dual beam transducers, major advances from the more traditional single beam. The inclusion of GPS into the datastream adds accurate spatial resolution to the densities and biomass estimates. These features make hydroacoustics a valuable option in quantifying EFH. Densities can be laid over geology, bathymetry, environmental quality, and positional data by GPS coordinates.

Hydroacoustic based estimates of density and biomass are usually of the total nekton community and are used to determine the density or biomass of a single species. Hydroacoustics does not provide species composition, so some type of species identification is required. Hydroacoustic studies of salmonids have produced methods to determine species based on target strength and pulse width (Burwen, 1998). Elaborate artificial neural networks (ANN) have been developed that, under circumstances of monospecific schooling, can accurately identify species. Haralabous and Georgakarakos (1996) used such an ANN to distinguish sardine, anchovy and horse mackerel in the Mediterranean. These ANN have been used successfully with offshore species. This technology has not been applied in estuaries where the complex and dynamic nature of species composition makes species identification problematic. Furthermore, during times of intense migration, larvae, juveniles, or sub-adults of several different species can be nearly identical in size making acoustic identification nearly impossible.

Very high nekton densities act to affect acoustic data in more than one way. Densely populated water columns (e.g. tidal passes), which occur during these migrations, can act to reduce the resolution of data by making it impossible for the system to separate single targets. Rottingen (1976) reported acoustic and real densities of 10 cm sprat, *Sprattus sprattus*, at up to

2000 individuals per m^3 in a 2.7m^3 net cage. At higher densities, the relationship between real and acoustic densities became non-linear. It is likely that the real density necessary to reduce acoustic resolution would be lower for a water column with smaller, heterogeneous targets as in an estuarine tidal creek. Densely schooling fish cause the energy returning to the transducer to be reflected and refracted by multiple targets, encountered on the sound waves' return trip to the transducer. This interference deteriorates the data on individual targets. Acoustic target strength (TS), or length estimates, can also be affected by fish schooling, with schooling aggregations of fish being assigned higher average target strength than non-schooling concentrations (Foote, 1981). This was shown in diurnal fluctuations in target strength (TS) among cod, which school in the daytime and disperse at night (Edwards and Armstrong, 1983; MacLennan et al., 1989; MacLennan, 1990). The problem of artificially inflated TS was not unique to cod; many densely schooling species show the relationship (MacLennan 1996, Barange 1996). In addition, high densities of large fish resulted in lower estimated biomass by up to 50 % (Appenzeller and Leggett, 1992) due to acoustic shadowing, or extinction of energy from the transducer by absorption by targets in the foreground. Corrections can be made, and biomass and density data are likely reliable in these high densities out to a certain distance as long as critical assumptions are met (Soule, 1996).

1.1 Objectives

The primary goal of this study was to evaluate split-beam hydroacoustics as a tool for sampling the total nekton community in a shallow water estuary. I sought to construct a practical, economic deployment method for long-term continuous monitoring with this new acoustic system, as its development would allow for much farther-reaching research in the future. My objective was to test this new tool by examining fall frontal passage effect on total

nekton abundance and biomass. For the purposes of this study, atmospheric frontal passages, or fronts, are defined as beginning at the time from which winds first shift from south to west and ending when winds finally return from the north and east to the south.

It is important to note that the hydroacoustic estimates of biomass and density flux associated with the frontal passages are of the total nekton community sampled and not indicative of any species-specific migrations.

1.2 Hypothesis Testing

Hypotheses for the study were broken into two temporal levels: seasonal and frontal. On the seasonal level the effects of fronts in relation to net seasonal differences in total abundance and biomass were tested. The null hypothesis for the seasonal level was that there was no difference in total biomass and density during the fall 2000 season. The second level involved individual fronts, which were contrasted for sequential differences in effect as well as for differences based on frontal event strength. The null hypothesis for the frontal level was that there was no difference in total biomass and density for the fronts sampled during the fall 2000 season.

The effects of hydrostatic, and in this study barometric, pressure upon fish have been shown to affect fish behavior (Pavlov et al., 2000; Zakharchenko et al., 1997) and could be the ultimate cue to which nekton are responding during cold front passage. Rapid increases in pressure could immediately be felt by nekton thereby triggering either a migration or avoidance response, both resulting in movement out of the marsh to deeper water. Pressure increases were therefore a focus of this study. I recognize that barometric pressure, water level, and water temperature are all affected by frontal passages. The interaction of these parameters, as a front passes, is important in modeling the data.

Barometric pressure changes were used in this study to quantify frontal intensity and particular attention was paid to rising barometric pressures as the ultimate cue for emigration. The frontal level hypothesis tested was that the total nekton community would emigrate from the estuary with fluctuation in barometric pressure associated with a cold front.

2. Materials and Methods

2.1 Study Site

This study was conducted in Bayou Tartellon adjacent to The Louisiana University Marine Consortium's (LUMCON) field station at Port Fourchon, Louisiana (Figure 1, 2). This tidal creek empties directly into the Gulf of Mexico through Belle Pass. The bayou drains most of a 3800-acre semi-impoundment of *Spartina alterniflora* dominated marsh, accounting for approximately 70% of water movement (Karlsson, 1999). Acoustic and environmental monitoring equipment were deployed from a pier extending approximately 10 meters into the tidal channel. The channel is approximately 75 meters wide with an average depth of 4.5 meters and a 6-meter deep channel in the center. The field station supplied power and a convenient place for work and lodging.

Tides at the site were diurnal (mean tidal range 0.34 ± 0.15 meters). Because of the diurnal nature of the tides, most falling tides (71%) occurred during daylight hours, whereas most rising tides (79%) occurred at night. Mean density and biomass estimates for tidal stage (falling or rising) and coinciding diel stage (day or night) were closely related (3.17 fish per cubic meter for falling tide versus 3.29 for day; and 1.81 fish per cubic meter for rising tide versus 1.66 for night) indicating that the tidal stage and diel stage variables were probably collinear. Diel stage was dropped from the model in favor of tidal stage, which is assumed to more indicative of passive and to some extent active nekton migration. Diel activity rhythms or vertical migrations may be important, but in this case, the relation between tidal stage and diel stage confounds analysis of diel effects. In an earlier hydroacoustic study performed 0.8 km downstream from this study's sample site, Karlsson (1999, unpublished) showed no differences in nekton density or biomass between day and night samples for spring, summer or winter.

Slightly more sampling time (55%) was spent sampling rising tides than falling tides (45%). This difference is probably due to brief periods of intense outgoing tide driven by the strong northerly winds of a frontal passage being compensated for by longer, more gradual incoming tides with little augmentation from weaker southerly winds evident following frontal passage.

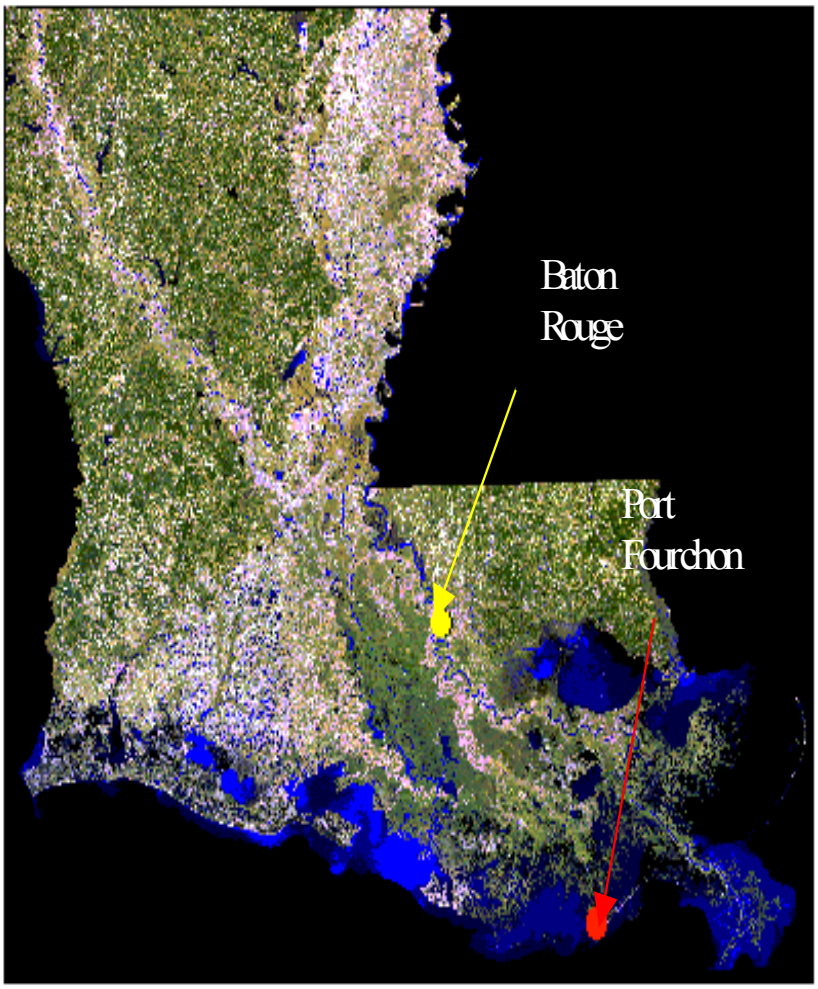

Figure 1. State map of Louisiana showing the location of the Port Fourchon sampling site in relation to Baton Rouge.

Figure 2. Aerial photograph of the sample site

2.2 Hydroacoustic Array

The acoustic system was set up on the pier in a weatherproof container ($1m^3$). The acoustic system consisted of a 420kHz BioSonics DE 6000 Scientific Digital Echosounder connected to a laptop computer. Two analog 2^0 by 6^0 split-beam, horizontally-elliptical transducers with 50 ft analog cables were deployed in the channel. One transducer was deployed approximately three meters out from the dock facing up from the bottom in approximately 3m of water. This upward-facing transducer was mounted to a weighted plate and lowered to the bottom with a four-point monofilament harness. The monofilament harness is invisible to the transducer insuring a clear path for the acoustic beam. The horizontal transducer was mounted to a bracket allowing for full adjustment in the vertical and horizontal planes as well as depth

control and was deployed at the edge of the pier looking perpendicularly across the channel near mid-depth (Figures 3, 4). The bracket was constructed using 3' sections of 4" aluminum pipe bolted together with a vertically tilting aluminum bracket pinned at its vertical center to the terminal end of the pipe. The top side consisted of a bracket upon which a star-drag reel was attached. The reel was strung with Dacron line run down the center of the connected aluminum poles and attached to the top of the bracket with a swivel. Rollers were welded at the entrance and exit points of the line into and out of the piping to reduce friction. Constant tension was kept on the bracket by reeling the line tight until the bracket was locked upright. Vertical adjustments were then made by reducing the drag on the reel allowing the bracket to tilt downward with the weight of transducer. The pole-mounted assembly was attached via two scaffold clamps to a vertical standoff on a plate bolted into the pier. The transducer was attached to the bracket with four bolts. The cable was secured to the pole mount to insure no slack could become tangled on the apparatus or hang in front of the transducer. The mounted transducer was then deployed to mid-water depth and the angle adjusted to produce an echogram free of bottom or surface interference. Depth and horizontal angle were fixed by tightening the scaffold clamps.

2.3 Acoustic Data Collection and Analysis Parameters

Data from both transducers were collected at a threshold of –65 dB, equaling approximately a 6.25 mm fish total length (Love 1971). Pulse widths were set at 0.4 ms, and ping rates were set to 5 pings per second. Source levels for the upward and outward transducers were 224.0 and 224.3 db/μPa, respectively. Absorption coefficients were dependent upon entered values for ambient salinity and water temperature and were 0.12 dB/m for the October and November data and 0.11 dB/m for December. Accurate water temperatures were difficult to input prior to collection, as temperature fluctuated with frontal

passage. Data were processed with BioSonics Visual Analyzer 4.0 for density, size frequency, and biomass.

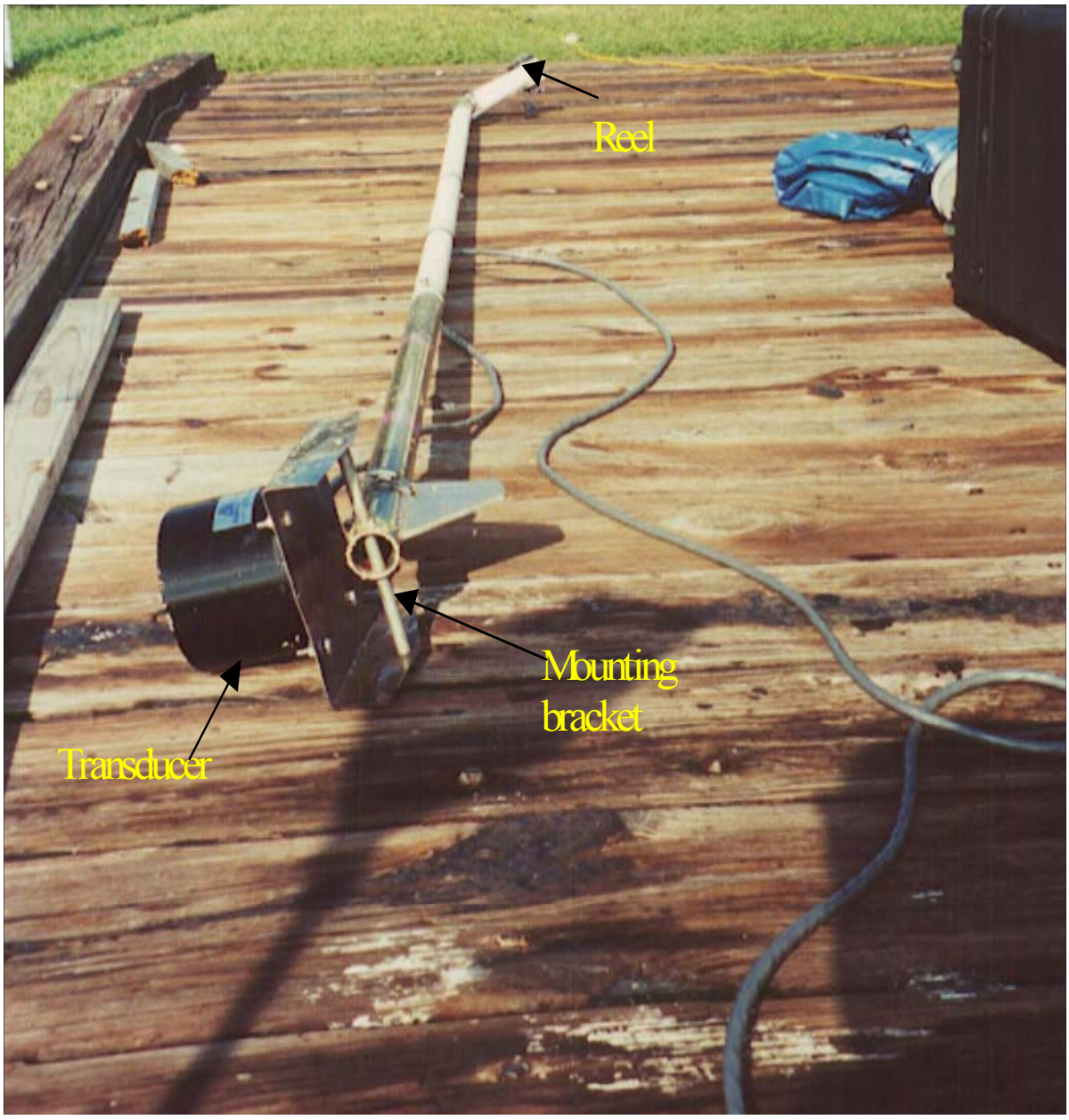

Figure 3. The horizontal transducer attached to its bracket.

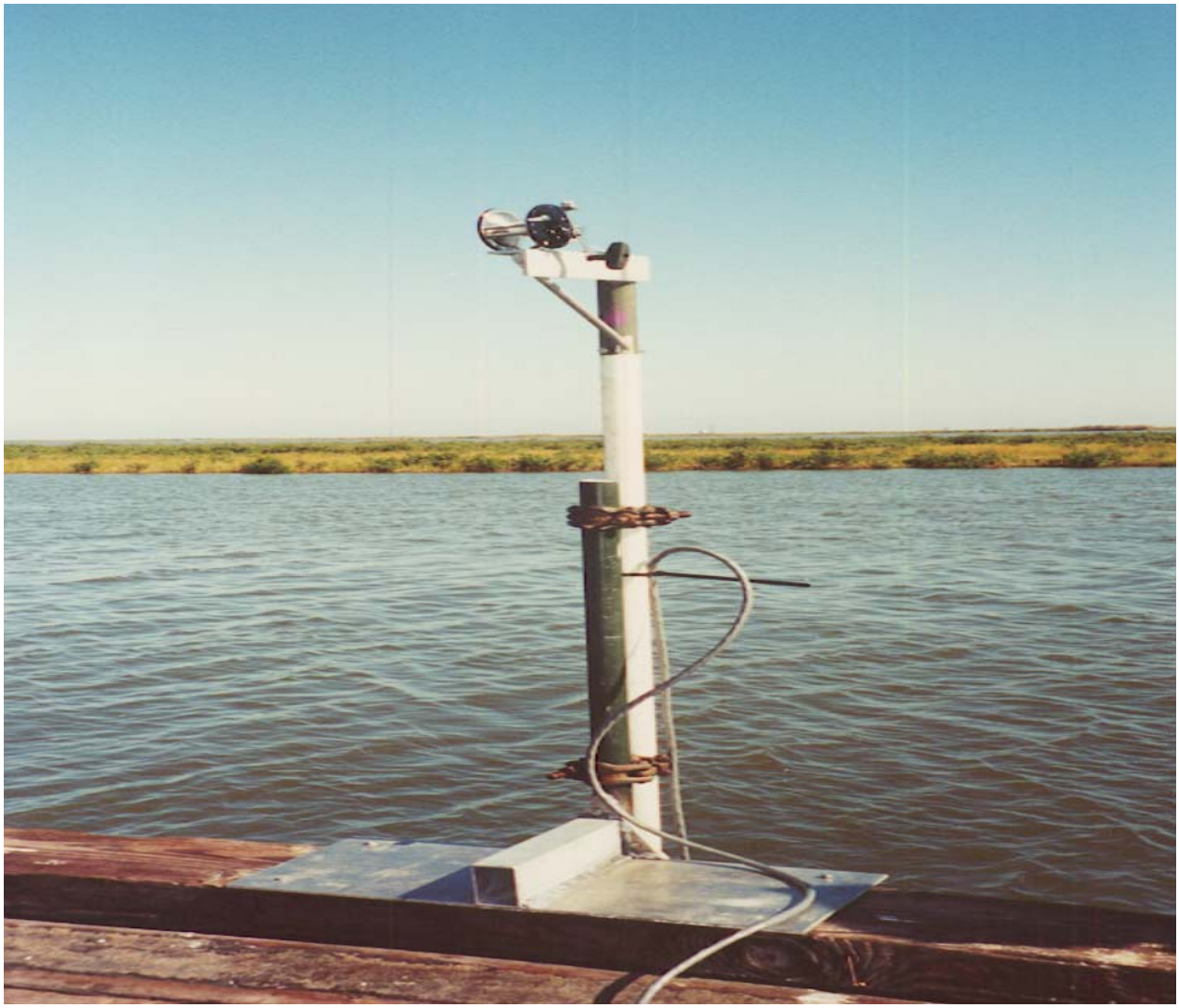

Figure 4. The horizontal transducer deployed at the edge of the dock, looking perpendicularly across the canal.

The vertical transducer was deployed for measurement of target strength, or acoustic size estimates. Data for the upward transducer were collected in one stratum from 0.7 m from the face of the transducer to 0.7 m from the surface to reduce near-field and surface interference. The stratum ranged in depth from 1.5-2.0 meters of water depending upon the tide.

Data from the horizontal transducer were used to estimate target strength, density, and biomass, and to determine direction and velocity of target movement. The horizontally flattened beam of the elliptical transducer reduced noise and interference from the surface and bottom

allowing for a cleaner signal further out into the creek than a circular dual beam transducer. The horizontal transducer sampled out to its calibrated limit of 30 meters. Data from the outward transducer were collected from 0.7 m from the transducer to 30m and divided equally into 3 strata of approximately 9.8 m each. Stratum one of the outward data was closest to the transducer with stratum three farthest away. Only data from stratum one was used for analysis due to problems created by extremely high schooling densities sampled (see Results Section 2.9.4). From this point on, only data from stratum one will be discussed unless otherwise noted.

Data output from Biosonics Visual Analyzer 4.0 used in the statistical analysis included volume backscattering (Sv), target strength (TS), and total targets per cubic meter (FPCM). Volume back scattering, or "the amount of energy back scattered from the school or layer to the echosounder transducer" in dB (Johannesson and Mitson 1983), is defined by the equation:

Equation 1. $Sv = \rho_c \Sigma(C^2)/\Sigma samples$ where:

ρ_c is the density scaling constant, C^2 the squared digital counts and samples the number of samples (BioSonics 1999). In the analysis, Sv was transformed into a proxy of biomass, Fish Energy (FE), following the equation $FE = 10^{(SV/10)}$. Target strength (TS), or the "measure of the reflecting power of a single target expressed in decibels" is calculated as:

Equation 2. $TS = ES - 2B - SL - RS$ for a split-beam transducer where:

ES = echo strength on the composite beam, SL = system source level, RS = through system gain at 1 m distance from the transducer (V/ μPa) and B = the ratio of the transmitted intensity of the acoustic beam at the angular coordinates (θ_1, θ_2) to the transmitted intensity on the acoustic axis of the transducer, expressed in dB, B is further defined as:

Equation 3. $B = \alpha\theta^2_1 + \beta\theta^2_2$ where:

the constants α and β are parameters measured from the two axes of the transducer's beam pattern response (BioSonics 1999).

TS is used in the calculation of total length (TL) for a target given in the equation:

Equation 4. $TS = 19.1*\log_{10}(TL) - 0.9\lambda-23.9$ (Love 1971) where:

λ = the frequency of the transducer.

Fish per cubic meter (FPCM) is the acoustic measure of total fish density for a range ΔR equal to:

Equation 5. $A_iB_rV^2$ where:

A_i = the density scaling constant, B_r = to a range dependent factor and V^2 = the average squared echo voltage from the layer ΔR (BioSonics 1999).

Preliminary data analyses were performed using BioSonics VTRACK analyzer. The VTRACK software was reported to provide target direction of movement and velocity from split-beam data. Analysis was abandoned when it was determined that results from V-TRACK processing were inaccurate due to the inability of the software to handle data from densely populated water columns (Jim Dawson- representative of Biosonics, personal communication).

2.4 Sampling Schedule

Five sampling trips were made during the fall of 2000 coinciding with frontal passage events; 6-8 and 13-15 October, 9-11 and 13-19 (divided into two samples by fronts) November, and 16-18 December. The 6-8 October front sampled was the second frontal event of fall 2000. The 13-15 October sampling trip resulted from an attempt to sample a front which was predicted to pass but stalled and never reached the coast. It is included in the sample for comparison of nekton density and biomass to the frontal passages sampled in the study. Highest frequency of fall frontal passages is typically 3-5 days. Three fronts were sampled within the ten-day period

from 9 to 19 November and they should be representative of the mid-fall period of strong fronts and increased frontal intensity. The December frontal event sample was taken to capture the response of nekton to later frontal passages and for comparison of biomass and nekton density to frontal passages earlier in the season.

Sampling was interrupted on November 17th by an electrical storm, which knocked out power to the echosounder. No damage was done to the equipment and sampling was restarted on the 18th when power was restored and the storm subsided. I intended to conduct sampling 24 hours prior to frontal passage through 24 hours after passage, but weather patterns proved unpredictable and this design was not always realized, in which case the closest possible schedule was followed.

The echosounder was programmed to multiplex the two transducers to run consecutively for 5 minutes each, once, every 30 minutes, resulting in 2 files of horizontal and vertical data per hour. A sampling rate of twice per hour was determined to be beneficial as it allowed for continuous data collection over a day, during and between predicted tidal periods without exceeding computer data storage limitations. Data from the horizontal transducer were frequently corrupted by passage of boats en route to and from a nearby boat launch. Several files had to be discarded. Most of these were collected during daylight and favorable weather conditions, when boat traffic was the highest. The upward transducer was protected from interference by being close to the pier; its beam was out of the way of boats.

2.5 Environmental Data

Environmental data were recorded with an YSI-6000 environmental monitor deployed from the pier. The YSI recorded dissolved oxygen, salinity and water temperature every 15 minutes. Data were stored on the YSI until downloaded to a laptop. Atmospheric data were

downloaded from the Coast Guard weather buoy GDIL1 stationed nearby at Grand Isle, Louisiana via the National Data Buoy Center website (www.ndbc.gov) and consisted of wind speed and direction, barometric pressure, water height, and atmospheric temperature. In a previous study, performed 0.8 km downstream, Karlsson (1999) reported a very close correlation with negligible lag time between water heights reported from the GDIL1 buoy and measurements taken onsite.

2.6 Net Sampling

Nekton were sampled with two types of trawls on the following dates: 10 October, 10, 14, 16, 17, and 19 November, and, 16 and 18 December. During the November 13-16 nonfront, and the November 16-18 and December 16-18 fronts, additional trawl samples were also taken. All samples were collected between 6 and 8 am, depending upon weather, during predicted falling tides, as the focus of the project was to sample the emigration during the fall frontal season. Biological samples consisted of one tow each of a surface trawl and a benthic trawl to sample as much of the water column as possible. Surface trawls consisted of two 12.19 m^2 wing nets (combined into one sample) with a net mesh size of 2.75 centimeters; a 0.635 cm nylon mesh insert was sewn from mid-length to the cod end. The mesh insert in the wing net allowed for the capture of smaller nekton. Benthic samples were taken an otter trawl with 7 m^2 mouth opening and 3.3 cm nylon mesh. Twenty-minute tows were made in the channel where acoustic sampling was performed.

Biological samples were sorted by species, and total length (cm) and wet weight (kg) were determined. Larger catches were sub-sampled by species (n=50). Total number of individuals for the species sub-sampled was calculated by dividing the weight of the total wet weight of the species by mean individual weight.

Comparisons involving the hydroacoustic and trawl data were performed using length frequency data from the wing-net samples. The portion of the water column sampled by the wing nets overlapped a greater portion of the water sampled by the horizontal transducer than did the portion of the water column sampled by the otter trawl. Samples from the otter trawl were used to report species composition.

2.7 Interpolation and Rates of Change

Environmental data were interpolated or selected to coincide with acoustic data. Atmospheric data available from the National Data Buoy Center's GDIL1 station were hourly, whereas acoustic data were collected at half-hour intervals. Atmospheric data were interpolated to half-hour intervals for the acoustic collection times. On site environmental data were sampled by the YSI every 15 minutes and the data point closest to the acoustic sample time was used (±7 minutes). Rates of change for barometric pressure and water level were calculated based on intervals between the interpolated data. Rate of change for water level was utilized as a proxy for current and the direction of nekton movement as it was assumed that nekton move in the direction of tidal flow. Ranges of barometric pressure for each sample period were calculated as a measure of frontal strength and were assigned to the variable "BPRange".

2.8 Categorical Variables

Several categorical variables were created to model combined effects of continuous variables, i.e., barometric pressure, wind speed, air temperature, and water level. These continuous variables all respond to frontal passage and I had hoped that the categorical variables would capture the combined effects. Categorical variables for water level and barometric pressure are presented in Table 1.

I used the frontal strength index (FSI) reported by Perez et al. (2000) as a weighted measure of frontal strength. The formula takes into account changes in barometric pressure, air temperature, and windstress. Twenty-four-hour rates of change for barometric pressure, and air temperature were calculated based on their formula, and windstress was calculated based on the formula: (Equation 6) $U=A*U^2$ after Hsu (1993). Threshold values for each variable were set in their model, and only those atmospheric events exceeding the thresholds for all three variables were deemed a "strong front". The variable 'FSI' had three categories and was created to express the classification of a frontal event based on their method as strong or weak. A new category of "strong return" created with thresholds equal –1 times the values of the thresholds for a "strong front", i.e., the threshold for barometric pressure change for a "strong front"= 7.2 mb/24hr (Perez et al., 2000), the threshold for barometric pressure change for a "strong return" in this study=-7.2 mb/24hr. Windstress was not entered into this additional characterization of an event as a "strong return", since a negative value for windstress is not possible.

Table 1. Values for the categorical variable Tidal Stage, and the corresponding values of water height hourly rate of change (Water Height Rate of Change <0 = Tidal Stage "Falling", Water Height Rate of Change ≥0 = Tidal Stage "Rising")

Categorical Variable	Continuous Variable	Continuous Variable Value	Categorical Variable Value
Water Level Stage	Water Height Rate of Change	< 0	Falling
		≥ 0	Rising
Barometric Pressure Stage	Barometric Pressure Rate of Change	< 0	Falling
		≥ 0	Rising

2.9 Statistical Analysis

2.9.1 Normality

Preliminary analysis of acoustic data indicated non-normality, indicative of patchy spatial and temporal nekton distributions, common to density and abundance samples. ANOVA was abandoned in favor of logistic regression, allowing for the separation of the "signal" from "background levels" of density and biomass within the tidal creek.

2.9.2 Logistic Regression

Traditional ANOVA was not used for analysis of horizontally collected acoustic data given the preponderance of low and zero values in the data examined. Binomial logistic models were constructed using the seventy-fifth percentile of "fish energy" (FE) ($7.00*10^{-5}$) or fish density (2.70 FPCM) values as a threshold. These models were used to evaluate the probability of biomass or density levels within the creek that exceeded the seventy-fifth percentile. The seventy-fifth percentile was picked because it separated the "background" and "signal" data more clearly than did the mean (Figures 5 & 6).

The use of logistic regression in ecological sampling was described by Trexler and Travis (2001). It has been shown to be useful with data that have a large proportion of zero values when error is usually not normally distributed. In most cases analysis consists of converting the dependent variable into a discrete form (e.g., presence/absence, agree/disagree, etc). The regression model then assumes a binomial distribution of errors (Trexler and Travis 2001, Garrison et al 2000). Binary response variables were created for FE and FPCM by establishing threshold levels equal to the 75^{th} percentile separating a response from background levels. These binary variables were then used to fit the logistic regression models.

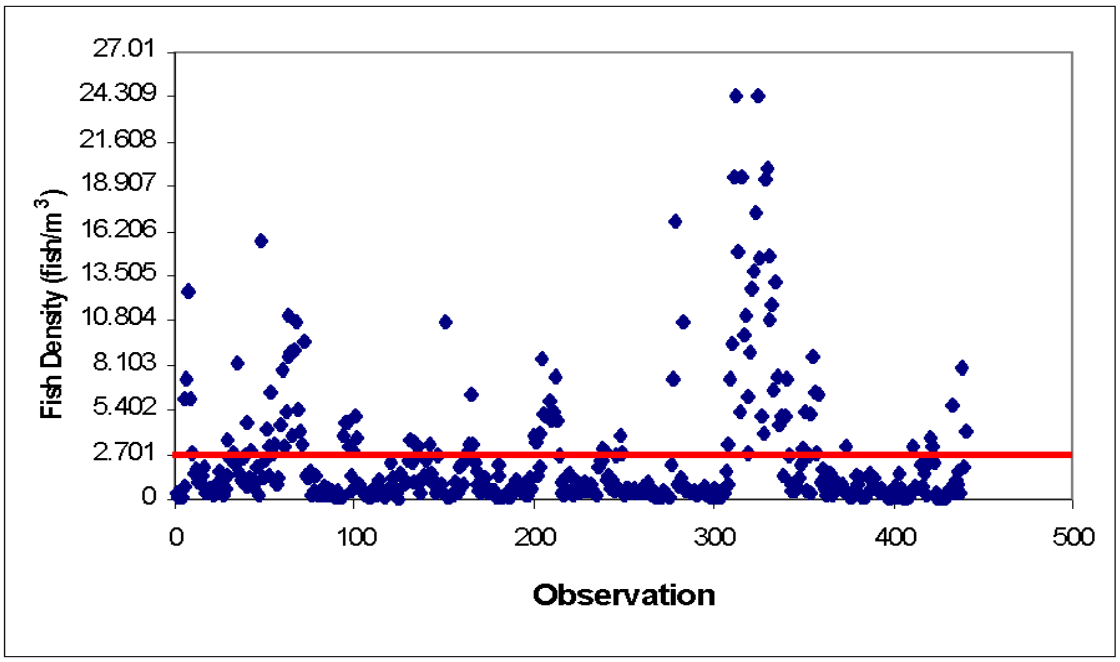

Figure 5. The distribution of total fish densities with the 75th percentile (2.70 fish/m^3) marked as a horizontal line. The 75th percentile was used as the threshold to divide densities into signal, and background.

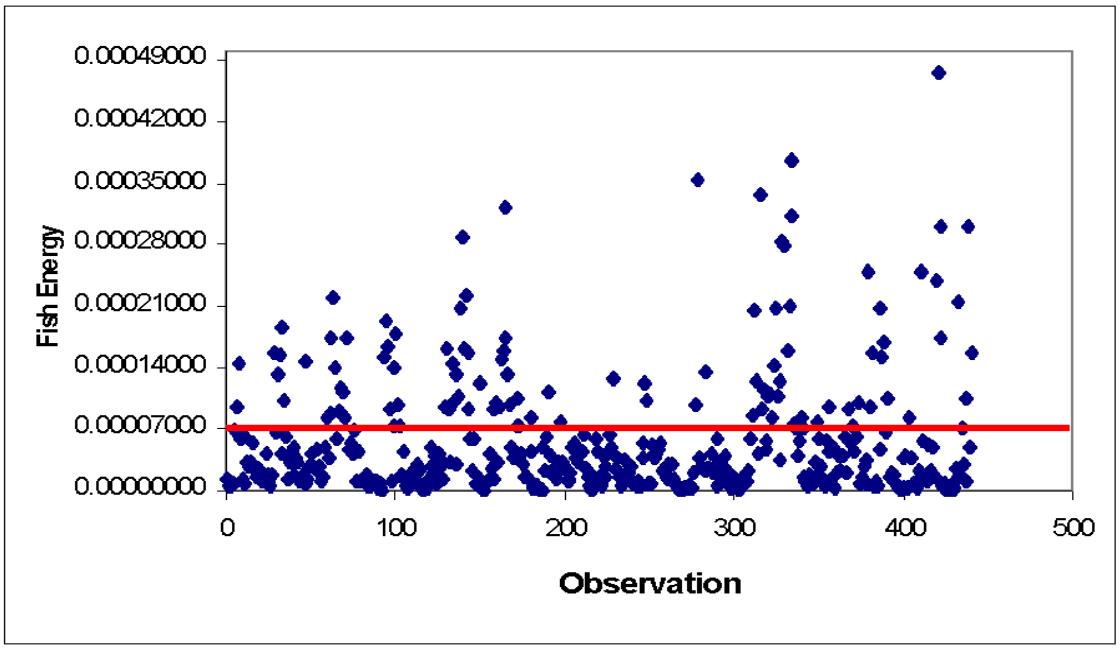

Figure 6. The distribution of fish energy in stratum 1 from the horizontal transducer with the 75th percentile ($7.00*10^{-5}$) marked as a horizontal line. The 75th percentile was used as a threshold to divide fish energies into signal and background levels.

The Statistical Analysis System (SAS 2000) includes a program that performs logistic regression (Proc Logistic). When run with the intercept option, it produces a Type III Analysis of Main Effects, which provides an estimate of the significance of Class Variables, based on a Maximum Likelihood Test (Chi Square test of significance α=0.05) that is used for comparing within class variables. This was the primary test used to determine effects.

2.9.3 Model Design

Preliminary models for FE and FPCM were initially fit with water temperature range (calculated as the maximum water temperature during a frontal sample minus the minimum water temperature over the same period) as a variable in the model. Since water temperature range was not significant in this model, it was eliminated from further models in favor of barometric pressure range (BPRange) and FSI (which incorporated rates of change in air temperature and barometric pressure). Models used in this study were fit to test for the effects of barometric pressure fluctuation associated with frontal passage on biomass (fish energy) and nekton density (FPCM). Barometric pressure was selected as a measure of frontal effects on nekton due to previous reports that nekton behavior was associated with pressure gradients and acclimation to increased pressures (Pavlov et al 2000, Zakharchenko et al. 1997). A frontal level model was fit to explain variation of the dependent variables FE and FPCM using the independent variables sampled, which included BPRange, Tidal Stage, BPRange*Tidal Stage, Barometric Pressure Stage, Tidal stage*Barometric Pressure Stage, and FSI. The frontal model was designed to test the effect of each independent variable as an ultimate factor in inducing total nekton migration.

Barometric pressure stage was designated as either rising (indicative of the movement of a cooler, denser air mass over the area) or falling (indicative of the post-frontal return to warmer,

less dense air from the Gulf of Mexico). Rising barometric pressure was hypothesized to be the ultimate frontal passage cue that induced nekton to emigrate. Barometric pressure stage was fit into the frontal level logistic regression model to test for effect on FPCM and FE above the 75th percentile threshold (indicating movement into the tidal creek during or following frontal passage, respectively). If nekton migrated passively in the direction of the current, then nekton density and biomass would be high during falling water levels (ebbing tides) and rising barometric pressure, as nekton emigrated with the onset of the front. If nekton relocated into the estuary after frontal passage, nekton density, and biomass would be high on falling barometric pressure and rising water levels (flooding tides).

The range of barometric pressure (BPRange) for a front (calculated as the maximum barometric pressure during the frontal sample minus the minimum over the same period) was used as a measure of frontal intensity. I also hypothesized that more intense frontal events would result in greater responses in total nekton density and biomass. More intense fronts would cause nekton to emigrate from the estuary in response to the greater physiological effects of more intense fluctuations of barometric pressure. In addition, a more comprehensive measure of frontal intensity, FSI (incorporating barometric pressure change, air temperature change and windstress), was tested as a measure of the effects of frontal intensity on nekton migration. Few instances of conditions exceeding the thresholds of FSI after Perez et. al. (2000) indicative of either a "strong front" or a "strong rebound" were sampled during this study.

The seasonal level model was designed to test the hypothesis that the initial fronts of a season would illicit greater emigration of the total nekton community than subsequent fronts by testing for variation among fronts (whether the emigration associated with frontal effects varies over the fall season). FE and FPCM were modeled against Front, Front*Tidal stage, and Water

Temperature. Tidal stages (rising or falling) within individual fronts were examined by the Front*Tidal stage interaction to determine whether net import or export of nekton density or biomass was occurring for each front. Tidal stage was fit into the model to determine whether import or export of nekton density or biomass is occurring over the entire study. Water temperature was placed in the model to test the alternate hypothesis that migration during the fall is a gradual, more continual "bleeding off" associated with gradual decreases in water temperature over the entire fall season.

2.9.4 Chi-Square

Acoustic data collected closest to the times of net samples for both the upward and outward facing transducers were compared to the net-sampled data. Chi-square tests were performed on the length-frequency distributions of the upward transducer, outward transducer and wing net collections. Length-frequency data from the otter trawl were not used, since its larger net mesh size made it less representative of targets sampled acoustically and since a smaller overlapping portion of the water column was sampled by the otter trawl and acoustic methods. The Chi-square tests were set up to test equality between two distributions (P-value < 0.05) for each sample date. Similar tests involving the separate total distributions over all dates for the upward and outward transducers were run independently against the wing net. In addition, Chi-square tests of the length distribution of the upward transducer data against the outward transducer length distribution data were performed for each "front" sampled, and total length distributions across all "fronts" sampled.

Acoustic data were initially broken into 25 bins by decibels from –35 to –60dB, a logarithmic scale equaling a range of total length from 114 to 1.38 cm. Acoustic data were limited to the 60 dB (1.38) mm to eliminate noise from sediment load, detritus, and plankton in

the water column. Due to the limitations of the upward transducer, for which the beam width was only 15.7 cm at the surface (1.5 meters), mean total lengths of greater than 15 cm were excluded from the Chi-square tests as targets larger than 15 cm could not be acoustically sampled by the upward oriented transducer. Very few individuals sampled either acoustically or by net, had mean total lengths greater than the 15.7 cm limit. Ten length-frequency bins of 1.5 each from 1.5 to 15 cm were created to aggregate the length-frequency distributions for upward, outward and wing net sampled length data. Lengths were assigned to bins in which they were equal to or lesser than the bin value (2 fish of 1.8 cm = 2 fish in the 3 cm bin). The number of all samples within a bin were summed and given the length value of the bin (2 fish of 1.8 cm + 3 fish of 2.6 cm = 5 fish in the 3 cm bin).

In some tests of the length-frequency distribution of a single transducer, outward or upward, against the wing net, adjustment to the length frequency was necessary to reduce the amount of cells with expected counts below 5 and make Chi-square a valid test. This adjustment consisted of collapsing the ends of the distribution, or summing the frequencies of the two largest and smallest length bins and assigning the smaller length for the larger end and the larger length for the smaller end (4 fish of 15cm + 10 fish of 13.5 cm = 14 fish of 13.5 cm, 8 fish of 3 cm + 6 fish of 4.5 cm = 14 fish of 4.5 cm). The ends of the distributions were collapsed until fewer than 25% of cells had expected values less than 5 making the Chi-square test valid. The adjustment truncated the length-frequency distribution and reduced the degrees of freedom for the distribution, but was necessary to normalize the test for Chi-square test assumptions.

2.9.5 Diversity

Shannon-Weaver index of diversity (H'), Pielou's evenness index (J') and Pielou's dominance index (1-J') were calculated for wingnet, otter trawl and combined totals for each

sample based on both biomass and abundance. Values for wing net collected data were compared among dates, as were values for otter trawl collected data, but no comparisons between wing net values and otter trawl values were made due to the difference in gear selectivity.

3. Results

3.1 Hydroacoustics

The amount of time and effort to install, initialize and sample a tidal creek with Biosonics' Split-Beam system, once refined, proved to be minimal. The bracket constructed for the attachment of the horizontally oriented transducer (horizontal transducer) to the pier was easily installed and the transducer easily attached to the bracket. The upward transducer, deployed on the bottom of the creek, (vertical transducer) was also installed with little effort. Both orientations yielded echograms indicating full coverage (from the bottom to the surface for the vertical transducer; from 0 to 30 meters out from the face of the pier for the horizontal transducer.) The weatherproof container was an excellent shelter for the system withstanding strong winds and rain and made for an easy place from which to operate. Two people could install all gear within one hour with minimal assistance. Adjustments to the depth, and vertical and horizontal angles of outward looking transducer were made upon installation to maximize the amount of water sampled and minimize surface and bottom noise with very little effort. Echograms were periodically checked to insure that the beam remained unobstructed during sampling. Only once, during the December sample was major adjustment needed as water levels dropped enough to expose the horizontal acoustic beam to the surface. The transducer was then lowered to mid-water depth and sampling continued.

Deployment of the upward transducer required minimal assistance from a second person to pass the transducer and mount to a person holding the boat in place for deployment. The harness deployment system worked flawlessly as it produced clean echograms with no interference from the monofilament or the bottom which would have indicated crooked deployment. The horizontal and vertical deployment systems were easily set up and provided quality echograms. Total cost for the horizontal mounting system was under $100, significantly

less than similar commercial designs while still providing full adjustability, durability and functionality. Since the completion of the fieldwork for this study, refinements have been made that will likely lead to further improvements. The two methods and equipment could easily be adapted to use from a boat or other platform with minor alterations making them flexible for several types of estuarine sampling. The deployment technique and equipment were considered successful for a proof of concept study.

The sampling site on the pier of the LUMCON facility was well suited for logistical operations, but proved to have some limitations. The canal was well suited for the study of migration events as it drains a large expanse of marsh; however, the hydrology and bathymetry of the site influenced results. The tidal channel contour causes several eddies to form on the opposite side from the pier. This was exacerbated by a canal entering the tidal channel from the north, immediately east of the pier. Tidal flow into and out of the canal and boat slip, coupled with the flow of the creek against the sea wall of the camp results in scouring against the sea wall and what appeared to be a large eddy in front of the pier extending well out into the creek. The eddy was easily visible from the pier; its form and rotation driven by tidal current.

Visual analysis of the horizontal echograms showed high target density and biomass and differences between and within samples. As noted in the introduction, high target densities limit data precision in several ways. Preliminary analysis for direction of movement and velocity with BioSonics VTRACK software proved to be affected by the above conditions. Results varied little regardless of tidal stage or frontal stage and failed to comply with both hypothesized movements and results from previous studies. Consultation with Jim Dawson of BioSonics on the shortcomings of the VTRACK software produced the conclusion that the software is unable to distinguish single targets within the water column populated by such dense aggregations of

small, similarly sized targets, thereby, rendering it impossible to track targets as they pass through the beam.

Similar problems arose with the accuracy of biomass and density data generated by the Visual Analyzer 4.0 program. As the beam of the transducer spreads over distance, it insonified a larger volume of water and therefore more targets. If densities within the beam exceed calibrated levels, assumptions necessary for accurate target strength, and volume backscatter calculations are not met. Adjustments must be made to the constants governing the loss of energy (due to backscatter) over time and the target identification parameters, as at high densities the software cannot accurately distinguish individual targets, or targets in the water column from the bottom echo return. Data are valid over a distance as long as assumptions are met with resolution negatively related to distance due to the increases in absorption of energy by targets, multiple scatters from multiple targets, and positive and negative interactions due to refraction and reflection of returns. Inspection of output from Visual Analyzer showed the influence of the violation of these assumptions in strata 2 and 3, (10-20 m and 20-30 m from the transducer). Nekton density data from stratum one were similar when compared to results from Karlsson's study (Karlsson, 1999). Therefore, I used data from stratum one for all statistical analysis. Data from strata two and three of the horizontal transducer were disregarded for this study. It is possible that, with the proper correction factors, data from strata two and three could prove useful in the future.

Target strength data were compared to the horizontal-facing transducer to determine if horizontal TS data were valid. Due to the shallow depth sampled, the vertically oriented transducer sampled 1.5 m of water (in a depth of 2 m). The cross sectional dimensions of the beam of the upward oriented transducer at its maximum range was 15.7 cm wide by 5.20 cm

high, equaling a surface area of 115 cm^2. This limited TS resolution to a 15cm fish. The volume of water sampled was 0.0127 m^3. Dimensions of the beam of the horizontally oriented transducer were much larger, 0.052 m wide and 0.017 m high for a surface area of 0.366 m^2, at 10 m. Volume of water sampled out to 10 m was 1.60 m^3.

3.2 Atmospheric Data

Hourly barometric pressure and water temperature data from the GDIL1 station from October through December show the variations associated with frontal passages (Figure 7). Ranges were calculated for barometric pressure, water temperature, water level and mean hourly rate of water level change (Table 2). Ranges were calculated as the difference of the minimum value from the maximum value during a front. The December 16-18 front had the greatest range of barometric pressure, 17.5 millibars; the lowest value occurring during the 13-15 October stalled non-front (3.9 millibars). The greatest range of water temperature (5.8 °Celsius) occurred during the 16-18 November front and the lowest range (1.7 °Celsius) occurred during the 13-15 October non-front. The 16-18 November front has the greatest range in water level (0.63 meters); whereas the 13-15 October non-front had the lowest tidal range (0.24 meters). Ranges of hourly rates of water level change occurred between a maximum of 0.13 meters per hour during the 13-16 November front and a minimum of 0.09 meters per hour during the 13-15 October non-front. (Note: Atmospheric data indicate that the 13-15 October front was not a frontal event due to low barometric pressure, rising water temperature, and low water level ranges; it is referred to as a non-front for the remainder of this study.)

3.3 Summary Statistics

Data for the hydroacoustic sampling were summarized to provide minima, maxima and means for fish energy and fish per cubic meter. The summary statistics below are not significantly different and are given to demonstrate the range of data points sampled.

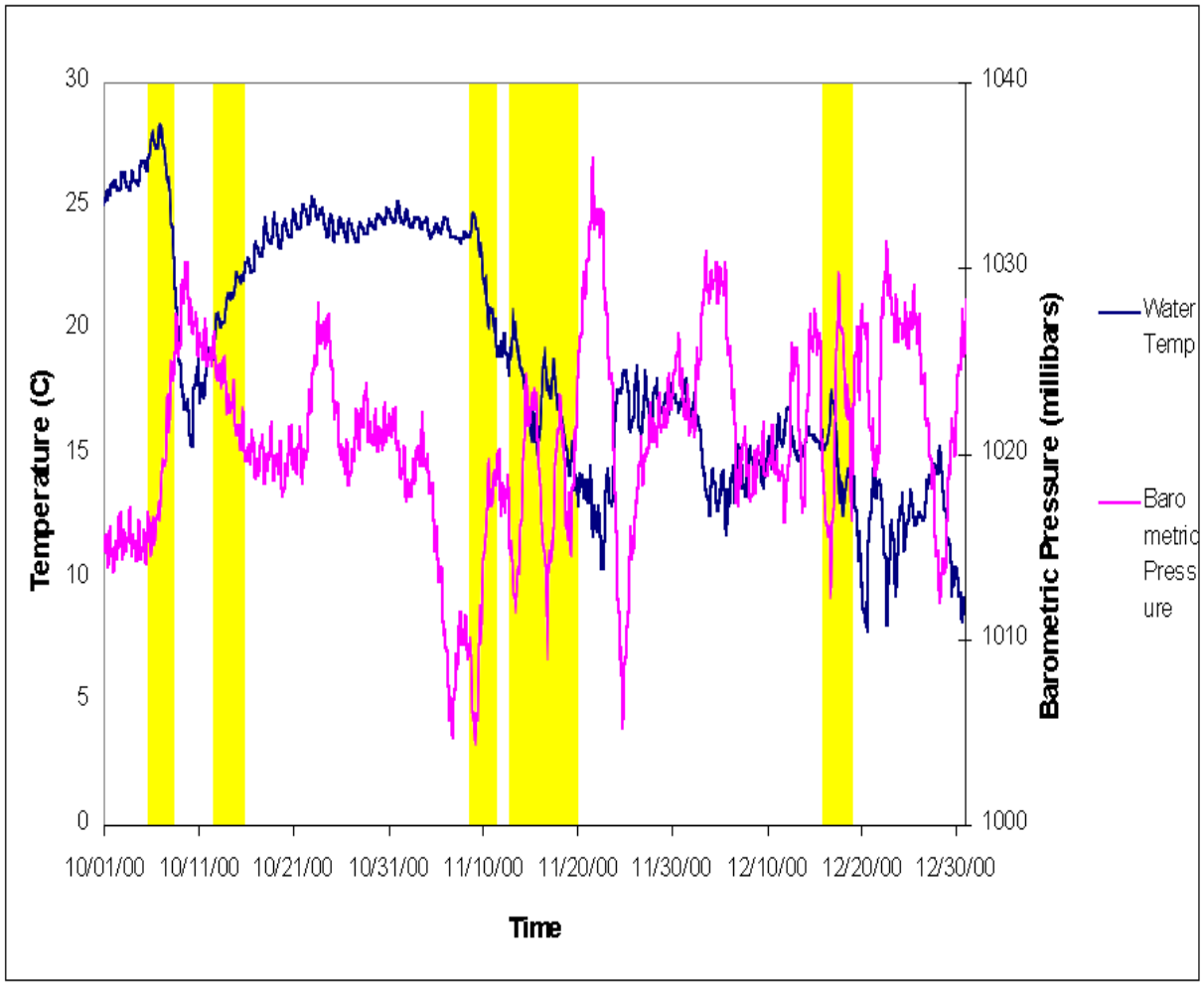

Figure 7. Barometric pressure (red) and water temperature (blue) for 10/1/2000 to 12/31/2000 for GDIL1 data buoy located on Grand Isle, La. Yellow highlighted areas represent sampling periods.

Table 2. Atmospheric data for the sampling periods in fall of 2000. Ranges were calculated as the difference of the minimum from maximum value for each front.

Front	Barometric Pressure Range (mb)	Water Temperature Range (C)	Water Level Range (ft)	Rate of Water Level Change Range (ft/hr)
6-Oct	13.0	7.40	1.51	0.49
13-Oct Non-Front	3.90	1.70	0.79	0.30
9-Nov	15.4	4.80	1.45	0.93
13-Nov	14.2	4.70	1.63	1.03
16-Nov	14.2	5.80	2.08	0.65
16-Dec	17.5	5.10	1.96	0.63

3.3.1 Fish Energy (Proxy for Total Nekton Biomass)

Fish energy (FE), a unit-less acoustic proxy of total nekton biomass calculated from SV (Equation 1), ranged from a minimum of $1.76*10^{-7}$ on a rising tide on November 18 to a maximum of $2.06*10^{-3}$ on the rising tide later the same day. The mean FE (± SD) for the study was $5.96*10^{-5} \pm 1.19*10^{-4}$. The November 16-19 front had the highest mean FE ($1.04*10^{-4}$), and the November 13-16 front the lowest mean ($3.34*10^{-5}$). FE was slightly higher during rising tides ($6.10*10^{-5}$) than on falling tides ($5.79*10^{-5}$).

3.3.2 Fish per Cubic Meter

Fish per cubic meter (FPCM), an acoustic estimate of total nekton density (Equation 4), ranged from a minimum of 0.02 FPCM on a rising tide on 18 November to a maximum of 24.4 on a falling tide on 17 November. The mean estimated FPCM for the study was 2.42 ± 3.72. The 16-19 November front had the highest mean FPCM (5.82), while the 16-18 December front had the lowest mean (1.01). Mean FPCM was higher during falling tides (3.17) than rising tides (1.82).

3.4 Frontal Model

3.4.1 Fish Energy (Total Nekton Biomass Proxy)

The frontal level model tested for differences among variables across the fronts sampled. Tidal stage was also included in the seasonal model and its means are reported above. Mean FE was slightly higher on rising tides, and only the 95% confidence interval of FE for rising tides exceeded the $7.00 * 10^{-5}$ threshold (Figure 8, Table 3). The "Tidal stage" (Tidal Stage), and the "BPRange*Tidal stage" interaction was significant at $\alpha=0.05$ (Table 4). The probability of exceeding the 75th percentile threshold of FE ($7.00*10^{-5}$) varied little for falling tides, and there was no apparent linear relation for FE means for falling tides and increasing barometric pressure

gradients. FE peaked ($6.63*10^{-5}$) at 14.2 millibars (13-16 and 16-19 November) and was slightly lower ($4.71*10^{-5}$) at 13 millibars (6-8 October). A plot of mean FE values for rising tides sampled (Figure 9) shows an increase in means with increasing barometric pressure range and a linear trend of increasing means with greater barometric pressure range. Based on mean FE, there was net export of biomass occurring at lower ranges of barometric pressure (<15.4 millibars), whereas net import of biomass appears to be occurring at higher ranges of barometric pressure (≥15.4 millibars). This change in net biomass movement could be related to the date of frontal passage, with stronger fronts coming later in the fall.

Table 3. Mean (MEAN), minimum (MIN), maximum (MAX) and standard deviation (STD) values of FE for BPRange at Rising and Falling tidal stages, and tidal stage.

BPRANGE	Tidal Stage	MEAN*10^{-5}	STD*10^{-5}	MIN*10^{-7}	MAX*10^{-4}
3.9	FALLING	5.51	6.28	8.28	9.25
13	FALLING	4.71	4.52	38.8	1.74
14.2	FALLING	6.63	9.05	12.0	5.09
15.4	FALLING	5.40	6.10	66.7	2.08
17.5	FALLING	5.47	6.24	9.10	2.49
3.9	RISING	2.82	3.88	7.54	1.79
13	RISING	6.28	6.00	65.4	2.20
14.2	RISING	5.98	2.16	7.69	20.6
15.4	RISING	8.38	7.72	27.9	3.21
17.5	RISING	7.08	10.6	1.76	4.75
Tidal Stage		**MEAN*10^{-5}**	**STD*10^{-5}**	**MIN*10^{-7}**	**MAX*10^{-4}**
FALLING		5.79	0.0000725	6.67	5.09
RISING		6.10	0.000147	1.76	20.6

Table 4. Results from the logistic regression analysis of the Frontal Level Model for fish energy (FE), establishing a binary distribution using the 75th percentile threshold (α=0.05).

EFFECT	DF	CHI-SQUARE	P>CHISQ
BPrange	1	1.47	0.24
Tidal Stage	1	4.75	**0.029**
BPrange*Tidal Stage	1	3.90	**0.048**
BPStage	1	0.37	0.54
Tidal Stage*BPStage	1	1.60	0.21
FSI	2	1.26	0.53

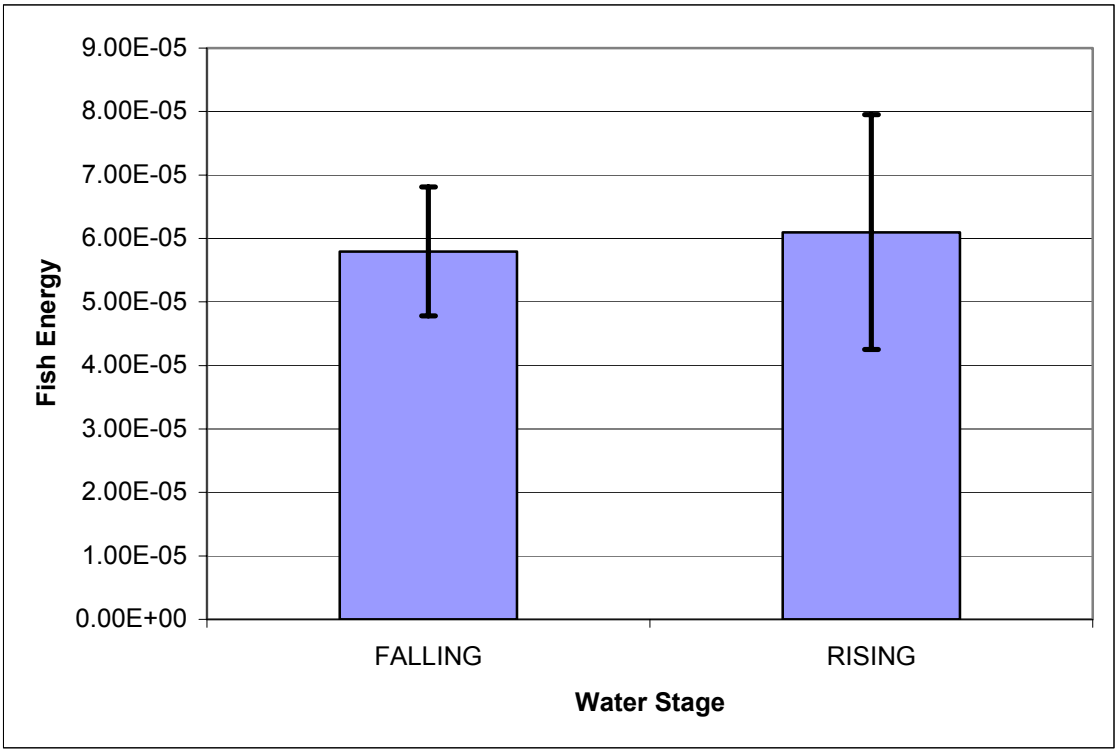

Figure 8. Mean Fish Energy (FE) by tidal stage (Falling or Rising) from hydroacoustic data collected at Bayou Tartellon October-December 2000; vertical bars represent the 95% confidence intervals of means

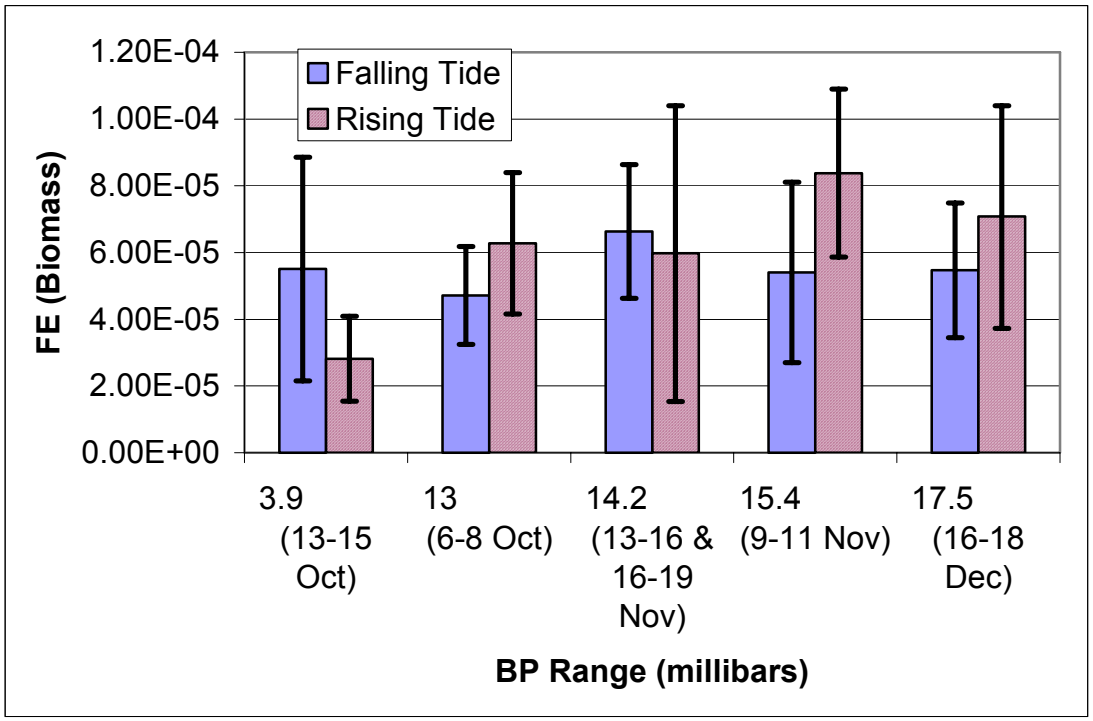

Figure 9. Mean fish energy for falling and rising tides for barometric pressure range (BPRange in millibars); dates in parenthesis are those for which the BPRanges were sampled from 6 October to 18 December; vertical bars represent the 95% confidence interval of the means.

3.4.2 Fish per Cubic Meter

Tidal stage (rising or falling) and the interaction of BPStage (barometric pressure stage – rising or falling)*Tidal Stage were significant in the frontal level model (Table 5). Mean, minimum and maximum total densities for the independent variables varied widely (Table 6). Mean density for falling tides were higher than mean density for rising tides (Figure 10). Mean falling tidal stage density exceeded the 75th percentile threshold for density (2.70 FPCM), whereas the threshold exceeded the upper limit of the 95% confidence interval for the mean rising tidal stage density, indicating a higher probability for density to exceed the threshold during falling tidal stage. Mean densities were higher for falling tidal stage for both rising and falling barometric pressure stages (Figure 11). The 75th percentile threshold (2.70 FPCM) exceeded the upper limit of the 95% confidence interval of the mean for rising tidal stage during

either falling or rising barometric pressure. Mean FPCM during rising barometric pressure was slightly (+0.39 FPCM) higher than during falling barometric pressure, although the means were not statistically different. The mean during a falling tidal stage was greater than during a rising tidal stage regardless of barometric pressure stage. The BPRange (barometric pressure range)*Tidal Stage interaction was nearly significant (p=0.076). Plots of mean and 95% confidence intervals for FPCM during rising and falling tidal stage associated with barometric pressure ranges sampled in the study (Figure 12) showed an increase for mean FPCM on falling tidal stage (5.07, Table 6) up to the 14.2 millibar range (13-16 and 16-19 November). Mean FPCM values for falling tides declined at higher barometric pressure ranges (>14.2 millibars) to FPCM values below those of weaker fronts (≤14.2 millibars). Means of FPCM on rising tidal stage peaked (3.22) at 13 millibars (6-8 October) and declined with increased barometric pressure range. The mean was higher for ranges of 13 or 14.2 millibars than all other ranges, as the threshold exceeded the upper limit of the 95% confidence interval for all ranges other than 13 or 14.2 millibars. Mean FPCM was greater on falling tidal stage for ranges up to 14.2 millibars, whereas mean FPCM was greater on rising tidal stage for ranges greater than 14.2 millibars. This shift in net migration may also be related to stronger fronts occurring later in the fall than weaker fronts.

Table 5. Results of logistic regression of the Frontal Level Model for nekton density estimates (FPCM), testing for the probabilities of FPCM exceeding the 75th percentile threshold (α=0.05)

EFFECT	DF	CHI-SQUARE	P>CHISQ
BPrange	1	0.0088	0.92
Tidal Stage	**1**	**5.9185**	**0.01**
BPrange*Tidal Stage	1	3.1421	0.08
BPStage	1	2.5862	0.10
Tidal Stage*BPStage	**1**	**3.9938**	**0.04**
FSI	2	1.7794	0.41

Table 6. Mean (MEAN), minimum (MIN), maximum (MAX) and standard deviation (STD) values for the BPRange*Tidal Tidal Stage (Barometric Pressure Range*Tidal Stage) interaction, BPStage*Tidal Stage (Barometric Pressure Stage*Tidal Stage) interaction, and Tidal Stage.

BP RANGE	TIDAL STAGE	MEAN	STD	MIN	MAX
3.9	FALLING	1.63	1.62	0.050	4.68
13	FALLING	3.38	3.65	0.122	15.6
14.2	FALLING	5.07	5.81	0.088	24.4
15.4	FALLING	1.15	1.05	0.074	3.55
17.5	FALLING	0.79	0.74	0.056	3.20
3.9	RISING	0.83	1.03	0.072	4.98
13	RISING	3.22	3.00	0.258	11.1
14.2	RISING	2.03	3.70	0.075	20.0
15.4	RISING	1.71	1.96	0.12	10.7
17.5	RISING	1.21	1.67	0.019	7.98
BP STAGE	**TIDAL STAGE**	**MEAN**	**STD**	**MIN**	**MAX**
FALLING	FALLING	3.33	4.81	0.0750	24.4
FALLING	RISING	1.62	3.20	0.0190	20.0
RISING	FALLING	3.09	4.32	0.0500	24.4
RISING	RISING	2.01	2.45	0.102	13.1
TIDAL STAGE		**MEAN**	**STD**	**MIN**	**MAX**
FALLING		3.17	4.48	0.0500	24.4
RISING		1.82	2.85	0.0190	20.0

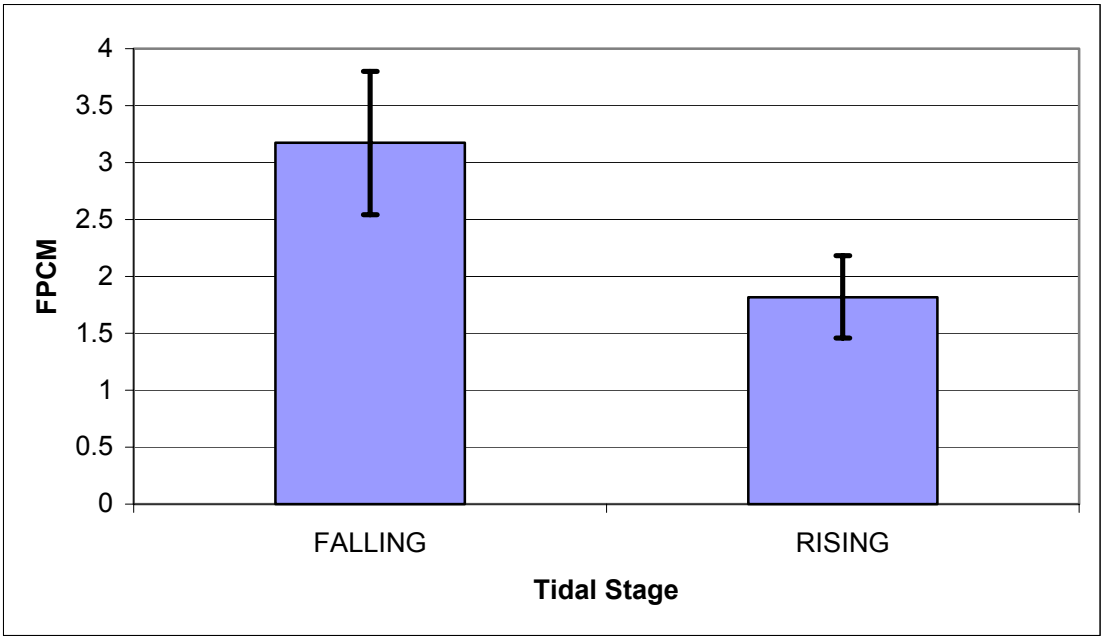

Figure 10. Mean nekton density (FPCM) estimated by split-beam hydroacoustics by tidal stages in Bayou Tartellon during October-December 2000.

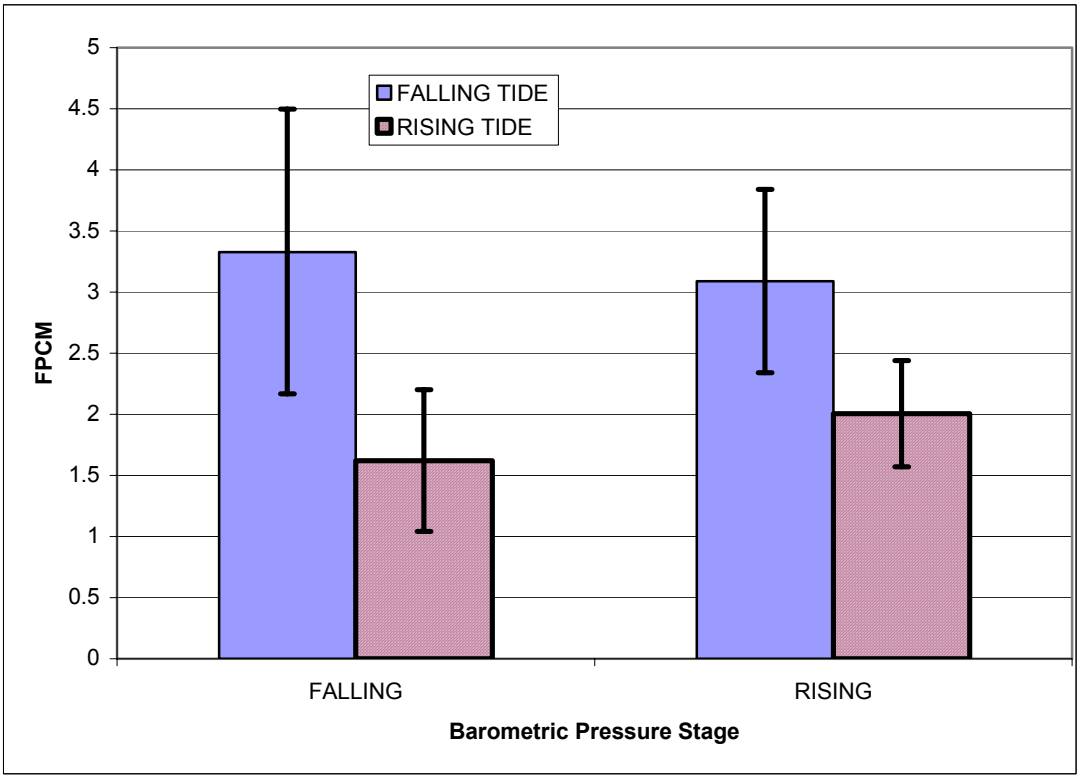

Figure 11. Mean nekton density (FPCM) estimated by split-beam hydroacoustics for barometric pressure stage (Rising or Falling) and tidal stage (Rising or Falling) in Bayou Tartellon during October-December 2000.

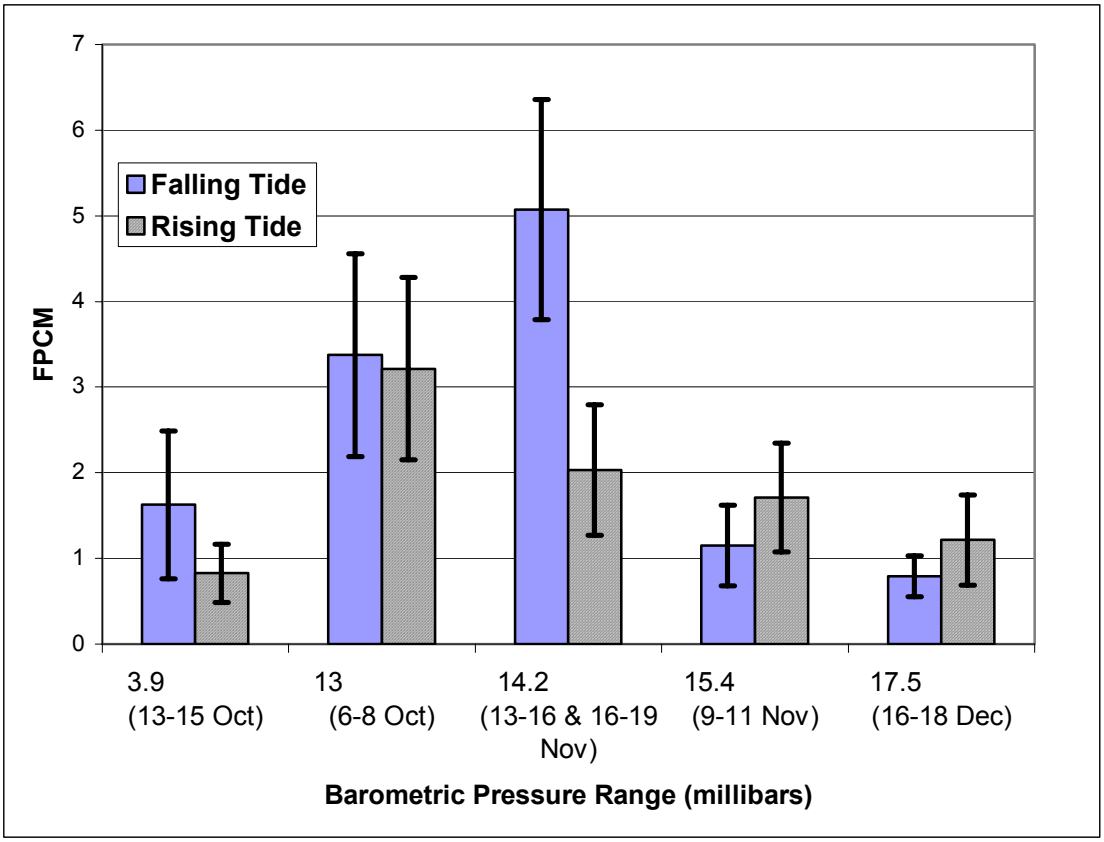

Figure 12. Hydroacoustic estimates of mean nekton density (FPCM) for rising and falling tidal stage in Bayou Tartellon during sampling events between October to December 2000 sorted by barometric pressure range (millibars); error bars represent the 95% confidence intervals of the means.

3.5 Seasonal Model

3.5.1 Fish Energy (Proxy for total nekton biomass)

In the seasonal level model, Front and Water Temperature (WTMP) were highly significant ($p<0.01$; Table 7). Visual analysis of the means and 95% confidence intervals for each front (Figure 13) showed a peak in mean biomass (FE = $1.04*10^{-4}$, Table 8) during the 16-19 November front. Means ($7.00*10^{-5}$) were greater for the 9-11 and 16-19 November fronts, and the 16-18 December front than other fronts, as the threshold exceeded the upper limit of the 95% confidence interval for fronts on 6-8 and 13-15 October, and 13-16 November. After an outlier (FE $2.05*10^{-3}$ occurring on a rising tide at 12.95 °C) was removed from the plot of FE by

temperature for rising and falling tides (Figure 14), there was no clear relationship between total biomass values exceeding the 75th percentile threshold and water temperature for either rising or falling tidal stage.

Table 7. Results from logistic regression analysis of the Seasonal Level Model for Fish Energy (FE), testing for the probabilities of FPCM exceeding the 75th percentile threshold (α=0.05), WTMP= Water Temperature

Effect	DF	Chi-Square	P>CHISQ
Front	**5**	**31.8163**	**0.0001**
Tidal Stage	1	0.7475	0.3873
Front*Tidal Stage	5	9.1131	0.1046
WTMP	**1**	**10.2845**	**0.0013**

Table 8. Mean, minimum (MIN), maximum (MAX) and standard deviation (STD) values of FE for the significant variables from the seasonal model, Front (by date) and the Front*Tidal Stage interaction.

FRONT	MEAN*10^{-5}	STD*10^{-5}	MIN*10^{-7}	MAX*10^{-4}	
Oct 6-8	5.43	5.26	38.8	2.20	
Oct 13-15	3.62	4.82	7.54	1.93	
Nov 9-11	7.30	7.27	6.67	3.21	
Nov 13-16	3.34	4.25	7.69	3.53	
Nov 16-19	10.4	25.2	12.2	20.6	
Dec 16-18	6.30	8.75	1.76	4.75	
FRONT	**TIDAL STAGE**	**MEAN*10^{-5}**	**STD*10^{-5}**	**MIN*10^{-7}**	**MAX*10^{-4}**
Oct 6-8	FALLING	4.71	4.52	37.9	1.74
Oct 13-15	FALLING	5.51	6.28	8.28	1.93
Nov 9-11	FALLING	5.40	6.10	6.67	2.08
Nov 13-16	FALLING	4.00	6.07	10.2	35.3
Nov 16-19	FALLING	8.96	10.6	12.2	50.9
Dec 16-18	FALLING	5.47	6.24	9.08	2.49
Oct 6-8	RISING	6.28	5.98	65.4	2.22
Oct 13-15	RISING	2.82	3.88	7.54	1.79
Nov 9-11	RISING	8.38	7.72	27.9	3.21
Nov 13-16	RISING	2.93	2.59	7.69	1.28
Nov 16-19	RISING	12.4	37.5	32.8	20.6
Dec 16-18	RISING	7.08	10.6	1.76	4.75

3.5.2 Fish per Cubic Meter

Front, Water Temperature and the Front*Tidal Stage interaction were significant in the seasonal level model (Table 9). Mean, minimum, and maximum total nekton densities varied widely for

the independent variables (Table 10). Plots of mean FPCM showed a peak total density (Figure 15) on 16-19 November (5.82 FPCM, Table 10) and a secondary peak (3.30 FPCM) on 6-8 October. Mean total densities for fronts on 9-11 (1.51) and 13-16 (1.73) November appeared similar. Mean densities for the non-front on 13-15 October (1.07) and 16-18 December front (1.01) were also similar. The probability for exceeding the 75th percentile FPCM threshold was highest for the 6-8 October and 16-19 November fronts. The 75th percentile threshold exceeded the upper limit of the 95% confidence interval of the mean FPCM for all other fronts sampled. Visual analysis of mean FPCM for rising and falling tidal stages during each front (Figure 16) showed a maximum for both falling (7.09) and rising (4.00) tides during the 16-19 November front. Other than these maxima, only the falling (3.38) and rising (3.22) tidal stage during 6-8 October and the falling tide (2.79) during 13-16 November had density means exceeding the

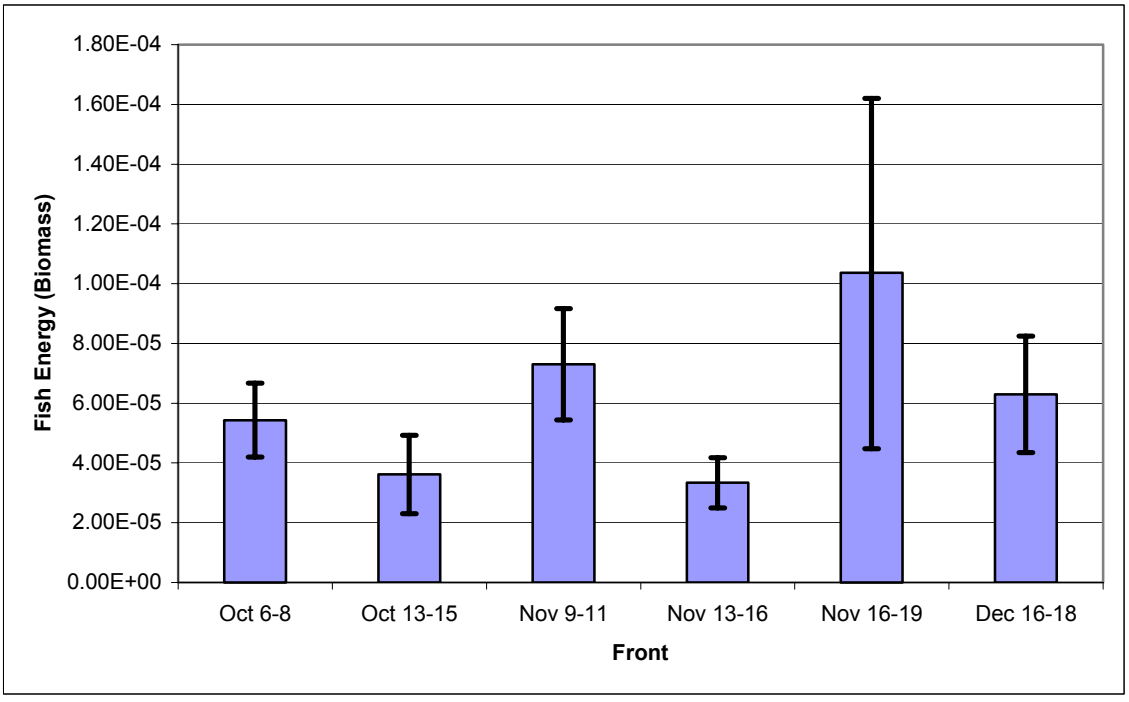

Figure 13. Mean values of Fish Energy (a hydroacoustic proxy for biomass) for frontal samples collected with split-beam hydroacoustics at Bayou Tartellon from sample dates between 6 October to 18 December 2001; error bars represent 95% confidence intervals of the means.

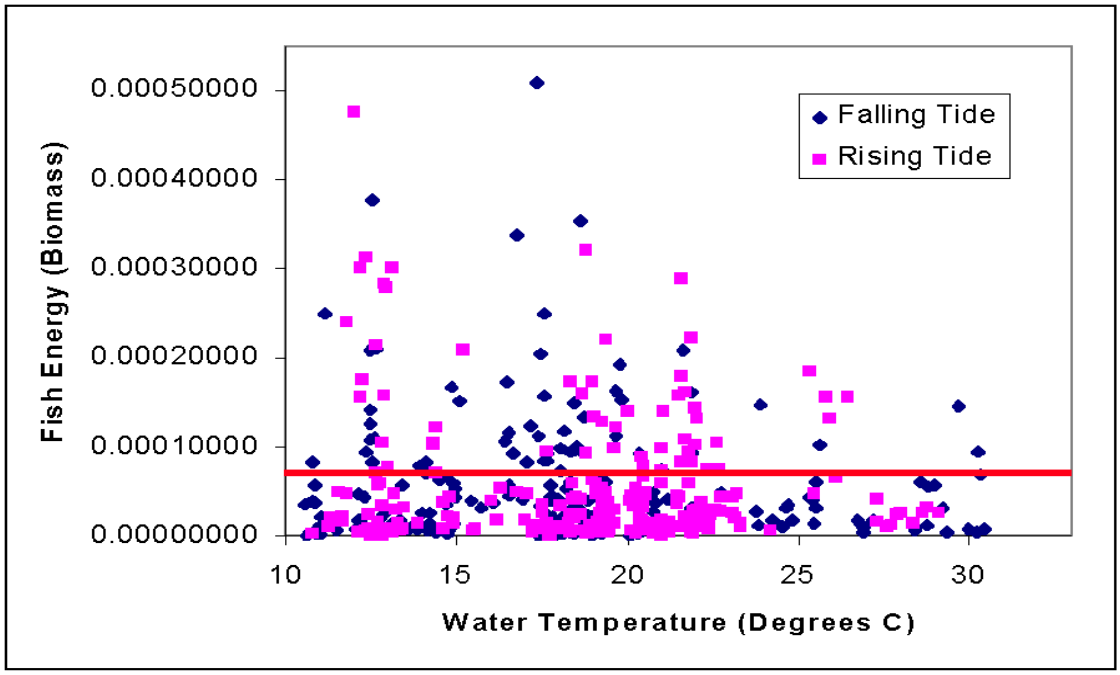

Figure 14. Fish energy (FE) collected with hydroacoustics at Bayou Tartellon during sample dates between 6 October - 18 December 2000 on rising tidal stage (pink square) and falling tidal stage (blue diamond) by water temperature (straight line represents 75th percentile threshold).

75th percentile threshold. The upper limit of the 95% confidence interval fell below the 75th percentile threshold for all other tides in the study, indicating a much lower probability of any single density value exceeding the threshold. There was a trend of net export of nekton based on differences in mean tidal densities until 16-19 November (with the exception of the 9-11 November front) and net import of nekton thereafter. Distribution of FPCM exceeding the threshold showed no relationship to water temperature for either rising or falling tides (Figure 17).

3.6 Biological Sampling

Wing net and otter trawl biomass and numerical abundance estimates derived during this study varied widely (Table 11, Figures 18 & 19). Biomass estimates from 20-minute wing nets trawls ranged from 2 kg on 18 December to 11.1 kg on 14 November. The overall study mean

Table 9. Results from logistic regression analysis of the Seasonal Level Model for total nekton density (FPCM), testing for the probabilities of FPCM exceeding the 75th percentile threshold (α=0.05), WTMP= Water Temperature.

Effect	DF	Chi-Square	P>CHISQ
Front	5	66.9	0.0001
Tidal Stage	1	0.0012	0.9722
Front*Tidal Stage	5	13.7	0.0174
WTMP	1	33.0	0.0001

Table 10. Mean, minimum (MIN), maximum (MAX) and standard deviation (STD) of hydroacoustic estimates of total density (FPCM) for Front and the Front*Tidal Stage (Sample*Tidal Stage) interaction from the seasonal model.

FRONT	MEAN	STD	MIN	MAX	
Oct 6-8	3.30	3.35	0.12	15.60	
Oct 13-15	1.07	1.27	0.05	4.97	
Nov 9-11	1.51	1.70	0.07	10.67	
Nov 13-16	1.73	20.50	0.75	16.70	
Nov 16-19	5.82	6.49	0.09	24.40	
Dec 16-18	1.01	1.31	0.02	7.98	
FRONT	**TIDAL STAGE**	**MEAN**	**STD**	**MIN**	**MAX**
Oct 6-8	FALLING	3.38	3.65	0.12	15.59
Oct 13-15	FALLING	1.63	1.62	0.05	4.68
Nov 9-11	FALLING	1.15	1.05	0.07	3.55
Nov 13-16	FALLING	2.79	3.44	0.10	16.75
Nov 16-19	FALLING	7.09	6.71	0.09	24.39
Dec 16-18	FALLING	0.79	0.74	0.06	3.20
Oct 6-8	RISING	3.22	3.00	0.26	11.13
Oct 13-15	RISING	0.83	1.03	0.07	4.97
Nov 9-11	RISING	1.71	1.96	0.12	10.66
Nov 13-16	RISING	1.09	1.35	0.08	8.44
Nov 16-19	RISING	4.00	5.80	0.12	20.04
Dec 16-18	RISING	1.21	1.67	0.02	7.98

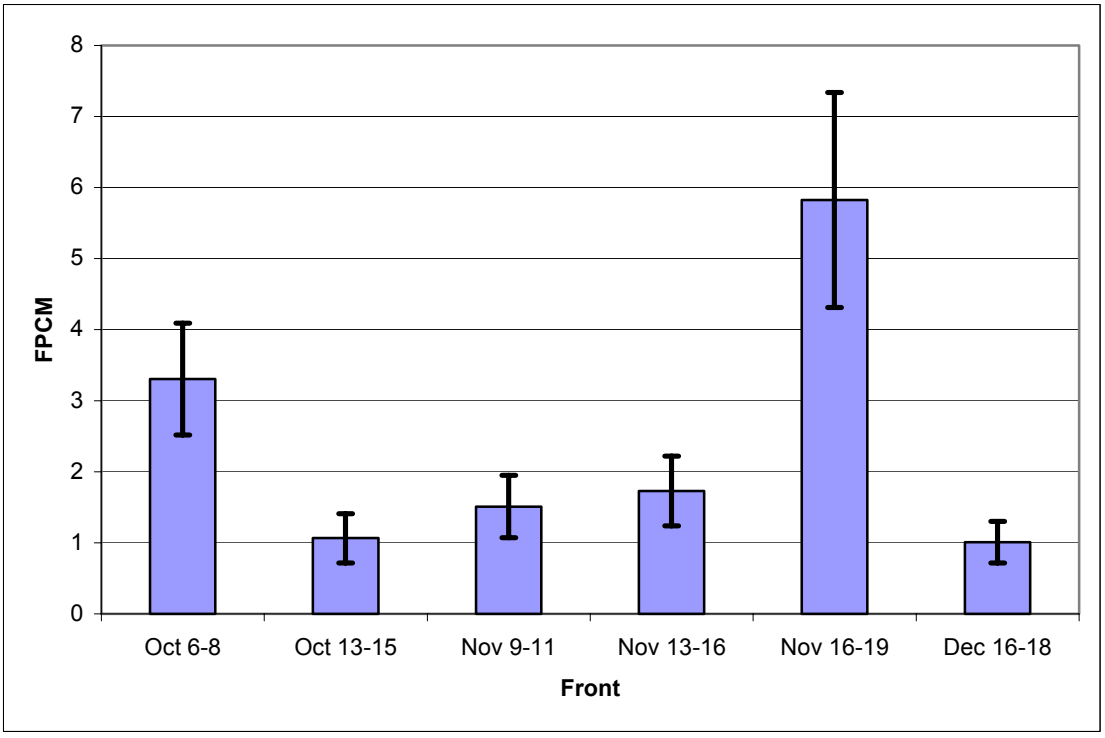

Figure 15. Mean hydroacoustic estimates of total nekton density (FPCM) present in Bayou Tartellon by sampling dates; error bars represent 95% confidence intervals for the means.

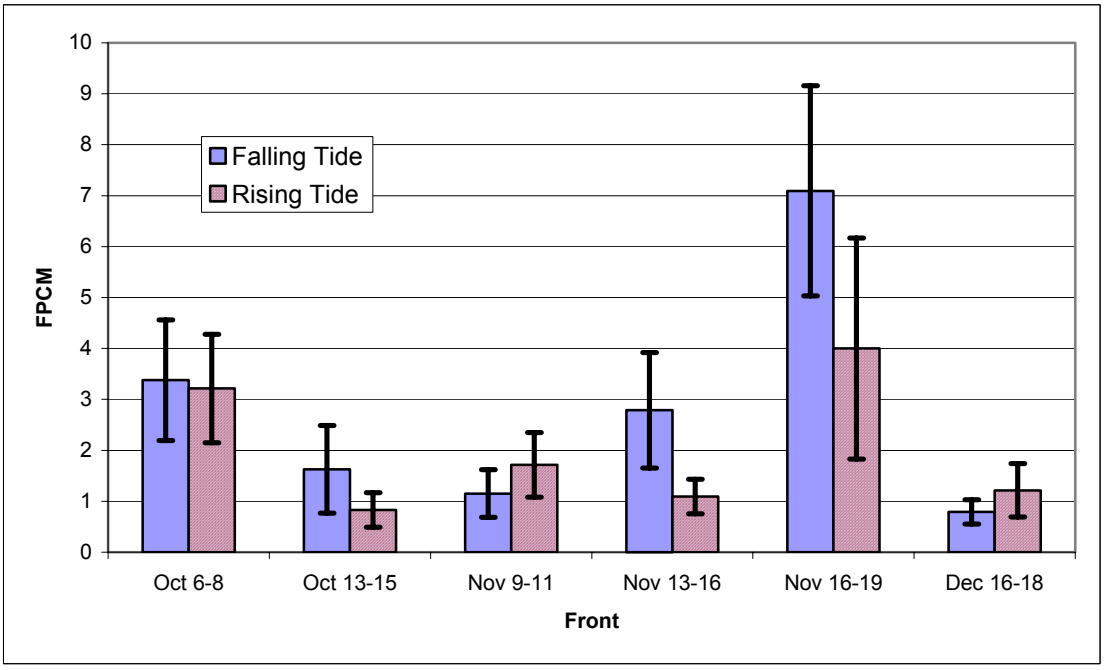

Figure 16. Hydroacoustic estimates of total nekton densities (FPCM) for tidal stages (Rising or Falling) for fronts sampled between 6 October- 18 December 2000 in Bayou Tartellon, Louisiana; error bars represent 95% confidence intervals for the means.

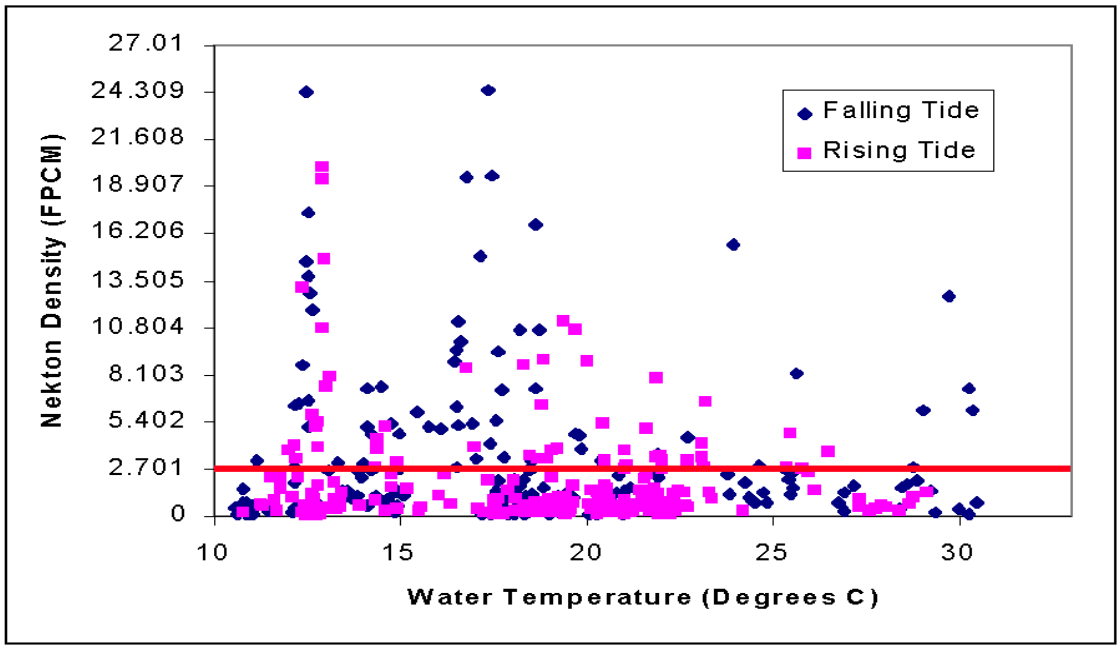

Figure 17. Hydroacoustic estimates of nekton density (FPCM) during rising and falling tidal stage and water temperature. Data were collected in Bayou Tartellon during sample fronts from 6 October - 18 December 2000.

was 6.3 kg. Otter trawl biomasses varied from a low of 2.1 kg on 18 December to 16.1 kg on 19 November, and the overall study mean was 9.1 kg. Numerically, wing net samples varied from 741 individuals (vertebrates and invertebrates) on 18 December to 8,366 on 19 November with a study mean of 3,880 individuals. Otter trawl samples had much lower numerical abundances ranging from 58 on 18 December to 646 individuals on 19 November with a study mean of 195 individuals.

The number of species caught per sampling trip ranged from a high of 27 on 16 November to a low of 12 on 18 December (mean of 19 species). Numbers of wing net-captured species and otter trawl-sampled species were similar; wing net species ranged from 19 (twice, 14 & 19 November) to 5 on 18 December with a fall mean of 12 species, while otter trawl species ranged from 17 on 14 November to 7 on 18 December with a mean of 11 species. Average total lengths for wing net samples ranged from 5.35 cm on 10 October to 6.40 on 17 December.

Average total lengths for the otter trawl samples varied from 9.75 cm on November 17 to 14.9 cm on December 18.

Table 11. Summary statistics, by sample date, of biological samples collected by wing-net (wing) and otter trawl (otter) during this study.

Date	Wing Wt (Kg)	Otter Wt (Kg)	Wing Abundance	Otter Abundance	Wing Species	Otter Species	Total Species	Wing AVG TL	Otter AVG TL
10/14	10.39	4.68	7399	535	17	13	22	5.51	9.85
11/10	1.43	2.54	1218	125	10	10	16	5.36	11.48
11/14	11.13	6.36	7015	132	19	17	27	6.18	10.87
11/16	5.19	12.81	130	64	11	10	16	5.85	12.47
11/17	1.96	11.88	808	85	12	12	21	5.52	9.75
11/19	10.82	16.09	8367	646	19	11	23	5.90	10.63
12/17	8.14	16.13	5366	344	10	13	21	6.40	13.84
12/18	1.19	2.13	741	58	5	7	12	6.16	14.91

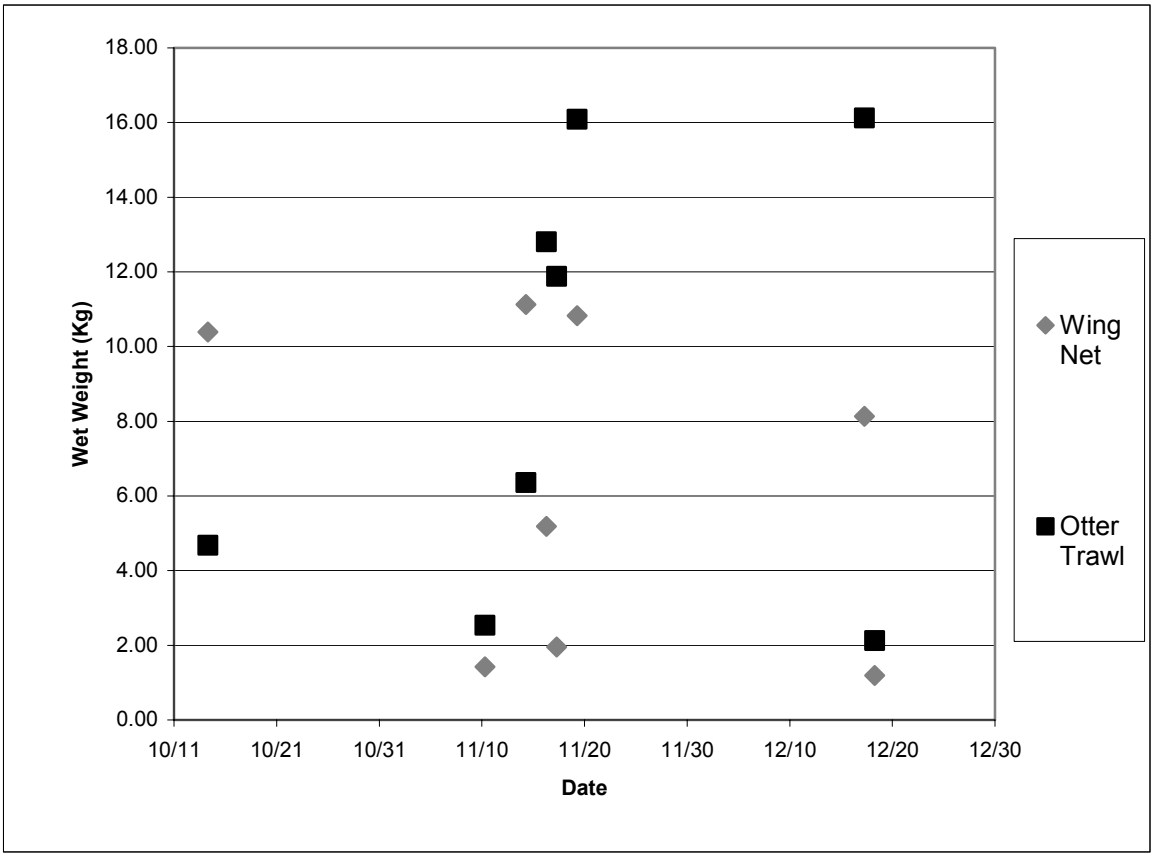

Figure 18. Mean wet weight (kg) for wing net and otter trawl samples collected in Bayou Tartellon from 10 October- 18 December 2000.

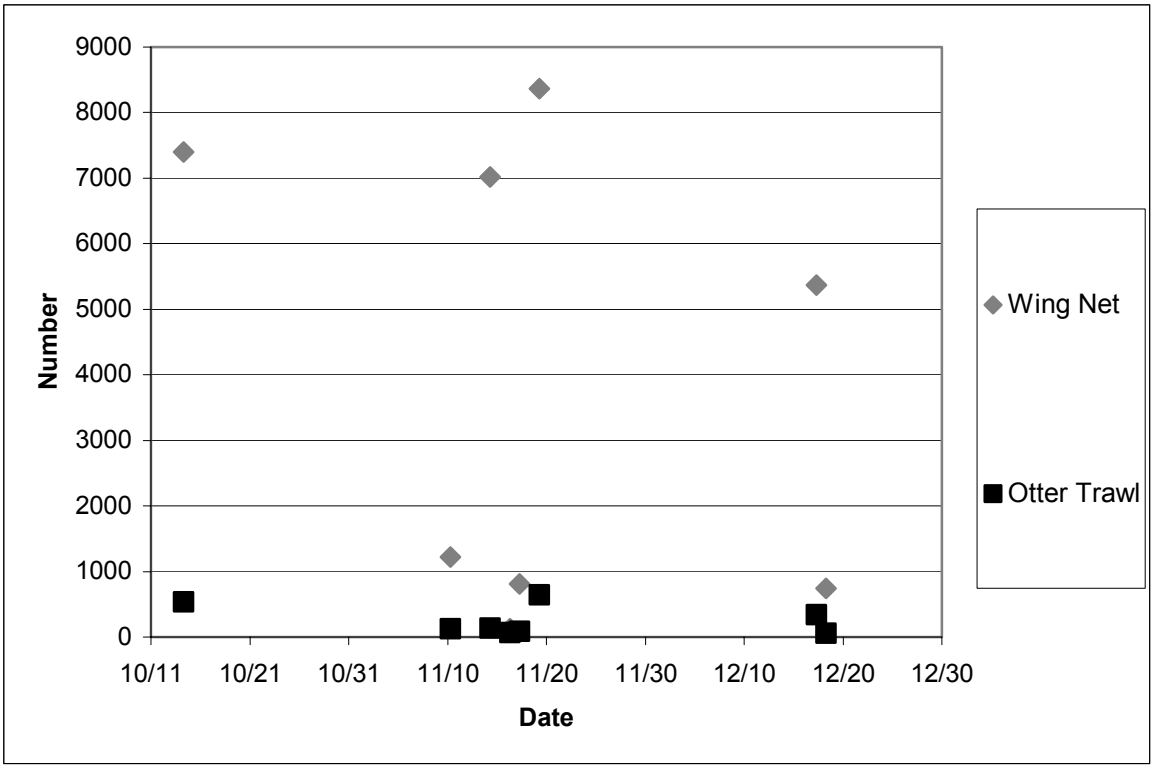

Figure 19. Abundances (total number of individuals) for wing net and otter trawl samples, by collection date, from 6 October- 18 December 2000 in Bayou Tartellon.

All biological samples were taken during outgoing tides; hence, trends in abundance represent only emigrational patterns. Numerically, bay anchovy, *Anchoa mitchilli*, were dominant throughout the study, comprising up to 89% of the total catch on October 14. In December, bay anchovy were displaced by the rough silverside, *Membras martinica,* which made up 76% of the total numbers caught on December 17 and 72% on December 18 (Appendix A). Bay anchovy were also dominant in biomass based on wet weight through the November 16 sample; bay anchovy biomass peaked (56% total weight) on October 14. Moon jelly, *Aurelia aurita*, were collected during the November 16 and 17 samples and made up 78% and 14%, respectively, of total catches by weight. The 17th and 18th December samples were dominated by *M. martinica* making up 31% and 32% of total catches by weight, respectively.

The top three species by (total mass and number) collected in the wing net during this study were *A. mitchilli*, *M. martinica*, white shrimp (*Paneaus setiferus*). For the otter trawl, the top three species by total mass were Atlantic stingray (*Dasyatis Sabina*), silver perch (*Biardiella chrysoura*), and spot (*Leiostomus xanthurus*) (Figures 20-23). Collectively they made up 97 % of the species catch by number and 58 % by weight. The only exception to this pattern was low abundance and weights occurring within the 16 and 17 November samples, which coincided with the dominance of jellyfish over that period. Bay anchovy and white shrimp declined in both abundance and weight over the study period. Silver perch increased in number and weight to a high on November 10, and then rapidly declined. Weight and numbers of rough silverside and spot increased throughout the sampling period. Atlantic stingray appeared only after 10 November and remained relatively high thereafter. Weight and abundances for all species declined sharply with the December 18 sample.

Staggered trends in abundance among species with shared food resources were apparent. For example, bay anchovy was abundant early in the study and decreased in number later in the fall; as anchovy decreased, rough silverside increased in abundance. Spot and silver perch showed a similar opposing trend. Spot increased in abundance through the fall, and silver perch decreased after being abundant earlier in the fall. Peaks in abundance early in the season by prey species, e.g., shrimp and bay anchovy, were followed by increased abundance of predator species such as Atlantic stingray and spotted seatrout (*Cynoscion nebulosus*, see Appendix) later in the fall.

Wing net sample collections had less diversity and evenness and higher dominance in both numerical abundance and biomass than otter trawl samples due to the initial dominance of bay anchovy and, later, rough silverside (Table 12). Diversity was highest for the November 16

and 17 samples for both wing net (H'= 0.49 and 0.40, respectively) and otter trawl (H'=0.77 and 0.78, respectively) samples. Evenness was also highest for the same sample dates for both the wing net (J'= 0.49 and 0.38, respectively) and otter trawl (0.81 and 75, respectively), which coincided with the appearance of jellyfish, *Aurelia arita*. High catches of jellyfish could have resulted in lower catches of other nekton due to avoidance by other species, grazing pressure from *A. arita* or lowered sampling efficiency due to clogging of the wing nets and otter trawl with jellyfish. Highest values of dominance occurred with high abundances of bay anchovy and the rough silverside.

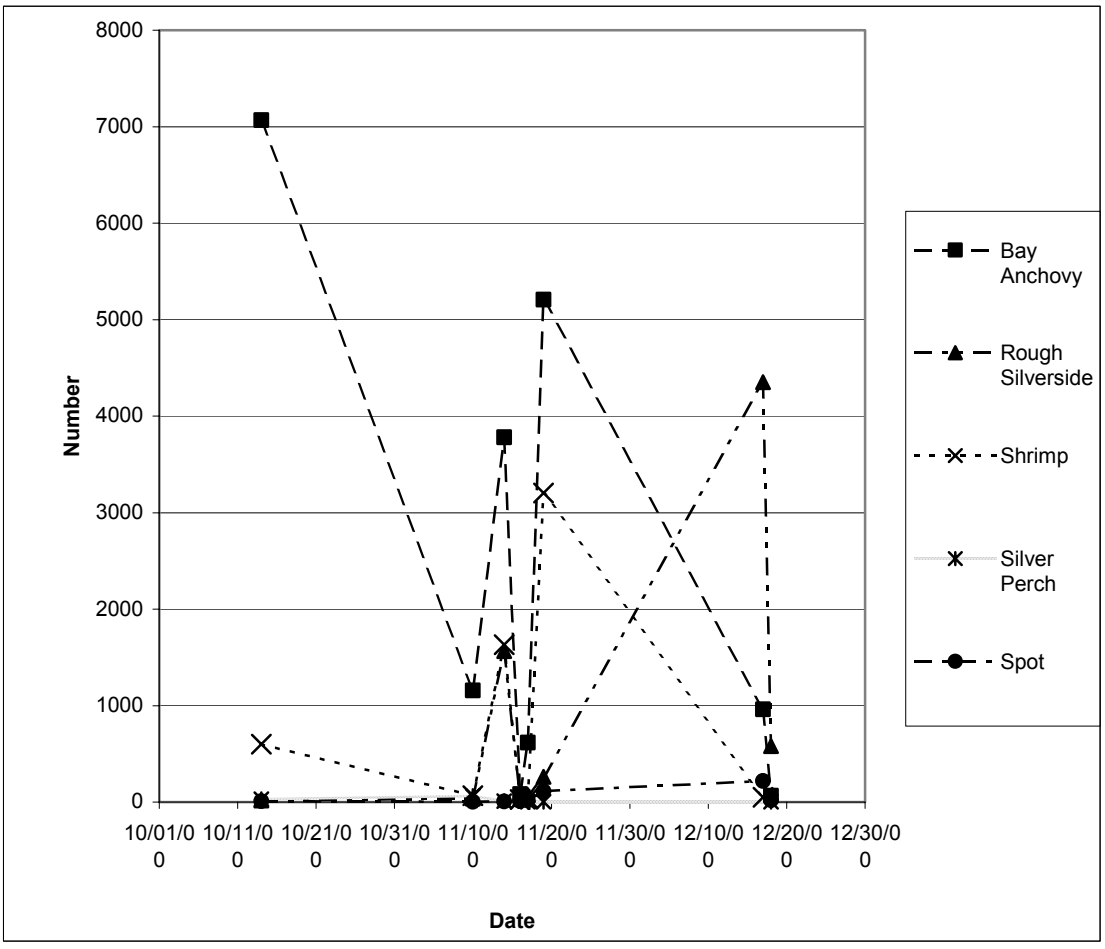

Figure 20. Numerical abundance of the six most dominate species (bay anchovy, rough silverside, white shrimp, silver perch, and spot) taken by wing net and otter trawl in Bayou Tartellon from 6 October to 18 December 2000.

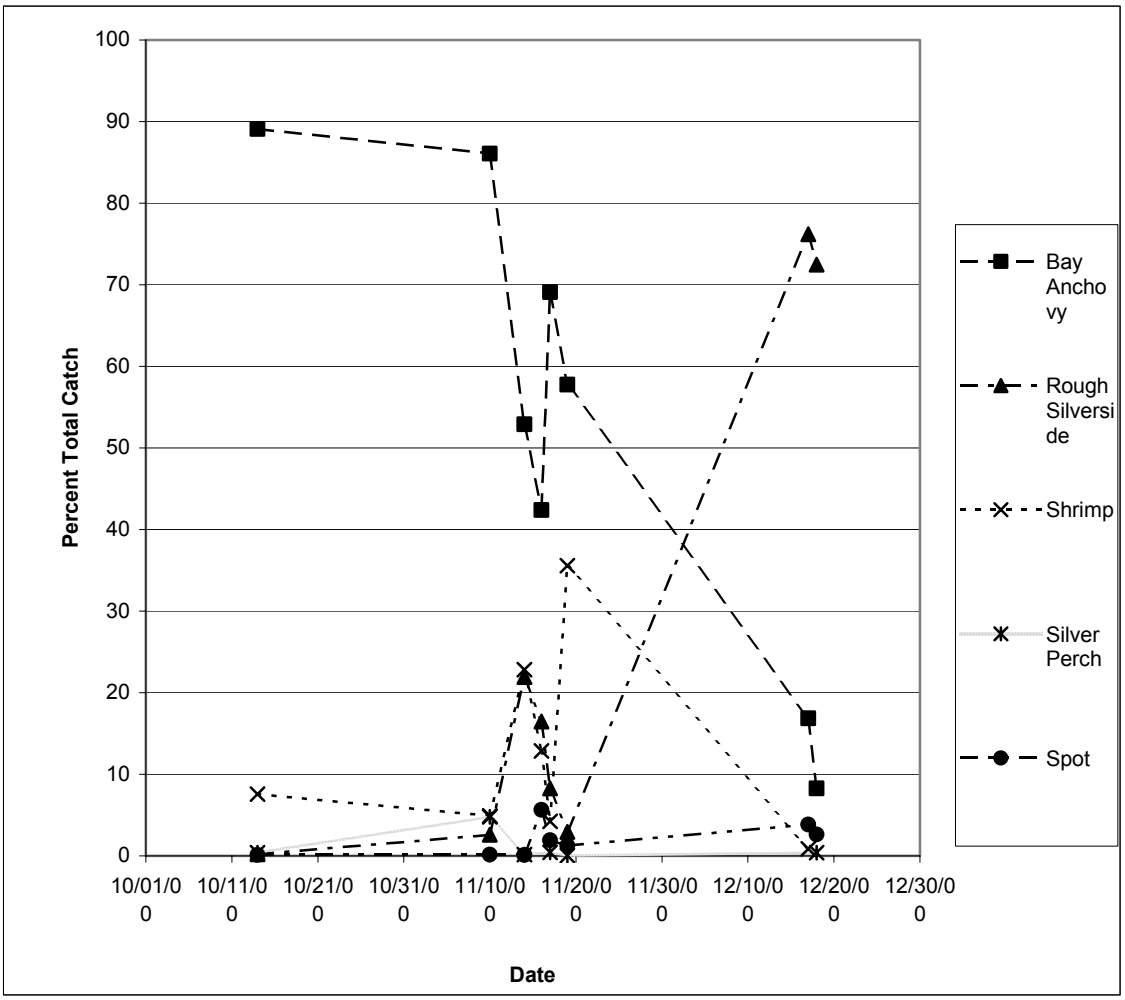

Figure 21. Percent total catch (by number) for the six most dominate species (bay anchovy, rough silverside, white shrimp, silver perch, and spot) taken by wing net and otter trawl in Bayou Tartellon from 6 October to 18 December 2000.

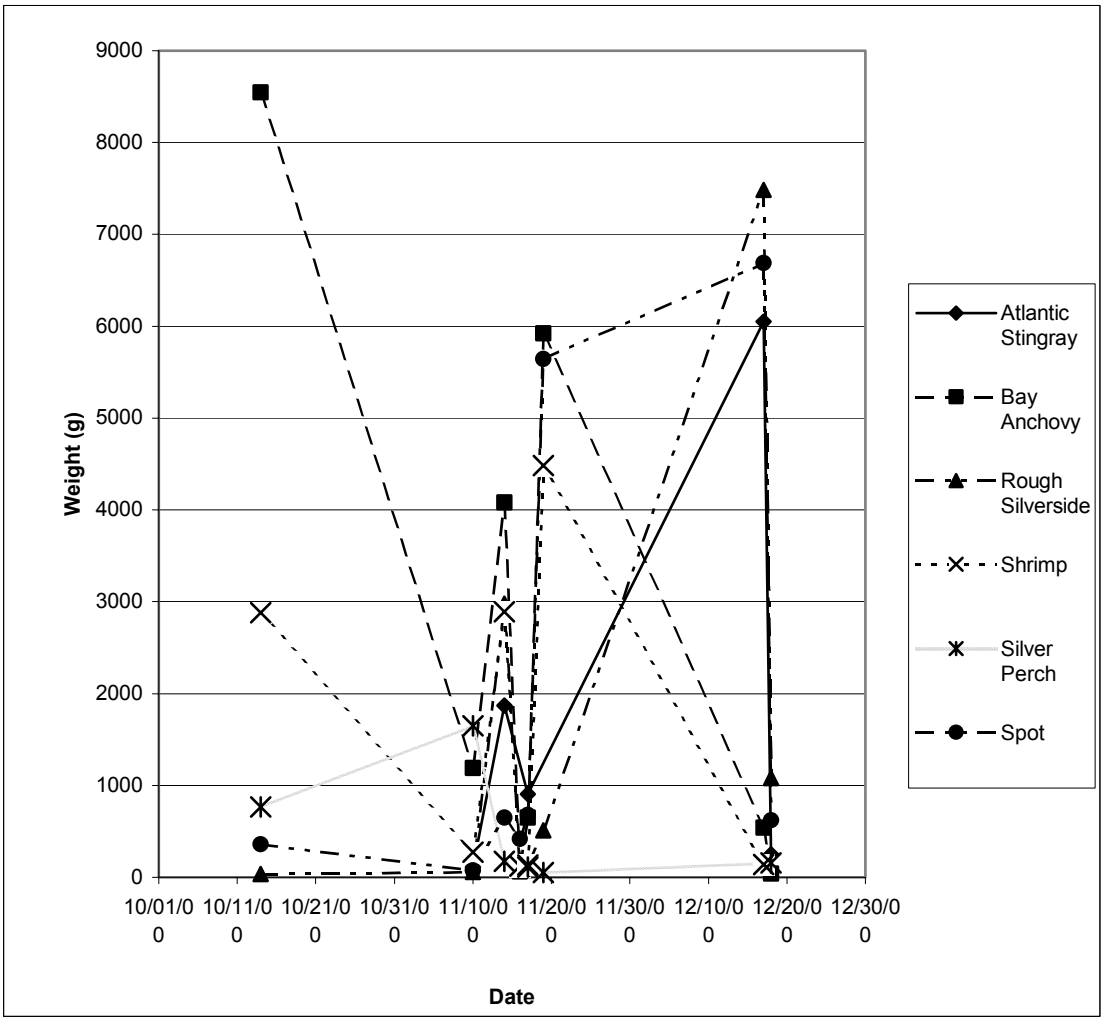

Figure 22. Biomass for six dominate species, Atlantic stingray, bay anchovy, rough silverside, white shrimp, silver perch, and spot taken by wing net and otter trawl in Bayou Tartellon from 6 October to 18 December 2000.

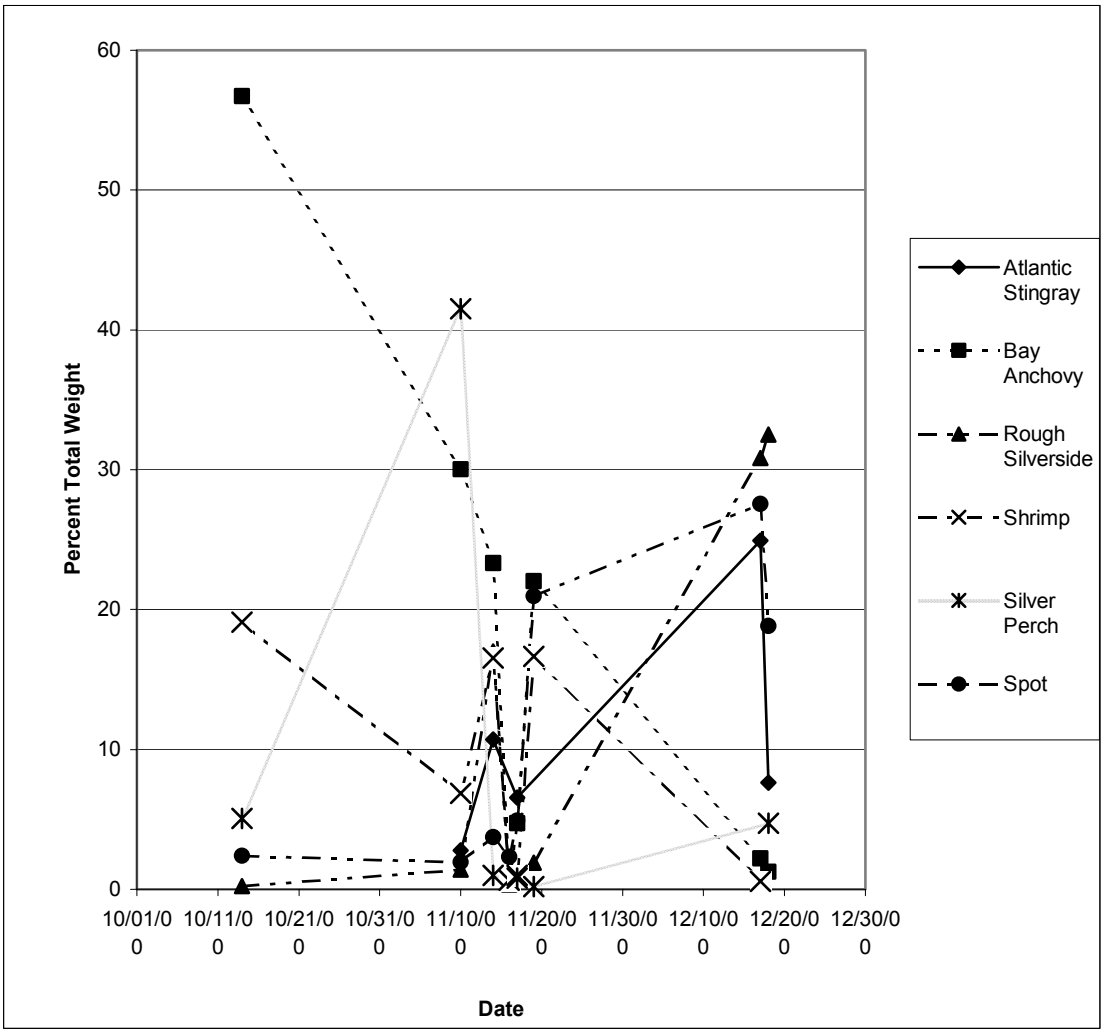

Figure 23. Percent total biomass for six dominant species (Atlantic stingray, bay anchovy, rough silverside, white shrimp, silver perch, and spot) taken by wing net and otter trawl in Bayou Tartellon from 6 October to 18 December 2000.

Table 12. Species composition statistics based on species abundances of nekton samples taken in Bayou Tartellon from October to December 2000. H'= Shannon Weaver index of biodiversity, J'= Pielou's Evenness statistic, 1-J'= Pielou's Dominance statistic

Date	Otter Trawl H'	Otter Trawl J'	Otter Trawl 1-J'	Wing Net H'	Wing Net J'	Wing Net 1-J'
10/14/00	0.41	0.37	0.63	0.12	0.09	0.91
11/10/00	0.48	0.48	0.52	0.12	0.11	0.89
11/14/00	0.86	0.70	0.30	0.47	0.37	0.63
11/16/00	0.77	0.81	0.19	0.49	0.49	0.51
11/17/00	0.78	0.75	0.25	0.40	0.38	0.62
11/19/00	0.58	0.56	0.44	0.36	0.28	0.72
12/17/00	0.55	0.49	0.51	0.23	0.23	0.77
12/18/00	0.69	0.81	0.19	0.30	0.43	0.57

3.7 Length Frequency Analysis

Length-frequency analyses of acoustic data were performed on all data for each front. Target strength data came directly from output from Biosonics' Visual Analyzer. Target strength data were converted into length using Love's (1971) equation (Equation 4). The results of the chi-square tests for equal length-frequency distributions for the total nekton community combined generated by the vertical and horizontal acoustic data showed a significant difference between the distributions of the two acoustic sets (all sampling dates combined- Table 13). The large sample size (n for horizontal 361,869, and n for vertical 27,035) resulted in a very powerful Chi-square test capable of detecting very small differences between the two distributions. Length frequencies for the two acoustic orientations appeared similar for most fronts, and for the total dataset (Figures 24-30). Although significantly different, the vertical and horizontal distributions appeared comparable, indicating that length estimates from the horizontal transducer may be as representative as vertical transducer estimates.

There are several possible explanations for the statistical difference between the two distributions. The horizontal transducer sampled a much larger volume and reduced the chance

that a few large or small targets could influence its length frequency distribution. The horizontal transducer sampled a greater portion of the tidal creek habitat, stretching from the dock to 10 m, whereas the vertical transducer was restricted to sampling a much smaller volume of water near the dock. Length frequencies from the horizontal data are therefore considered more representative of the water column and, therefore, the density estimates based on those length frequencies should be accurate.

Length-frequency distributions for the total nekton community were generated for wing net samples for each sampling date, and for all samples combined. Chi-square tests for equal distributions showed highly significant differences between the two collection methods for all comparisons (Table 14). The small sample size and mesh size for the otter trawl collections invalidated Chi-square test results (due to the presence of greater than 25% of cells with expected counts less than five), despite efforts to correct the problem by collapsing the ends of the distributions. Wing net collections in contrast sampled the upper water column, a larger portion of the entire water column, and included smaller targets due to the insertion of the 0.635 cm mesh lining. Therefore, data from the two methods were incomparable. Otter trawl data was used for species composition and diversity measures for the lower water column.

Length-frequency distributions for each wing net sample and the five-minute horizontal acoustic samples immediately adjacent to the net collections were constructed and tested with a Chi-square test for equal distributions for each sample and across all samples combined. Results from the tests for equal distributions for horizontal acoustic and wing net

sampled data were valid and significantly different, although the ends of the acoustical distributions for some dates had to be collapsed (Table 15). Small individuals (<6cm) comprised a greater percentage of the horizontal acoustic distribution for all sample dates and across all

samples (Figures 31-39). Distributions for the wing net data were influenced by the high abundance of one or two species, normally *A. mitchilli* or *M. martinica*.

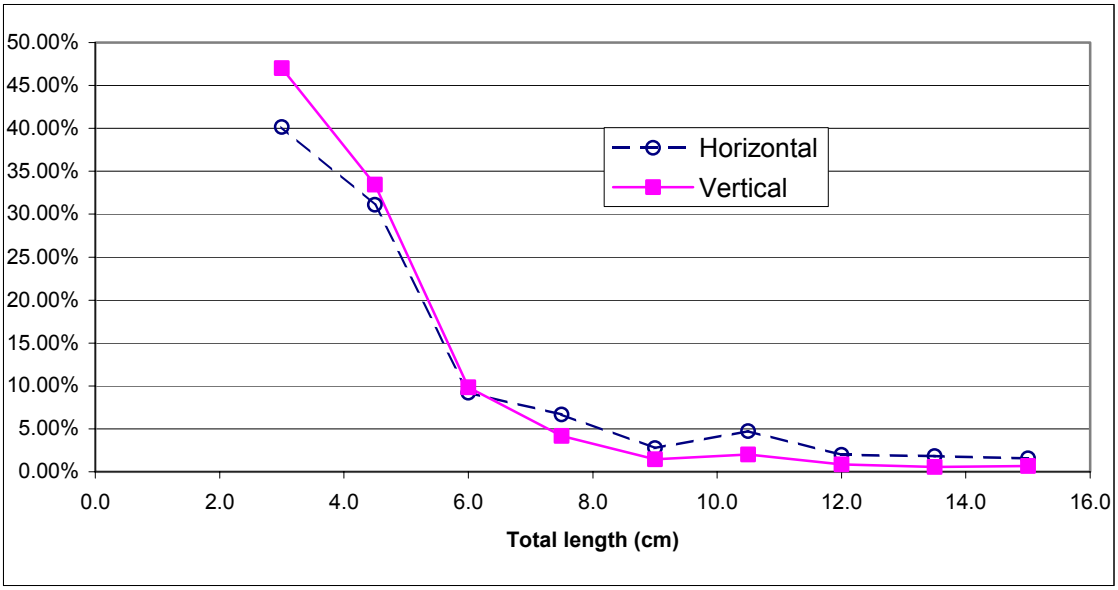

Figure 24. Length-frequency distributions (TL) generated by a horizontal and a vertical transducer in Bayou Tartellon from October 6-8, 2000.

Table 13. Results from a Chi-square test of equal length frequencies estimates from horizontal- and vertical-facing transducers taken during October 6 through December 18 in Bayou Tartellon (P<0.05 denotes significantly different).

Front	DF	Chi-Square	P
Oct 6-11	8	487.8638	<.0001
Oct 13-15	8	1448.657	<.0001
Nov 9-11	8	1225.95	<.0001
Nov 13-16	8	86.1019	<.0001
Nov 16-19	8	860.6588	<.0001
Dec 16-18	8	2375.539	<.0001
Oct 6-Dec 18	8	4356.714	<.0001

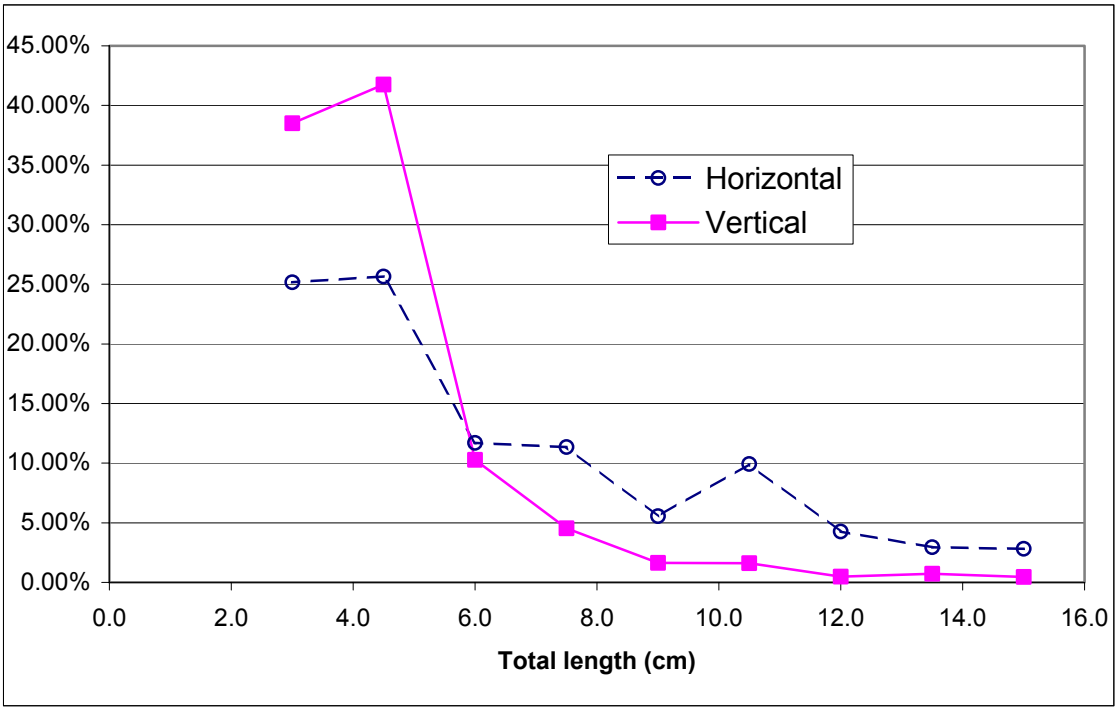

Figure 25. Length-frequency distributions (TL) generated by a horizontal and a vertical transducer in Bayou Tartellon from October 13-15, 2000.

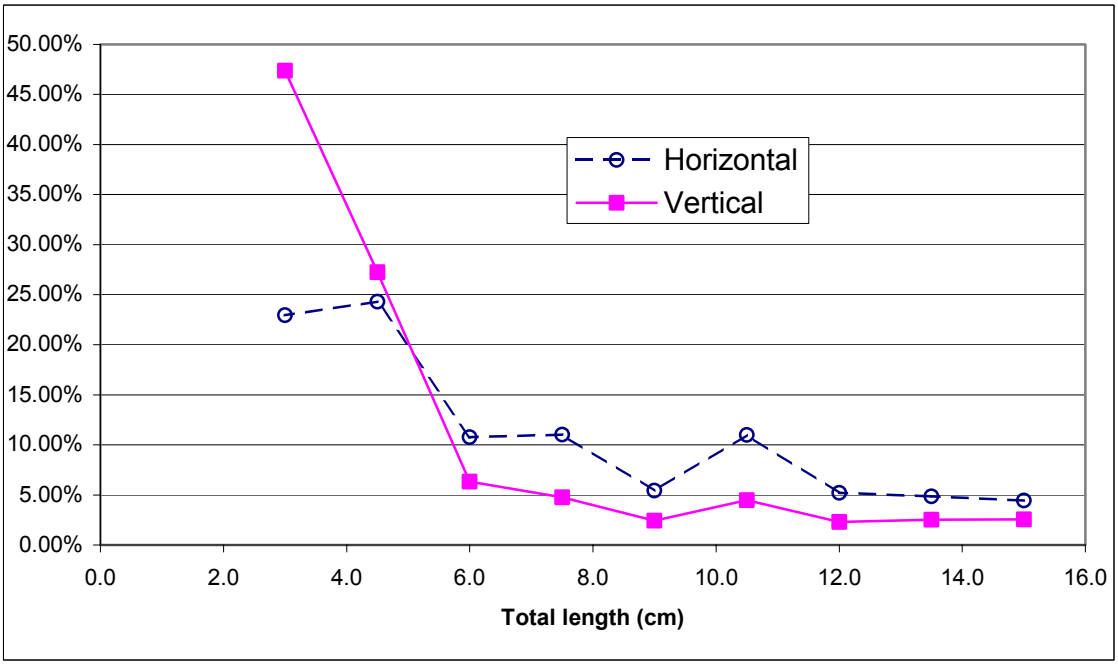

Figure 26. Length-frequency distributions (TL) generated by a horizontal and a vertical transducer in Bayou Tartellon from November 9-11, 2000.

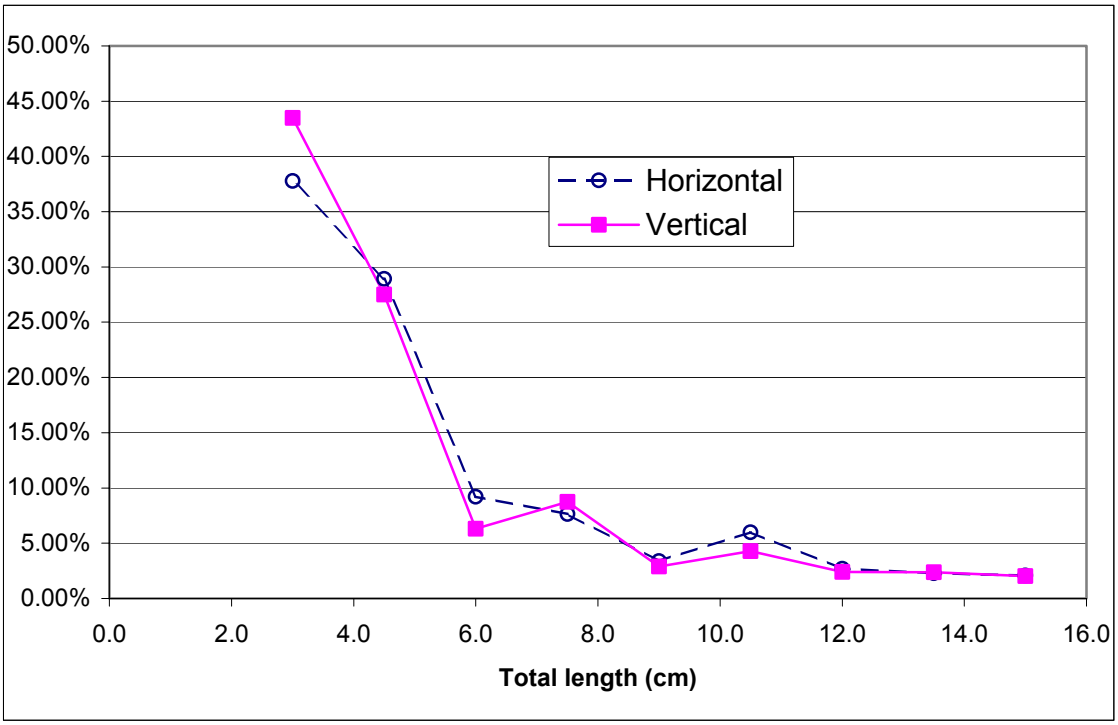

Figure 27. Length-frequency distributions (TL) generated by a horizontal and a vertical transducer in Bayou Tartellon from November 13-16, 2000.

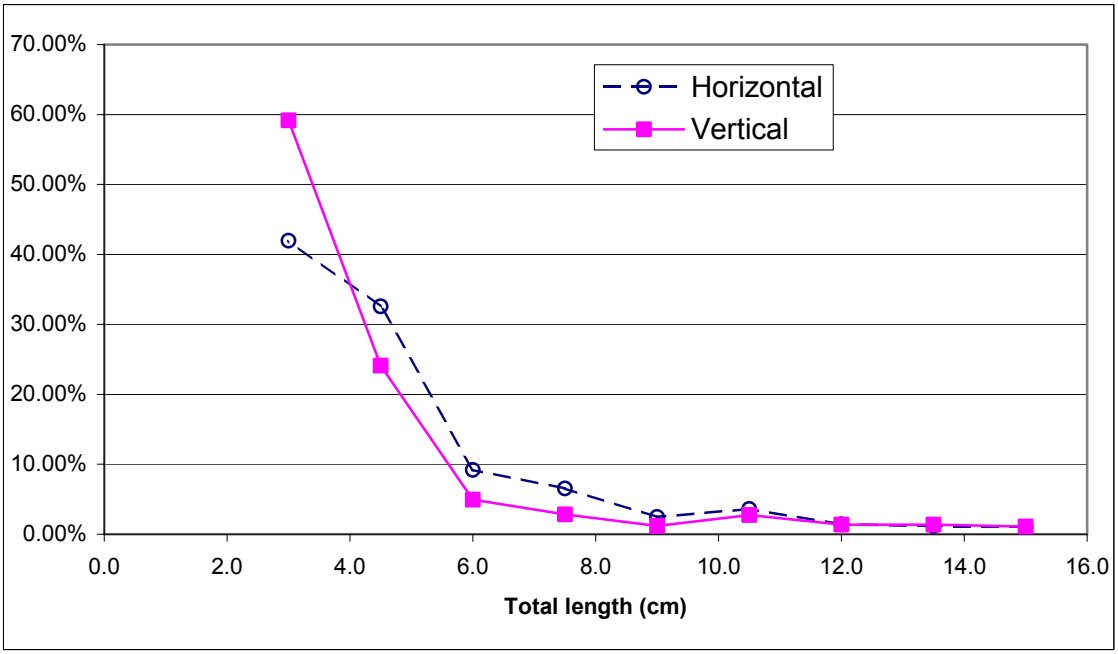

Figure 28. Length-frequency distributions generated by a vertical and an horizontal oriented transducer in Bayou Tartellon from November 16-19, 2000.

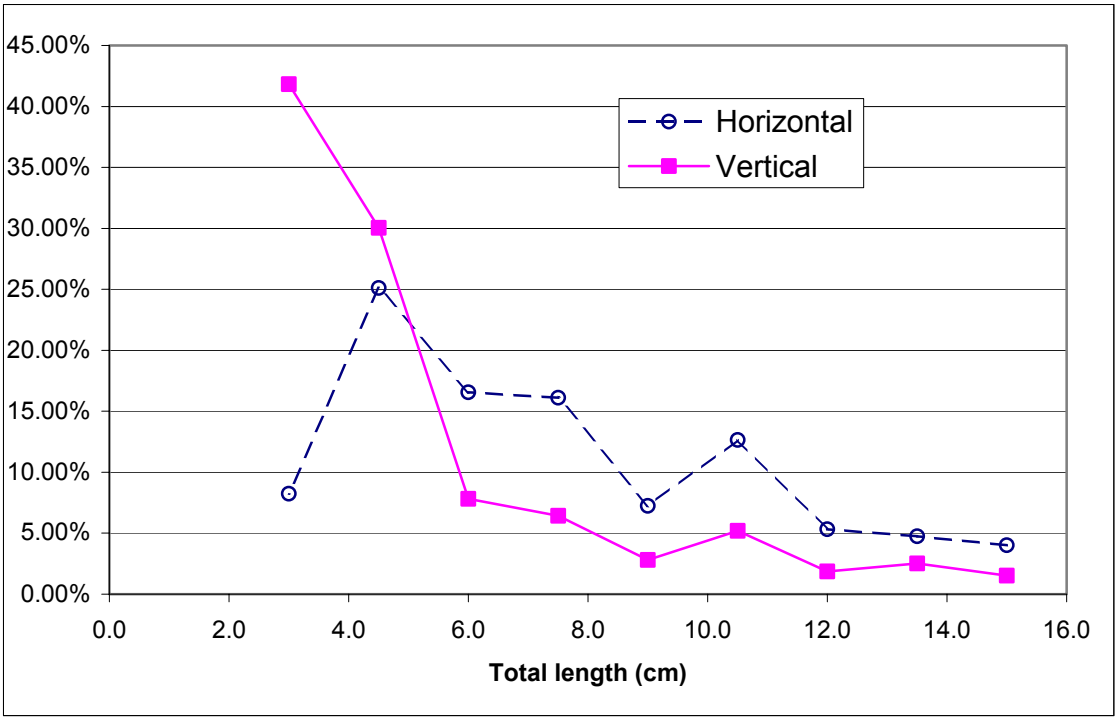

Figure 29. Length-frequency distributions generated by a vertical and a horizontal transducer in Bayou Tartellon from December 16-18, 2000.

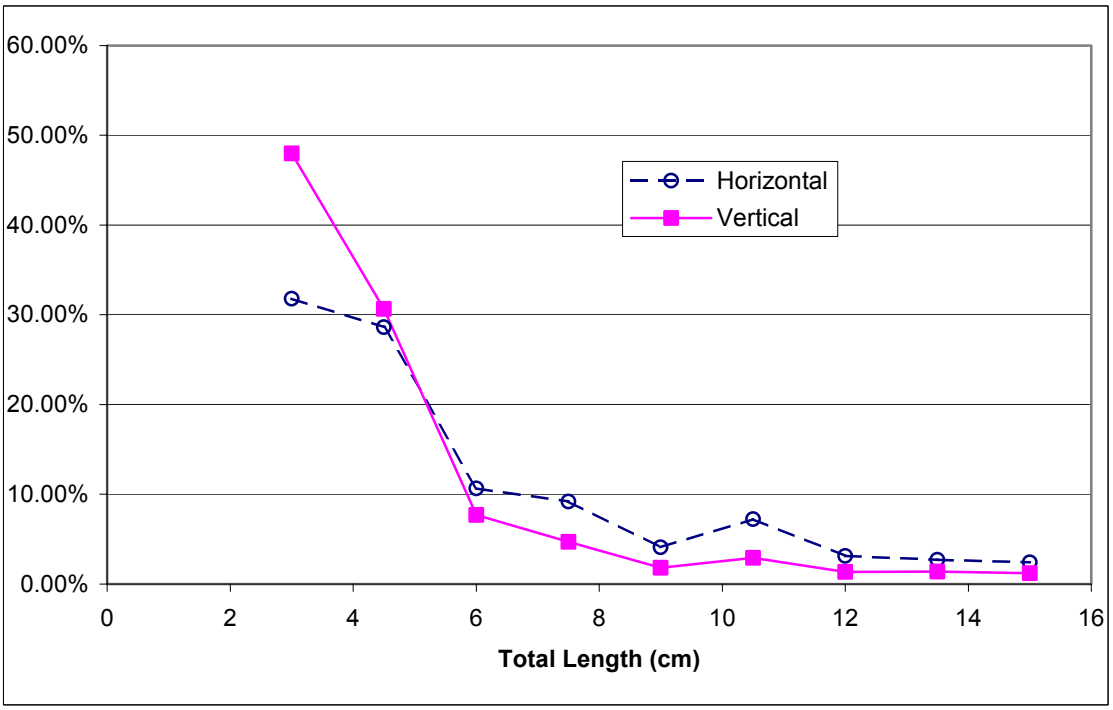

Figure 30. Length-frequency distributions generated by a vertical and a horizontal transducer in Bayou Tartellon from six sampling periods from October 6th to December 18th, 2000.

Table 14. Results of Chi-square tests for equal distributions of length frequencies for otter trawl and wing net sampled data in Bayou Tartellon in Fall 2000.

DATE	DF	Value	P
13-Oct	1	1261.161	<.0001
10-Nov	4	1162.191	<.0001
14-Nov	1	5061.368	<.0001
16-Nov	3	170.914	<.0001
17-Nov	1	813.113	<.0001
19-Nov	3	8219.043	<.0001
17-Dec	3	5565.047	<.0001
18-Dec	2	767.1836	<.0001
ALL	8	25076.68	<.0001

Table 15. Results of Chi-square tests for equal distributions of length frequencies for wing net samples and horizontal acoustic data in Bayou Tartellon in Fall 2000.

DATE	DF	Value	P
13-Oct	1	19.7112	<.0001
10-Nov	8	1252.706	<.0001
14-Nov	5	6868.22	<.0001
16-Nov	1	4.6035	0.0319
17-Nov	1	98.7944	<.0001
19-Nov	3	596.0196	<.0001
17-Dec	7	3600.725	<.0001
18-Dec	8	891.6355	<.0001
ALL	8	24188.18	<.0001

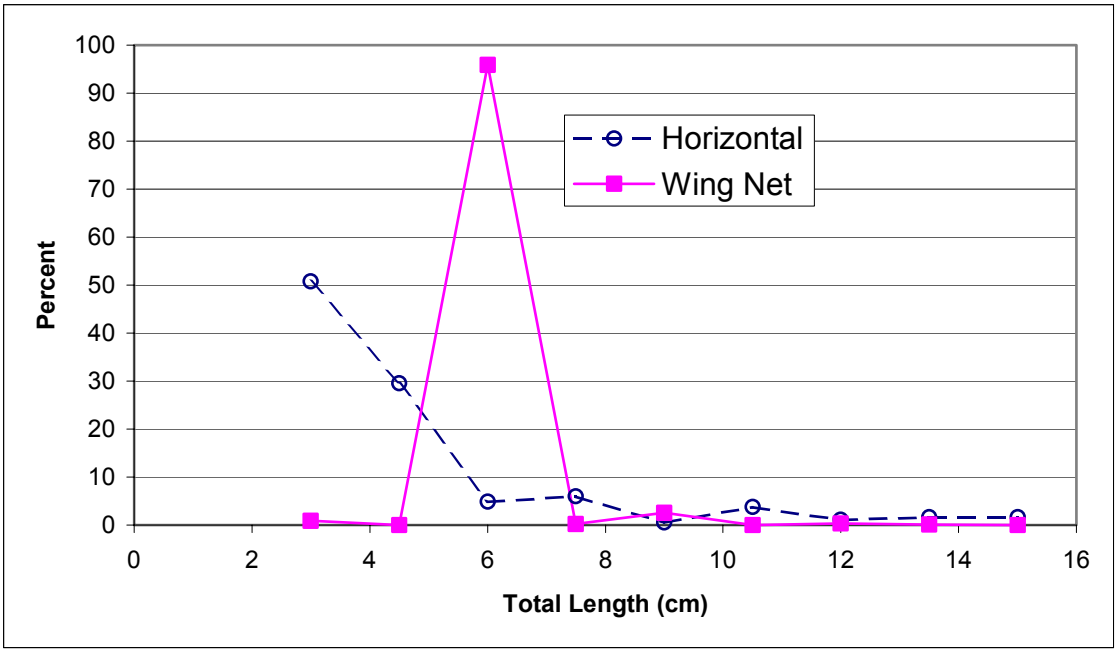

Figure 31. Length frequency distributions for data collected via wing net and horizontal hydroacoustics on 14 October 2000 in Bayou Tartellon. Horizontal data were converted to TL based on Love (1971).

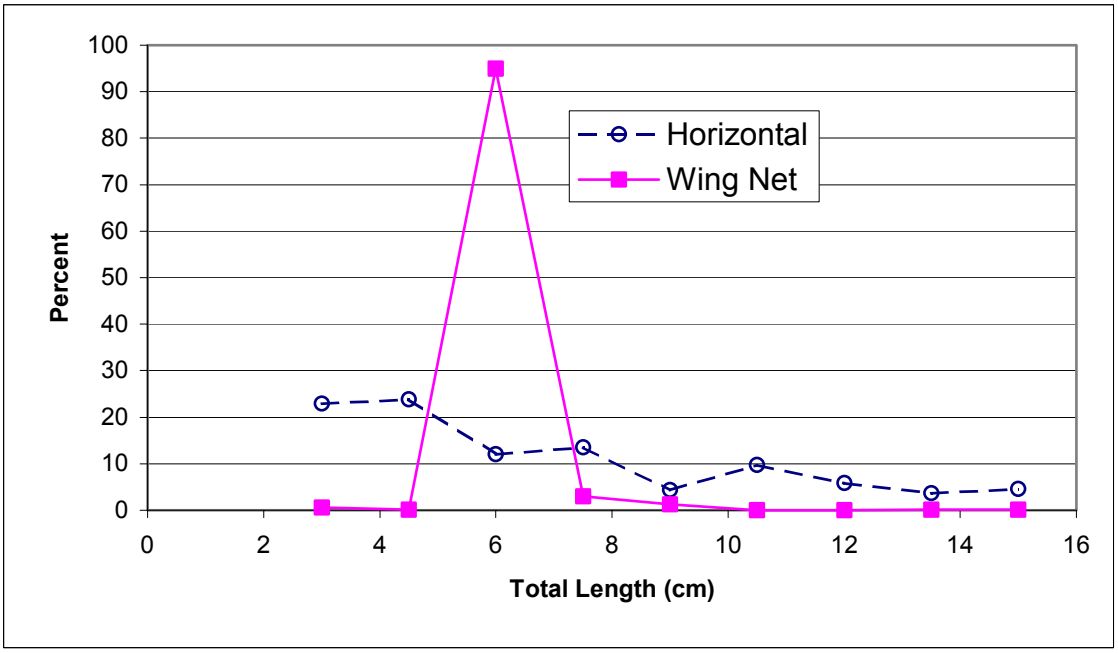

Figure 32. Length frequency distributions for data collected via wing net and horizontal hydroacoustics on 10 November 2000 in Bayou Tartellon. Horizontal data were converted to TL based on Love (1971).

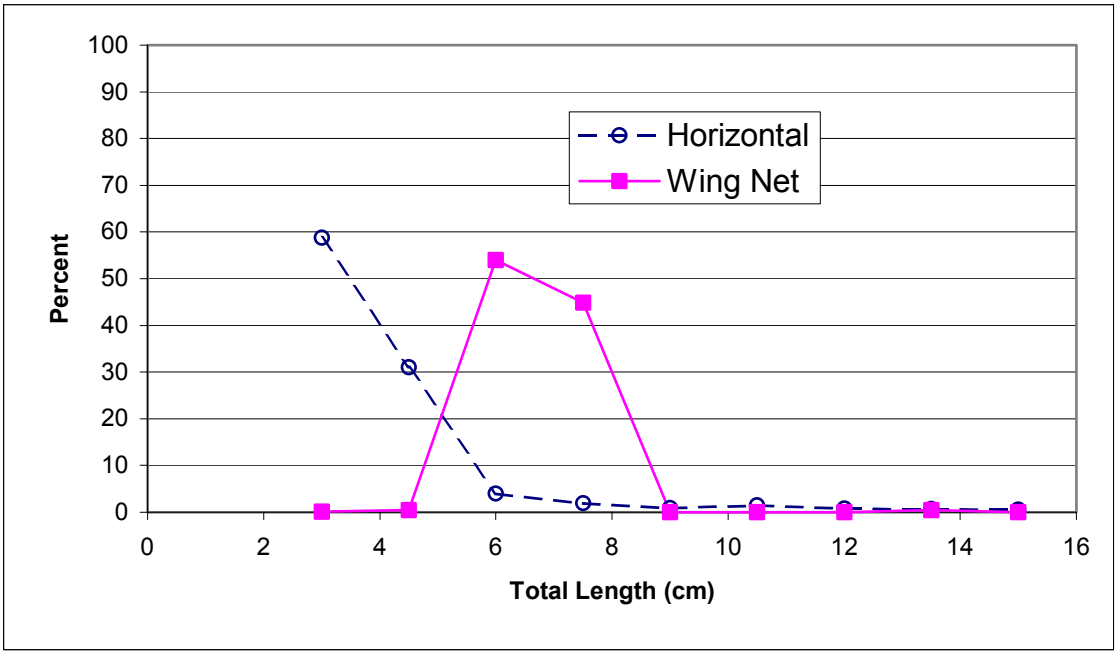

Figure 33. Length frequency distributions for data collected via wing net and horizontal hydroacoustics on 14 November 2000 in Bayou Tartellon. Horizontal data were converted to TL based on Love (1971).

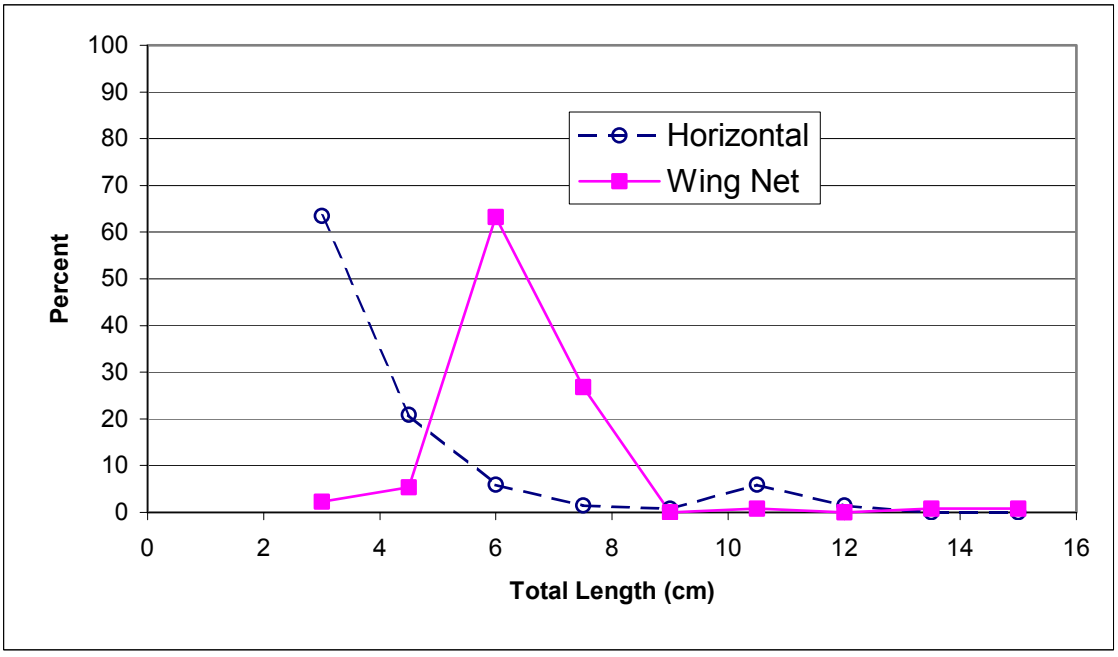

Figure 34. Length frequency distributions for data collected via wing net and horizontal hydroacoustics on 16 November 2000 in Bayou Tartellon. Horizontal data were converted to TL based on Love (1971).

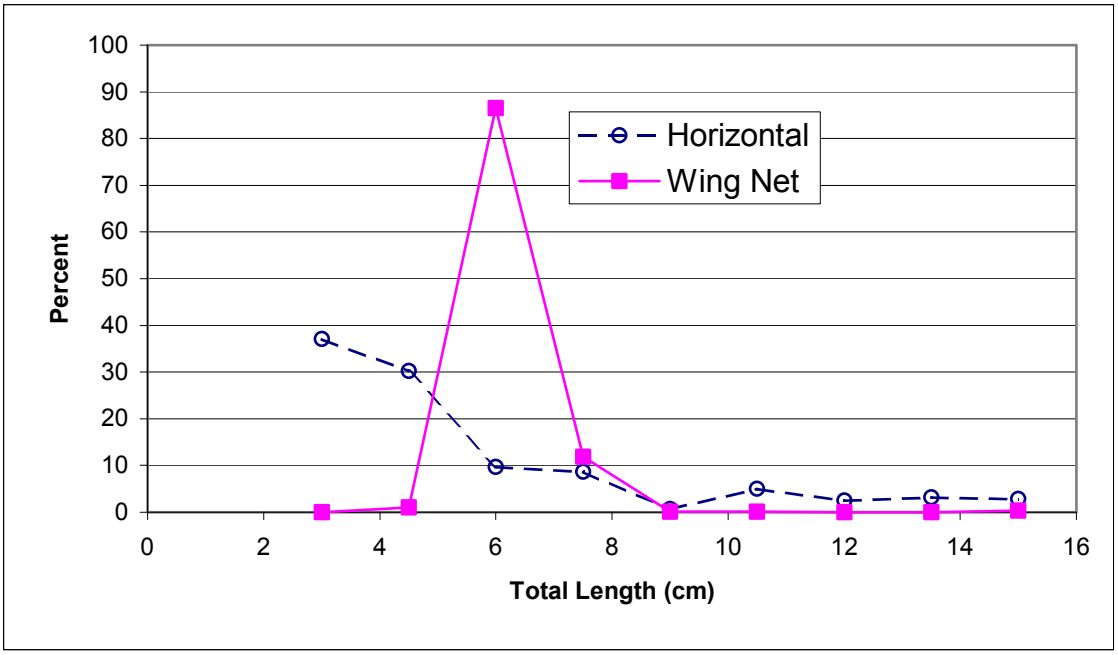

Figure 35. Length frequency distributions for data collected via wing net and horizontal hydroacoustics on 17 November 2000 in Bayou Tartellon. Horizontal data were converted to TL based on Love (1971).

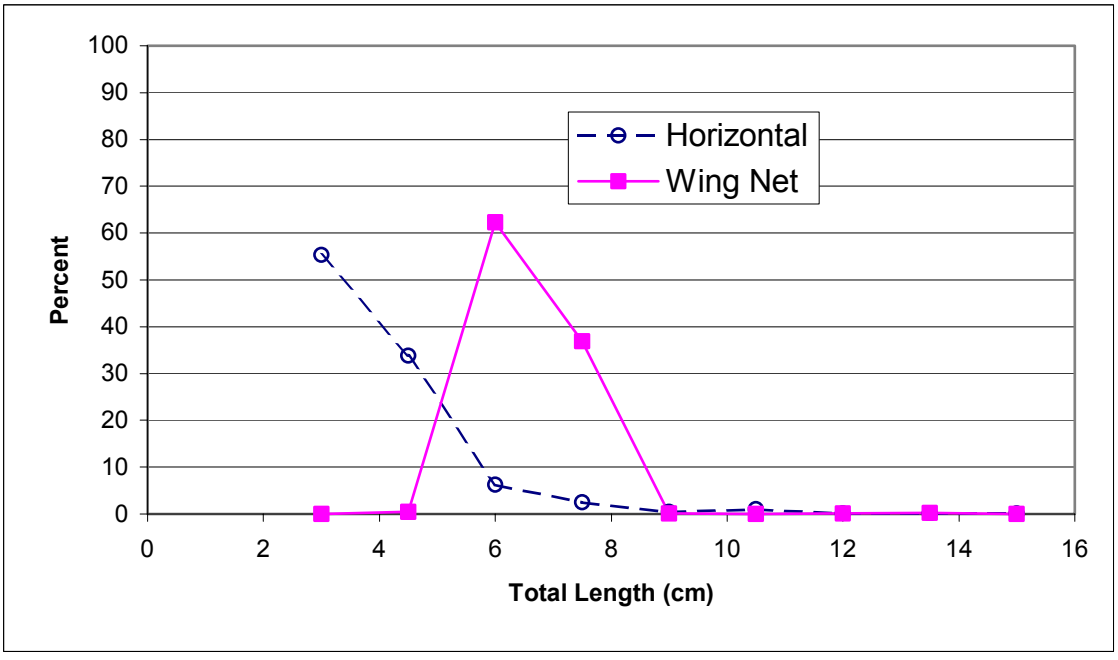

Figure 36. Length frequency distributions for data collected via wing net and horizontal hydroacoustics on 19 November 2000 in Bayou Tartellon. Horizontal data were converted to TL based on Love (1971).

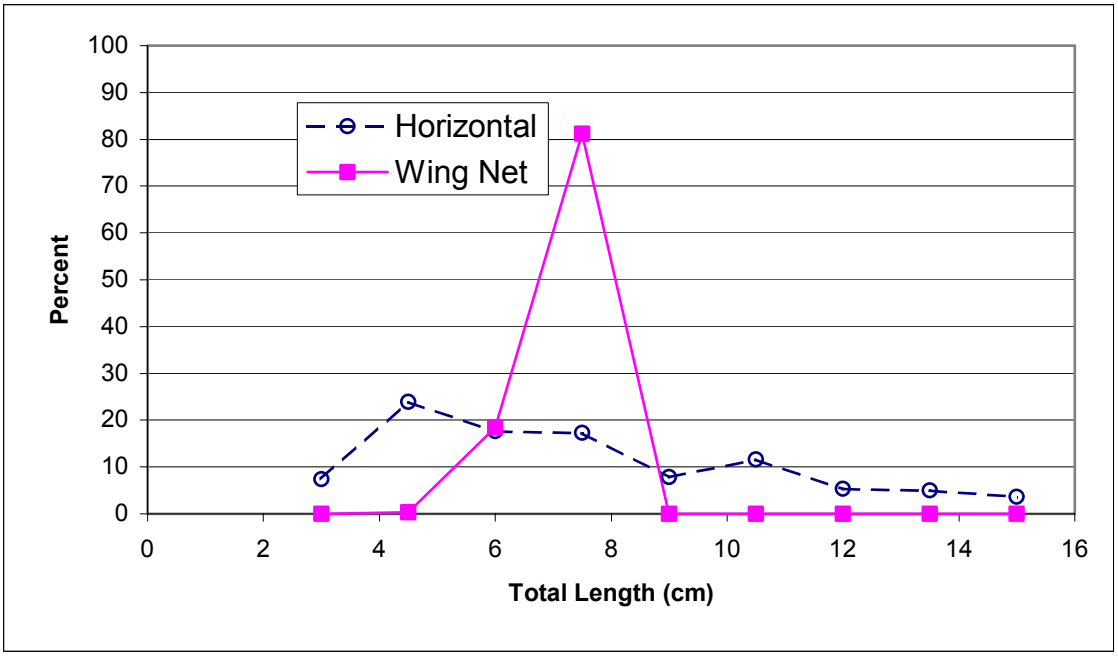

Figure 37. Length frequency distributions for data collected via wing net and horizontal hydroacoustics on 17 December 2000 in Bayou Tartellon. Horizontal data were converted to TL based on Love (1971).

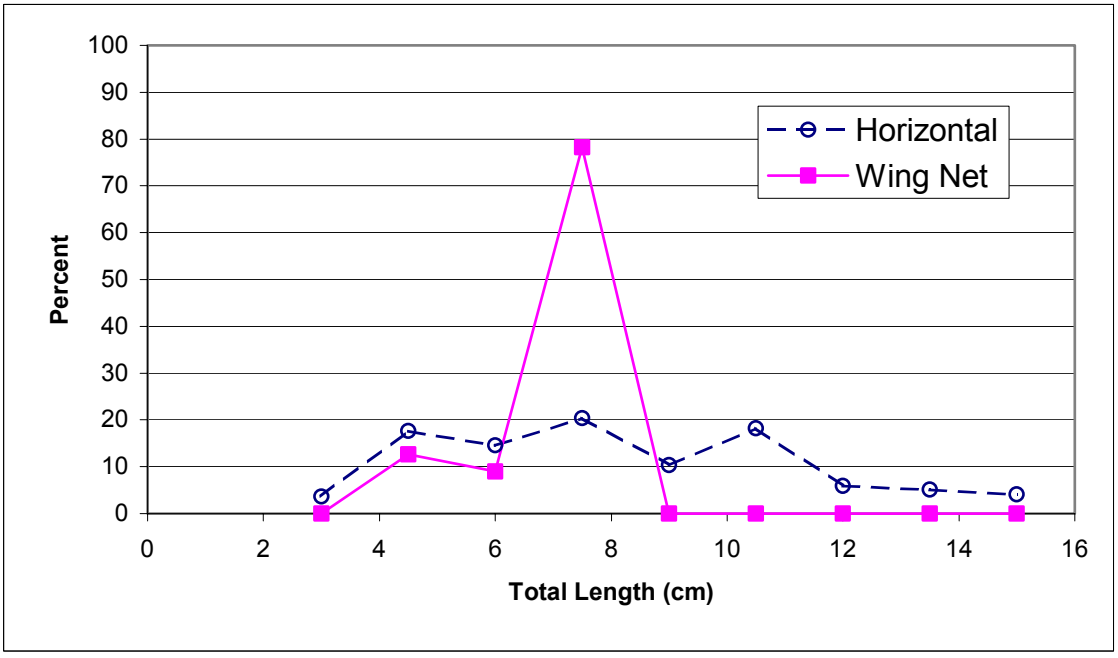

Figure 38. Length frequency distributions for data collected via wing net and horizontal hydroacoustics on 18 December 2000 in Bayou Tartellon. Horizontal data were converted to TL based on Love (1971).

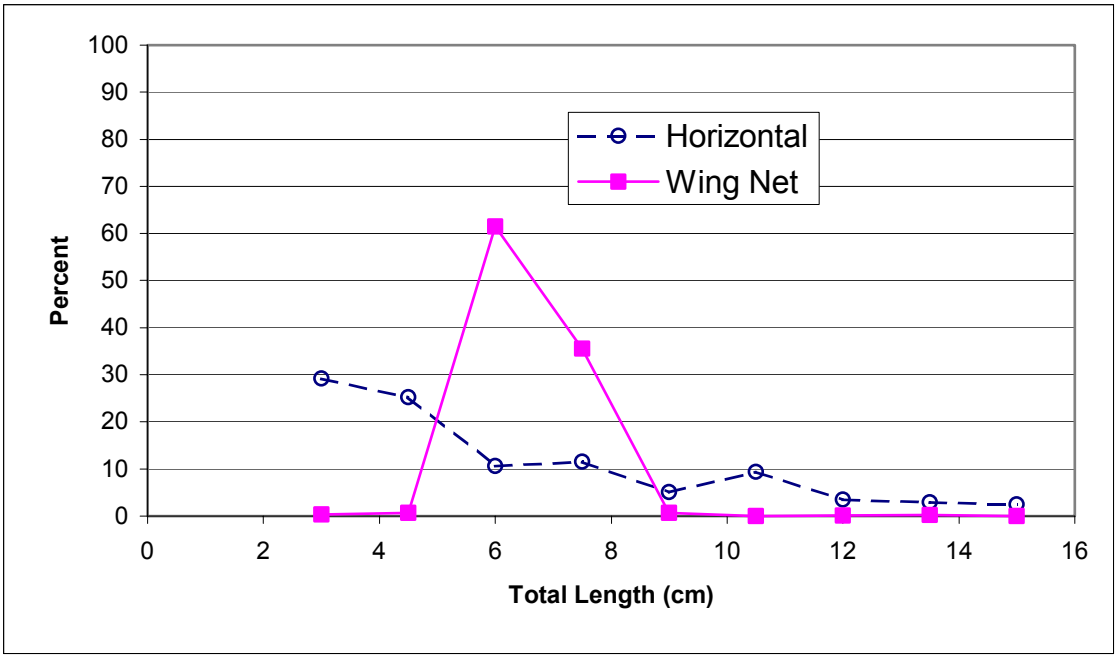

Figure 39. Length frequency distributions for data collected via wing net and horizontal hydroacoustics from 14 October to 18 December 2000 in Bayou Tartellon. Horizontal data were converted to TL based on Love (1971).

4. Discussion

4.1 Hydroacoustics

4.1.1 Deployment and Analysis

The hydroacoustic system used in this study proved effective for sampling estuarine habitat and successfully capturing the signal of frontal migration events. Equipment deployment required only minimal assistance from a second party and generally was completed in less than two hours. The bracket designed for the horizontally oriented transducer allowed for adjustment in the vertical and horizontal planes as well as adjustment to the vertical angle of the transducer. The ability to fine tune depth and vertical angle of the transducer allowed sampling out to the calibrated range (30 m from dock, or mid channel). The vertically oriented transducer was also easily deployed with assistance from a second party, and worked adequately for comparison to horizontal acoustic data, but was constrained by depth. It would prove more useful in deeper water columns.

The two BioSonics 420 kHz elliptical split-beam transducers worked well throughout the sampling season. The elliptical shape of the horizontally-oriented transducer's beam allowed for a greater volume of water to be sampled in this shallow water setting as opposed to a typical conical beam. When mounted with the widest axis of the beam on the horizontal plane, the vertical axis was much narrower than a traditional conical beam, reducing surface and bottom interference. The much larger cross sectional area and volume of water insonified by the horizontal transducer made it more useful in estimating nekton densities and biomass than the vertical transducer. Data from the vertical transducer was useful for length frequency comparison for accuracy with estimates from the horizontal transducer. In shallow estuarine

environments, horizontal orientation of transducers for estimates of density and biomass is necessary and would appear representative based on my results.

The actual sampling location did prove to be somewhat disadvantageous and affected acoustic data-analysis. Several eddies were present in front of the pier from which the horizontal transducer was mounted; these hydrologic factors complicated analysis by confounding determination of target direction of movement and velocity with the VTRACK software. I concluded that measurements of direction and velocity of targets were misrepresentative of the entire tidal creek, where most of the flow was more uniform (unidirectional) and tidally driven.

The distortion of movement direction, and velocity combined with the software's inability to detect single targets in densely packed schools (Jim Dawson- representative of Biosonics, personal communication) led me to abandon the calculation flux (i.e., transport rates) based on directional velocity of targets.

Due to these periodically high nekton densities, only data from the first ten meters of the horizontal transducer were used in the study, a conflict which was not known prior to, or during, sampling and initial data analyses (Jim Dawson- representative of Biosonics, personal communication). Data collected via the horizontal transducer beyond ten meters exhibited an artificial elevation of target strength and fewer targets (resulted in decreased density). Had this discrepancy been known prior to the initial sampling events, corrections could have been made including inputting for data collection offsets, moving the sampling site to a less congested tidal creek, or otherwise altering collection methods. This phenomenon artificial target strength elevation was documented in previous studies of densely schooling species (Rottingen, 1976; Foote, 1981; Edwards and Armstrong, 1983; MacLennan et al., 1989; MacLennan 1990; Nielsen and Lundgren, 1999; Appenzeller and Leggett, 1992; Soule, 1996).

4.1.2 Data Comparisons

Sample FE means for the collection were much higher than mean FE reported by previous investigators seen at an oil and gas platform and two artificial reefs, all three sampled in 100 meters of water in the Gulf of Mexico (Wilson et al., in press) (Figure 40).

Target strength and total nekton density data (from within ten meters) were similar to a previous study using dual beam hydroacoustics in the same area just 0.8 km downstream of the sample site in this study (Karlsson, 1999, unpublished). Karlsson's study used vertically oriented dual-beam hydroacoustics, but the results of her study are comparable to my results (Jim Dawson- Biosonics representative, personal communication). She reported mean densities of 5.54 fish/m^3 for spring, 2.43 fish/m^3 for summer and 2.15 fish/m^3 for winter. These densities are similar to the mean for this study, 2.42 fish/m^3 and minimum and maximum mean densities for all fronts, which were 1.00 fish/m^3 during 16-18 December, and 5.82 fish/m^3 during 16-19 November (Figure 41). The similarity between estimates from this study and the Karlsson study are evidence that a horizontal transducer is an effective sampling technique.

The length frequency data from the horizontal transducer and wing net samples were different among sample dates and across all samples (Table 18). Both sampling gears recorded a preponderance of small targets, but I found a larger percentage of small targets in the acoustic samples (Figures 33-41). The split-beam system is calibrated to sample targets at least –60 dB in target strength, or a fish of 1.38 cm total length (Love 1971). The nylon insert placed into the wing nets had a mesh size of 6.35 mm, smaller than the minimum of the acoustically sampled target range. The 2.75 cm square mesh of the wing net would likely allow the passage of targets of 1-2 cm TL fish, so the smaller size ranges present in the water column were likely under-represented, hence the acoustic system is sampling smaller organisms than the wing net.

In addition, acoustic reflectivity differences were expected in the nekton community. Invertebrates and other nekton without swim bladders are sampled acoustically. They are recorded as being smaller than indicated by Love's equation (1971) due to their lack of a swim bladder (Mutlu, 1999). Mutlu reported target strengths for the common jellyfish,

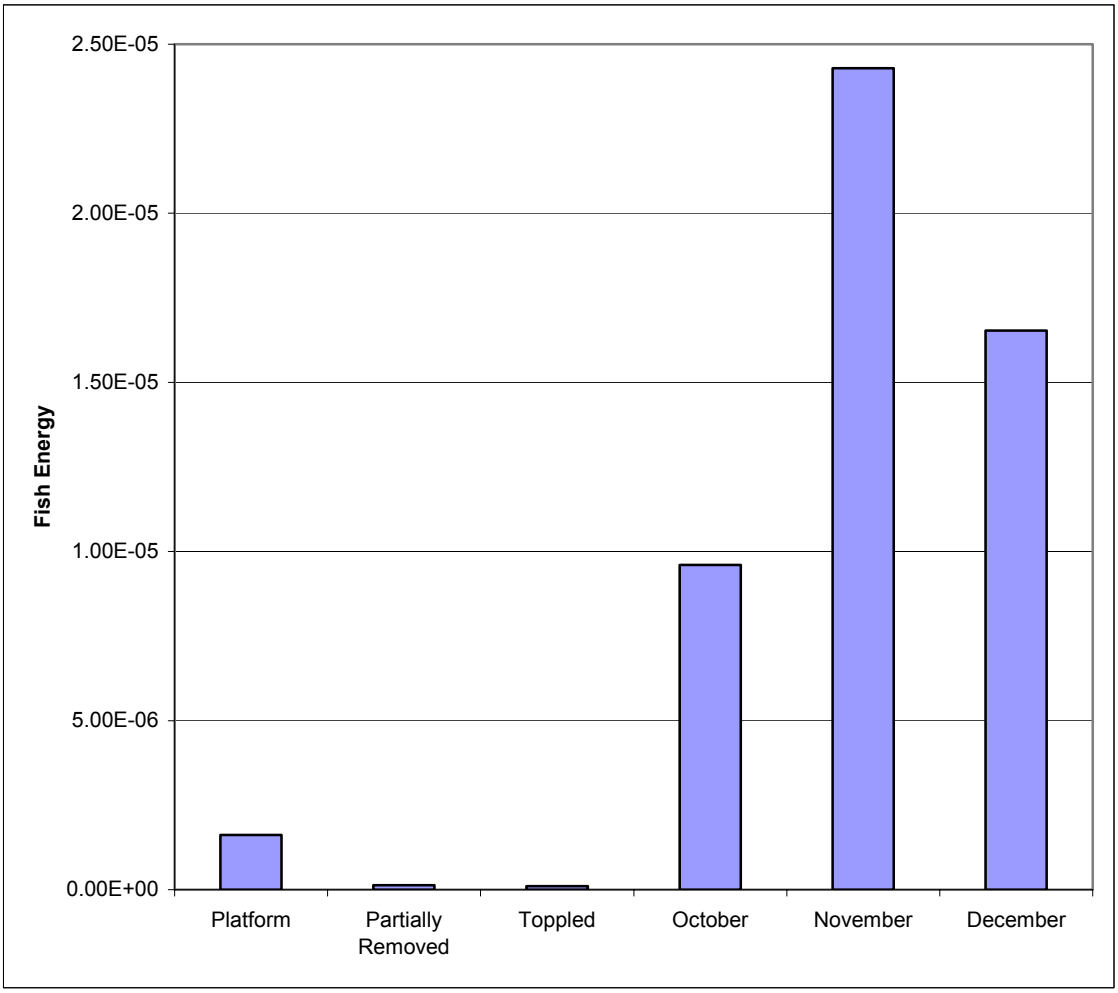

Figure 40. Comparison of hydroacoustic estimations of Fish Energy among monthly sample means for this study during October-December 2000 and estimates of three offshore environments: "Platform" denotes a standing petroleum platform; "Partially Removed" denotes a partially removed petroleum platform; "Toppled" denotes a toppled petroleum platform lying on the ocean floor. All three platforms are located near one another in the Gulf of Mexico in approximately 100 m of water (Wilson et al., 2001, in press).

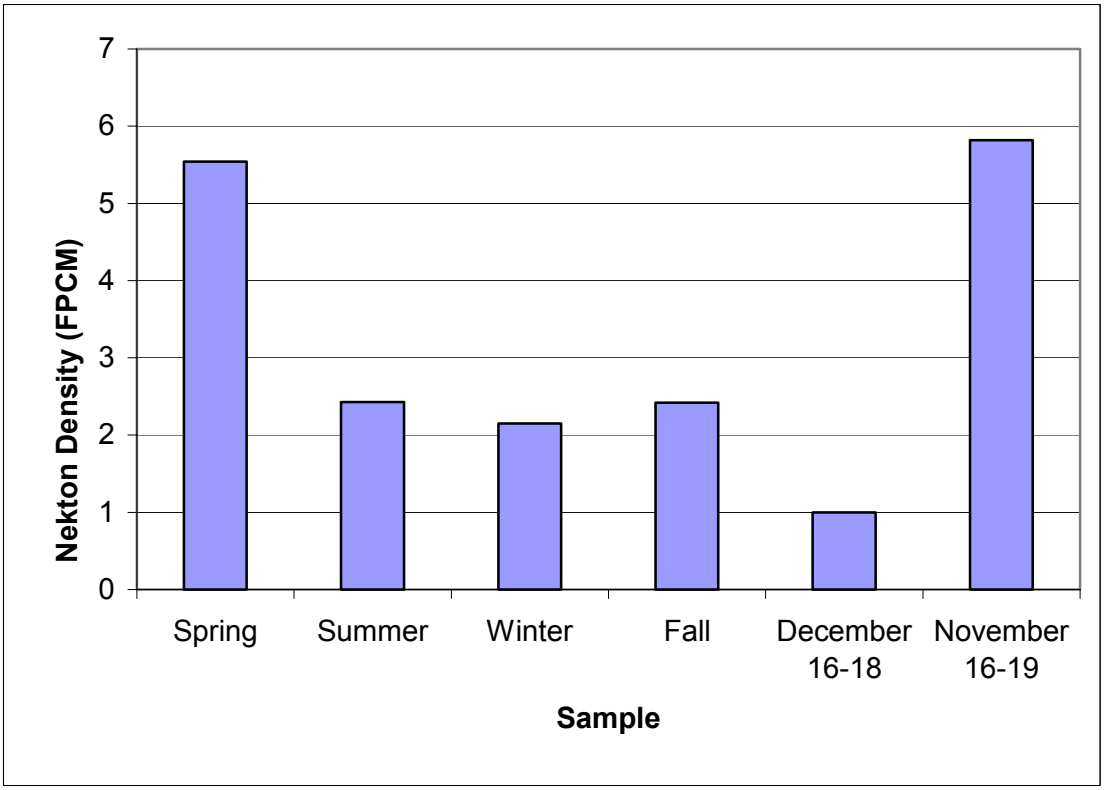

Figure 41. Comparison of nekton density estimates (FPCM) by season and minimum (December 16-18) and maximum (November 16-19) mean densities for fronts sampled during this study (Data for Spring, Summer, and Winter from Karlsson, 1999).

Aurelia arita, the same species sampled in this study, to be around –55 dB. The true diameters of the jellyfish were much larger than those estimated when using Love's equation (Equation 4), and target strength fluctuated with the contractions of the jellyfishes' umbrellas. Thus, it is possible that the shift towards smaller targets represented in the acoustic length frequency diagram could be indicative of the low total lengths assigned to shrimp and jellyfish. The low target strength values are not indicative of samples of densely packed nekton from previous studies (MacLennan et al., 1989; MacLennan, 1990; Edwards and Armstrong, 1983; Rottingen, 1976; Foote, 1981), where target strengths of nekton in densities above acceptable limits are assigned inflated target strength values. Length-frequency distributions for the hydroacoustic data compared to the wing net samples from 17-18 December (Figures 36 & 37), the only samples when white shrimp or jellyfish were not abundant, did have less of a shift toward the

smallest length classes in the acoustic data. Targets in the 6-cm size class were the most abundant acoustically on Dec 17-18, and larger size classes had higher abundances acoustically than in other samples (Figures 30-35). The horizontal transducer-based length frequencies over the 16-18 December front (Figure 38) had more, larger (>3 cm) targets than the results from other fronts and the total dataset (Figures 31-38 and 39).

The length-frequency data from the wing net, and the estimated length frequency from the vertical horizontal transducer were statistically different. The trawl and transducer data differences are explained above. The TS difference between horizontal and vertical transducers is more concerning. Since future estuarine studies will depend upon horizontal transducer-derived data for biomass estimates, it is important to have some evidence that a lateral acoustic perspective can be converted into biomass. These differences can be accounted for based on special differences in area sampled between the two transducers. The horizontal transducer sampled a much larger volume than the vertical transducer, i.e., a greater portion of the bayou's water column and, presumably, its nekton. The vertically-oriented transducer was limited to sampling only those targets moving near the dock and through a very short, narrow beam. The horizontal transducer sampled targets out to 10 meters from the dock and virtually throughout the vertical water column of the main channel. The greater number of targets from the horizontal data (>60,000 mean targets per front) decreases the influence of any one target or school of targets on the resultant length frequency distribution. However, the large sample size also increases the power of the Chi-square test to detect smaller differences between distributions. Graphically, the distributions appeared to be visually similar (Figures 24-30) for each front and for all data across fronts. Prior to the execution of future studies, investigators should redo this type of comparison with better spatial precision.

Another drawback to hydroacoustic sampling in an estuary was the inability to distinguish species. In my study, this drawback resulted in not being able to determine responses for individual species to the atmospheric changes associated with the frontal passages sampled. Thus, the data were representative of the density and biomass fluctuations of the total nekton community. Responses of individual species to the fluctuations in barometric pressure, water temperature and other atmospheric variables were not captured, creating an obscuring effect on the results of the study. Where individual species may have reacted to the atmospheric variables and ranges as hypothesized, the changes in biomass and density of the total community would not show these individual responses; thus, this discussion is centered on the individual frontal- and seasonal-level effects of frontal passages on the total nekton community of the estuary. Focusing on the effects of frontal passages on the total nekton community provided estimates of the total nekton biomass and density flux during fronts, hypothesized to be important mechanisms behind fall migrations.

4.2 Frontal Model

The major purpose of this study was to determine the effect of barometric pressure fluctuations associated with fall cold frontal passages on the total nekton community. This endeavor proved to be much more involved than initially thought. Prior to sampling I hypothesized that cold front events would have clearly distinct signals and effects on the total marsh nekton community with the barometric pressure fluctuation at the onset of a front acting as the ultimate cue for initiating the migration of the total nekton community from the marsh. This did not prove to be the case.

Barometric pressure stage (whether the barometric pressure was rising or falling) did not influence either total nekton biomass (measured as fish energy) or total nekton density (Tables 3

& 5) contrary to my hypothesis that fluctuating barometric pressure associated with frontal passage would trigger nekton emigration. Nekton density by tidal stage (whether the tidal level was rising or falling) was influenced by barometric pressure stage (Table 5) with a slightly higher mean density for rising tides associated with rising barometric pressure (+0.39 FPCM) than rising tides associated with falling barometric pressure (Figure 10). Density during falling tide was not different between barometric pressure stages, with means for both rising and falling pressure stages exceeding the 75^{th} percentile, whereas the threshold exceeded the upper limit of the 95% confidence interval for means during rising tides associated with either barometric pressure stage (Figure 10). Mean nekton densities associated with either rising or falling tidal stage being influenced by barometric pressure fluctuations were contrary to the hypothesized relationship that densities on falling tides associated with rising barometric pressures would be the highest for all levels of interaction.

Acoustical means for total nekton biomass and density in the study were influenced by tidal stage (Tables 3 & 5). Mean biomasses for rising and falling tidal levels did not appear to be different (Figure 8), although only the upper limit of the confidence interval for the mean rising tide biomass exceeded the 75^{th} percentile threshold ($7.00x10^{-5}$). Based on comparison of the means, there was no net flux of biomass over the entire course of the study, and in fact, net influx of biomass may have occurred. Mean nekton densities for rising and falling tides did appear different (Figure 10), with mean density during falling tides much higher (+1.35 FPCM). Mean falling tide density exceeded the 75^{th} percentile threshold, whereas the upper limit of the 95% confidence interval for mean rising tide density was lower than the threshold indicating a higher probability of density exceeding the threshold during a falling tide. Comparison of the means and confidence intervals indicates a net export (by number) over the course of the study. The

difference in mean biomass and nekton density for rising and falling tides indicates that the net export of fish density during the study was offset in net biomass by an influx of fewer, larger targets.

Neither of the two measures of frontal strength used in this study, i.e., Frontal Strength Index (FSI) and barometric pressure range (BPR), was significant in the frontal level model for either nekton biomass or density (Tables 3 & 5). FSI may not have been a good choice for frontal strength measurement, as it was originally calculated with wind stress as well and used in relation to sediment flux (Perez, et al. 2000). Behaviorally active nekton may very well respond to different forcing functions or, for that matter, stimuli than those that would affect purely passive sediment transport. I hypothesized that stronger fronts would illicit greater responses in nekton emigration than weaker fronts. In preliminary models, water temperature range for a frontal event proved insignificant and was removed from the final models.

Barometric pressure range did influence nekton biomass when it interacted with tidal stage (Table 4). Mean biomasses during falling tides varied little with barometric pressure range, peaking at 14.2 millibars (13-16 and 16-19 November, Figure 9). Means and confidence intervals for falling tide biomasses associated with the higher barometric pressure ranges, 13 millibars (6-8 October nonfront), 14.2 millibars (13-16 and 16-19 November), 15.4 millibars (9-11 November), and 17.5 millibars (16-18 December) did not appear to be different from mean falling tide biomasses associated with the lowest range, 3.9 millibars (13-15 October non-front), indicating no increased export of biomass with increased frontal strength. Means and confidence intervals for rising tide biomasses increased with higher barometric pressure ranges, and appeared to be different from mean rising tide biomass for the lowest BP range (13-15 October)

indicating an increased import of biomass with increased frontal strength, in direct contrast to what I hypothesized.

Mean total density during rising and falling tides, when associated with barometric pressure ranges, (Figure 12) peaked at 14.2 millibars (13-16 and 16-19 November), and declined with the higher ranges, 15.4 millibars (9-11 November) and 17.5 millibars (16-18 December) indicating that net export of total nekton decreased later in the fall, when many nekton had already left the estuary, and with stronger frontal events. Mean density during rising tide followed a similar trend, although mean density peaked at a barometric pressure range of 13 millibars (6-8 October) and then declined with higher ranges. Nekton export (based on density) occurred only during the relatively moderate fronts of 14.2 and 13 millibars, and there was no difference in nekton export between the strongest and weakest fronts. Mean falling tide densities were higher than mean rising tide densities when associated with the lower ranges (3.9 to 14.2 millibars). In contrast, mean rising tide densities were higher than mean falling tide densities when associated with the higher barometric pressure ranges (15.4 and 17.5), indicating a switch from net export of total nekton during earlier weaker fronts to net import during stronger later fronts, the trend also seen in net total biomass. An important caveat here is that water current was not measured, so import and export discussion assumes equal water flow in and out of the system.

The 13-15 October sampling period was not considered a frontal event, eliminating this sample, frontal intensity increased from October to December. This increase in frontal strength with time confounds the importance of frontal strength, as the increase could be partially due to the time of occurrence of the frontal (i.e., early or late in the fall). The importance of the barometric pressure range and tidal stage interaction is further confounded by the cumulative

emigration of nekton over the fall season. As organisms leave the estuary, the perceived subsequent impact of these ultimate factors drops as there are fewer nekton left in the estuary to respond.

4.3 Seasonal Model

Both total nekton density and fish energy (biomass) were affected by water temperature as a greater number of samples for both measurements exceed the 75th percentile thresholds at cooler temperatures. This pattern is evidence of greater movement through the tidal creek as temperatures dropped, which is influenced by sequential frontal passages as well as the gradual progression into winter (Figures 14 & 17). There appeared to be no trend in values exceeding the threshold during rising or falling tides across the range in water temperatures.

Mean total biomasses and nekton densities were significantly different among all fronts sampled (Tables 7 & 9). The 16-19 November front had the highest mean biomass and density (Figures 13 and 15). The fronts sampled varied in intensity and duration (Figure 7). Mean frontal biomass and total nekton density increased until 16-19 November and then declined thereafter with the exception of higher relative biomass than density for the 9-11 November and 16-18 December fronts. Visual analysis of mean nekton density for tidal stages during each front showed that the 9-11 November and 16-18 December fronts were the only frontal events with import of total nekton (Figure 16). The 9-11 November and 16-18 December fronts were the strongest based on barometric pressure range (15.4 and 17.5 millibars, respectively). During these two fronts, nekton may have been imported into the estuary due to an immigration response to greater pressure fluctuation or a possible net influx of water into the estuary forced by strong southerly winds just before the approach of stronger frontal passages with larger barometric

pressure ranges (Figure 7), or just after frontal passage as the estuary refills after having been significantly drained by the strong northerly winds.

Comparison of the means for total nekton biomass and density among the non-frontal 13-15 period and the frontal passages showed that, while relatively low, the October 13-15 means were not the lowest sampled for either biomass or density (Figures 13 & 15). Comparison of the means of density for tidal stages showed net export during the 13-15 October period. These comparisons suggest that in terms of mean total biomass or nekton density, or net nekton migration, frontal passages may vary little from non-frontal conditions in the fall, although comparison of conditions or events in early fall to conditions or events later in the season may be problematic.

The 16-19 November peak in nekton biomass and density in this study may be evidence of a pattern of increased biomass and density until mid-fall and decreased values thereafter. Falling tides within the 16-19 November front had the highest mean total density (7.09 FPCM, Table 10) of all tides per front, and the second highest mean total biomass (8.9572×10^{-5}, Table 8). Rising tides during the 16-19 November front had the second highest mean density for a sampled tide (4.00 FPCM), and the highest mean biomass (1.2386×10^{-4}). This front had relatively high ranges of barometric pressure (14.2 millibars), water temperature (5.8 degrees C), and a large tidal range (0.63 meters). This 16-19 November front could be considered the most important emigration event in this study. Luo and Brandt (1993) reported a similar trend in nekton biomass for Chesapeake Bay with a net emigration peaking in November with high densities on both tides. The discrepancy between net export of nekton and net import of biomass during the front could be explained by differential tidal use of the creek by species. Roundtree and Able (1992) reported that nekton catches during falling tides in a New Jersey tidal creek

were dominated by nonresident larvae and juveniles during emigrational events, where as seine samples taken along the banks of the creek (during the same events) were dominated by resident species. Subrahmanyam and Drake (1975) reported the late fall abundance of adults of some species only on high tides. These species were believed to be carnivores moving in to feed and included *Leiostomus xanthurus,* which was also taken in this study. In a study of eight falling tides in a South Carolina tidal creek sampled with a channel net in January, Shenker and Dean (1979) reported low catches of adults (<1 kg per species) in all but one sample when *Menidia menidia*, the Atlantic silverside, was abundant (3.77 kg).

The trend of net import of total nekton biomass and export of total nekton density is likely misrepresentative of seasonal emigration during frontal events. The larger targets present during the incoming tides accounting for the higher biomass could be nekton moving with the incoming tide to forage. These targets could be moving up into the marsh to feed, lingering and feeding at the mouths of distributaries as the tide falls and then perhaps moving out along the bottom or along the edges of the tidal creek where they are not ensonified by the acoustic beam. This evasion during falling tides, along with the greater abundance of small targets on an outgoing tide, would account for the greater total biomass during incoming tides. Since no samples with the otter trawl, which would sample these species, at least along the bottom of the channel, were conducted during rising tides this phenomenon is speculative.

I conclude that it is unlikely that any single parameter associated with frontal events independently elicits a response from the total nekton community of the estuary which is contrary to the seasonal hypothesis that barometric pressure changes were the most important factor keying the estuarine emigration of the total nekton community. Most likely, multiple factors are operating simultaneously or accumulatively. For example, the succession of fronts

over the fall season may have a compounding affect, where the effects of each front are in some way additive. As the season progresses, fronts become stronger and more frequent, eventually occurring approximately every three to six days. My assumption for the seasonal hypothesis that the initial fronts of the fall would induce the largest migrational response in the nekton community is also contradicted. The November 16-19 sampled front was the third within a week, preceded by two fronts very similar in strength. The strength of the November 16-19 front, coupled with the occurrence of two strong fronts immediately preceding the event, may have been enough to effectively trigger a large-scale ubiquitous response in the nekton resulting in the highest FE and FPCM values. The strength of an individual front does not seem to be important in eliciting a synchronized response in nekton, contrary to that proposed in the seasonal hypothesis. The strongest front determined by barometric pressure (17.5 millibars, 16-18 December) did not produce the largest nekton response, but it was also measured latest in the season. The accumulative effects of frequency, strength and relative date of occurrence within the fall season of fronts may be more important than individual frontal strength alone, contrary to my seasonal hypothesis that frontal strength alone would determine nekton response.

If the increased intensity and frequency of fronts were the only factor determining the level of nekton response, then fronts later in the season would have the highest density and biomass signals. As the nekton community's response to fronts increases, more nekton emigrate from the estuary to deeper coastal water, leaving fewer animals remaining within the estuary. As such, fronts have both a positive and negative effect on subsequent events, cumulatively increasing nekton response, but decreasing the amount of estuarine nekton left to respond. This is seen in the highest biomasses and densities in the 16-19 November sample and lower values

during the 16-18 December samples. As the fall season progresses, the estuary becomes less thermally hospitable resulting in lower abundances and biomasses.

Species diversity varied widely over the sampling season. Diversity for the wing net data ranged from a low of 0.12 on October 14 to a high of H'=0.49 on November 16. The diversity of the wing net samples was strongly influenced by the numerical dominance of one species, bay anchovy, from early October through mid-November and the subsequent dominance of rough silverside in December (Figures 20-23). Diversity within otter trawl samples was typically higher and exhibited a smaller range (0.41 on October 14 to 0.86 on November 14). The November 16 sample captured a transport event of jellyfish into the estuary. Predation by jellyfish, avoidance of jellyfish by smaller nekton, or decreased sampling efficiency of the nets due to clogging by jellyfish, or combinations of these factors could explain the decrease in abundance (dominance) of shrimp, anchovy and other species emigrating.

Numerical dominance of *A. mitchilli* in this study is supported in numerous other estuarine works (Condrey et al, 1995; Salinas et al 1986; Shenker and Dean, 1979; Zimmerman and Minello, 1984;). An extensive study by Rogers and Herke (1985) showed very similar trends in abundance during falling tides for white shrimp, speckled trout, Atlantic croaker, and bay anchovy during the same time periods.

The specific responses to barometric pressure, water temperature, salinity and dissolved oxygen of each non-resident species determine when that species will react and emigrate from the estuary. Species most sensitive to frontal passage, and those reacting earliest in the season to frontal passage, are most likely being triggered by the change in barometric pressure as the ultimate factor. Barometric pressure changes associated with frontal passages are immediately felt by nekton, especially those with relatively large swim bladders or other air bodies. The more

demersal species may not have to move as far or as rapidly to escape or remedy the effects of barometric pressure change. Species responding earliest may also have the lowest tolerances for water temperature changes, and the front-induced, brief decreases from the normal high average temperature may be enough to drive these early emigrants from the estuary. Water temperature tolerances would affect a greater portion of the nekton population, including demersal species, although the major thermal impacts occur later in the fall season and some thermal insulation in deeper water may lessen the effect. In a shallow, well-mixed estuary, however, this thermal insulation would be minimal, leaving even the relatively deep-dwelling species affected.

As indicated above, water temperature is likely the ultimate factor in the response of the later emigrating species. While frontal passages do bring brief periods of cooler temperatures, in Louisiana's estuaries average water temperatures remain warm, above 20 °C, well into November. Not until mid-November do water temperatures cool significantly and remain so. Demersal species may respond to a larger degree to temperature decreases than sudden barometric pressure fluctuations.

The physical process of "frontal forcing" on the estuarine hydrology whereby wind-driven currents may magnify or negate tidal ranges before, during and after a front may also play a role in nekton migrations. Rogers et al. (1993) hypothesized that such frontal forcing could play a substantial role in the estuarine immigration of Louisiana postlarval brown shrimp in the spring. Larval brown shrimp could rise up in the water column to be carried into the estuary by currents driven by the dominant onshore winds and "coastal setup" after a front. Likewise, the increased tidal ranges and currents associated with fall frontal passages could effectively flush out nekton which are at the end of their estuarine lifecycle and wash in those nekton in the

estuarine recruitment phase of their life histories. This physical effect of frontal passages on the estuarine hydrology is likely to be important.

Just as no one environmental factor affects nekton uniformly, it is unlikely that the nekton react totally independent of one another. Removal of prey species from an area will lead to the ultimate displacement of predator species from the area as well. This can clearly be seen in the sequential emigration first of prey species such as white shrimp and the subsequent emigration of predator species, i.e., spot, speckled trout and Atlantic stingray, from the estuary. This staggered emigration with some overlap would explain the peak in total abundance and biomass seen in the November 16-18 sample. The second half of prey migration coupled with the first half of predator migration may have occurred about this time and could have resulted in higher total abundances. Larger, acoustically derived, average total lengths estimates in the later samples supports this pattern as well. Roundtree and Able (1992) reported fall abundances of predator species fluctuated with abundances of prey species.

Lifecycle strategies among similar species based on environmental tolerances and competitive abilities can be used to explain timing of emigration. Subrahmanyam and Coultas (1980) point to staggered seasonal occurrence of species as adaptive strategies to avoid competition for limiting resources among similar species. Bay anchovy, one of the earlier responding species, and rough silverside, one of the dominant species in later samples, share plankton food resources within the estuary. Bay anchovy were far more dominant in abundance and most likely in biomass as well. Juvenile rough silversides, by postponing emigration (a behavior necessitating greater environmental tolerances) until later in the season (after most anchovy have left the estuary) could enjoy a foraging advantage in that they could dominate the planktivore community without the competition of a dominant potential rival. Likewise, spot

appeared to remain in the estuary longer than silver perch, a similar species, which may enable juvenile spot to grow for a brief period with lowered levels of competition.

4.4 Future Research

The integration of hydroacoustics with global-positioning systems (GPS), side-scan sonar, environmental, meteorological and biological data can generate three-dimensional GIS models relating nekton abundance, biomass and species composition to physical variables and processes such as bottom type, water quality, seasonal cycles, and environmental/physical forcing functions. The compilation of all these data will provide detailed models, by which habitats and relevant processes can be scaled in quantitative terms. The success and relative ease of deploying acoustic equipment experienced in this study suggest that hydroacoustic systems can be adaptable to many situations within coastal wetlands. The addition of a pontoon boat specially designed for acoustic sampling in shallow waters will allow for greater estuarine mobility across a wide range of habitats, while providing a stable, yet mobile, work platform.

In the field, continuous consideration should be paid to the quality of hydroacoustic data. The periodic problems associated with sampling densely packed schooling species seen in this study and reported elsewhere clearly indicates that sampling parameters such as TS threshold and analysis offsets must be periodicially adjusted. Data from this study, in which data sampled from farther than ten meters away appear to break acoustic sampling assumptions, would be an ideal test bed for preliminary work to see if parameter adjustments could be retrofitted until processed results from data from beyond ten meters becomes similar to the valid data from within ten meters.

Several alterations in sampling methods could be made to produce better results, such as, extending the sampling over the fall season to capture more fronts and periods between fronts,

and sampling more completely with appropriate net mesh sizes and over both tidal stages and day and night. In the future, a more appropriate site selection to escape the confounding effects of shoreline eddies and heavy boat traffic would possibly reduce or remove problems incurred during this study.

4.5 Conclusions

Hydroacoustics were successfully deployed with minimal effort in the study. The combination of hydroacoustics and biological sampling provided detailed information on total nekton biomass and density and limited species composition data for morning outgoing tides with much less effort than a study based solely on biological sampling would have required. The deployment system engineered for this study can be easily adapted to any number of settings and has since been successfully used mounted to the specially designed pontoon boat.

Validity and quality of hydroacoustic data pose a more significant challenge in estuarine settings. As seen in this study and many others, sampling systems with high schooling densities can produce inaccurate total densities, biomasses and target strengths, if not first properly amended with appropriate parameter offsets. This shortcoming along with the lack of species-specific capabilities in diverse ecosystems are the most substantial obstacles in the course of the practical use of hydroacoustics. As of yet, for the high density interference, it is necessary to consult with a seasoned hydroacoustician familiar with the limitations and physics of hydroacoustics. Preliminary work, like that completed in this study, can be processed repeatedly until the necessary offsets can be calculated to negate or reduce the effects of high schooling densities. Data from this study are ideal for future research directed at calculating such offsets, as the effects of high schooling densities were only periodically apparent in data sampled beyond ten meters. Data sampled from within ten meters did not reflect these high density effects,

typically manifested in higher average target strength, fewer individual targets, and lower densities. Different offsets and parameters can be entered in the data analysis until data from beyond ten meters are similar to data from within ten meters, and effects of dense schooling have been effectively removed.

Because hydroacoustics are not able to distinguish nekton by species, the data collected were analyzed to determine the effects of fall frontal passages on the total nekton community of the estuary. Individual species responses were not distinguished by the hydroacoustics, and effects on the total nekton biomass and density fluctuations did not represent the responses of individual species. The effects of fall cold front passages are significant when viewed as single events, with those effects felt differently by each species. On a seasonal scale, many other parameters are involved as ultimate factors in the migrations of the nekton community. Some species, including white shrimp, are affected by the initial fronts, most likely responding to the fluctuations in barometric pressure brought on by a front, since temperature effects are not great or long lasting early in the season. Other species react later in the fall, most likely responding to lower average water temperatures. Frontal passages in the late fall may decrease water temperatures enough and over a long period to trigger these later migrating species. Sequential emigration from the estuary by species is an important biological interaction. Species with similar life histories and trophic behaviors, such as bay anchovy and rough silversides, appeared to emigrate at staggered times in the fall which would allow rough silverside to remain in the estuary longer to take advantage of planktonic resources without competition from the earlier migrating numerical and biomass dominant. Probably the most significant biological interaction is the sequential movements of prey and predator. Prey species, including shrimp and anchovy, emigrated from the estuary in October through mid-November. Increased catches of predator

species, including Atlantic stingrays, spot and speckled trout, were seen in December, evidence of estuarine emigration from a now poorer food environment or following a food source. This sequence was reflected in a shift in dominance towards demersal species, as most upper water column species had previously exited.

The overall trends for total nekton biomass and abundance followed neither the frontally dominated or "bleeding off" models previously suggested. Total biomass and abundance peaked in mid-November giving a bell shaped model for the nekton community in the fall. The overlap of sequential migrations noted above combined with the cumulative effects of sequential fronts appears to have contributed to the mid-season peak. The initial fall fronts induced small, locally important reactions, but produced increased tidal pass abundances in the most sensitive species. As fronts strengthened and became more frequent, and mean water temperatures dropped, the effects of fronts grew, reaching the peak in mid-November. Strong fronts continued throughout the fall, becoming even more frequent, while their effects on the nekton community declined. This can be explained by a reduction in the nekton population caused by the emigrations triggered by previous fronts. In essence, nekton had been removed from the response pool by earlier fronts, leaving fewer individuals to respond, even though the fronts of the late fall were intense enough to trigger large nekton responses. This phenomenon can be likened to diminishing returns in an endothermic chemical reaction, in which the reaction of a reactant increases with introduced heat. Initial additions of heat create small reactions, until enough heat is added to induce a full-scale reaction. Subsequent additions of heat, however large, will produce only small reactions due to the spent nature of the reactants. The resultant bell-shaped curve for total nekton biomass and abundance over the fall may be indicative of a combination of the proposed frontally driven and continually bleeding off of species from the estuary.

References

Appenzeller, A.R., Leggett, W.C. 1992. Bias in hydroacoustic estimates of fish abundance due to acoustic shadowing: evidence from day night surveys of vertically migrating fish. Canadian Journal of Fisheries and Aquatic Sciences vol. 49, pp 2179-2189

Barange, M., Hampton. I., Soule, M. Empirical determination of in situ target strengths of three loosely aggregated pelagic fish species. ICES Journal of Marine Science, 53 1996

Biosonics, Inc. 1998. Guide to using the DT series, version 2.1.Biosonics, Inc, Seattle, Washington.

Boesch, Donald F, and Turner, R. E. 1984. Dependence of fishery species on salt marshes: the role of food and refuge. Estuaries vol. 7, no. 4a, 460-468

Bozeman, E.L. Jr. and J.M. Dean. 1980. The abundance of estuarine larval and juvenile fish in a South Carolina intertidal creek. *Estuaries* 3(2):89-97.

Burczynski, J.J. and R.L. Johnson. 1986. Application of dual-beam acoustic survey techniques to limnetic populations of juvenile sockeye salmon (*Onchorynchus nerka*). *Can. J. Fish. Aquat. Sci* 43:1776-1788.

Burwen, Deborah L., Fleischman, Steven J. 1998. Evaluation of side-aspect target strength and pulse width as potential hydroacoustic discriminators of fish species in rivers. Canadian Journal of Fisheries and Aquatic Science vol. 55 no. 11 1998.

Condrey, R., P. Kemp, J. Visser, J. Gosselink, D. Lindstedt, E. Melancon, G. Peterson, and B. Thompson. 1995. Status, trends, and probable causes of change in living resources in the Barataria and Terrebonne National Estuary Program, Thibodaux, Louisiana, 434 pp.

Dunbar, J.B. 1990. *Land Loss Rates, Report 2, Louisiana Chenier Plain*, U.S. Army Corps of Engineers, Waterways Experiment Station, Vicksburg, Miss., COE Tech Report GL-90-2.

Edwards, J.I., Armstrong, F. 1983. Measurements of the target strengths of live herring and mackerel. FAO Fish. Rep. 300, 69-70

Foote, K.G. 1981. Evidence for the influence of fish behavior on echo energy. In Soumala, J.B., ed. Meeting on Hydroacoustical Methods for the Estimation of Marine Fish Populations, 25-29 June 1979, vol. 2. Cambridge, Ma. Charles Stock Draper Laboratory Inc, pp 201-28

Gauthier, S., Boisclair, D., Legendre, P. 1997. Evaluation of a variable angle scanning method to estimate relative abundance and distribution of fish using a single-beam echosounder in shallow lakes. Journal of Fish Biology 1997 vol. 50 pp208-221

Gunter, Gordon. 1967. Some relationships of estuaries to the fishes of the Gulf of Mexico. In G.H. Lauff (ed), Estuaries. American Association for the Advancement of Science publication 83, Washington, DC

Haralabous, J., Geogakakaros, S. Artificial neural networks as a tool for species identification of fish schools. ICES Journal of Marine Science, 53 1996

Herke, W. H., E. E. Knudsen, Knudsen, P.A., and B. D. Rogers. 1992. Effects of semi-impoundment of Louisiana marsh on fish and crustacean nursery use and export. N. Amer. J. Fish. Manage. 12:151-160.

Herke, W. H., Rogers, B.D., Wright, K. L., and W. H Bradshaw. 1996. Postlarval *Penaeus aztecus* and *P. setiferus* transport into, and distribution within adjacent weired and un-weired ponds. Wetlands vol. 16, No. 2, June pp 197-207

Houde, E.D. and E.S. Rutherford. 1993. Recent Trends in Estuarine Fisheries: Predictions of Fish Production and Yield. *Estuaries* 16:161-176.

Hoss, Donald E., Thayer, Gordon W. 1993. The importance of habitat to the early life history of estuarine dependent fishes. AFS symposium 14:147-158

Hsu, S.A. 1988. Coastal Meteorology. San Diego: Academic Press

Hsu, S. A. and B. W. Blanchard. 1993. Meteorological Forcing on Louisiana Wetlands. Coastal Zone 1993 Proceedings, 8th Symposium on Coastal and Ocean Management July 19-23, New Orleans, La.

Johannesson, K.A., Mitson, R.B. 1983. Fisheries acoustics. A practical manual for aquatic biomass estimation. FAO Fish. Tech. Pap., (240):249 p.

Karlsson, Kris. 1999. The use of dual-beam hydroacoustics to estimate biomass flux through a tidal creek in Port Fourchon, Louisiana. M. Sc. Thesis. Louisiana State University and Agricultural and Mechanical College. Baton Rouge, Louisiana.

Knudsen, E.E., Rogers, B.D., Paille, R.F., Herke, W.H. and J.P. Geaghan. 1996. Juvenile white shrimp growth, mortality, and emigration in weired and unweired Louisiana marsh ponds. N. Amer. J. Fish. Manage. 16(3): 640-652.

Love, R.H. 1971. Dorsal aspect target strength on individual fish at any aspect. Journal of the Acoustic Society of America, vol. 49, no 3., pp 816-823

Luo, J. and S. B. Brandt. 1993. Bay Anchovy, *Anchoa mitchilli* production and consumption in mid-Chesapeake Bay based on a bioenergetics model and acoustic measures of fish abundance. Marine Ecology Progress Series vol. 98: 223-236

MacLennan, D.N. 1990. Acoustical measurement of fish abundance. Journal of the Acoustic Society of America. vol. 87, 1-15

MacLennan, D. N., Hollingworth, C.E. and Armstrong, F. 1989. Target strength and the tilt angle distribution of caged fish. Proceedings of the Institute of Acoustics I.O.A vol. 11, 11-21

MacLennan, D. N.. Menz, A., Interpolation of in situ target strength data. ICES Journal of Marine Science 53, 1996

McKenzie, L.S. III, M. Wascom, W. R. Keithly, R. E. Emmer, W. H. Hudwall, M. T. C. Johnson, F. Niami, and B. A. Touchet. 1995. Land use and socioeconomic status and trends in Barataria and Terrebonne Estuarine System. BTNEP publication # 23, BTNEP, Thibodaux, La, 184 pages plus appendix

Minello, T. J. and J. W. Webb, Jr. 1997. Use of natural and created *Spartina alterniflora* salt marshes by fisheries species and other aquatic fauna in Galveston Bay, Texas, USA. Marine Ecological Progress Series vol. 151 Mar 1977

Minello, T.J. and Zimmerman, R.J. 1983. Fish predation on juvenile brown shrimp, *Penaeus aztecus*, Ives: the effect of simulated *Spartina* structure on predation rates. *J. Exp. Mar. Biol. and Ecol.* 72:211-231.

Mitsch, W.J., J.G. Gosselink. 1993. Wetlands. Van Nostrand Reinhold, New York.

Mutlu, E. Target strength of the common jellyfish (Aurelia arita): a preliminary experimental study with a dual-beam acoustic system. ICES Journal of Marine Science 53, 1996

Nielsen, J.R., Lundgren, B. 1999. Hydroacoustic ex situ target strength measurements on juvenile cod (Gadus morhua L.). ICES Journal of Marine Science, vol. 56: 627-639, 1999

Pavlov, D.S., Sadnovskii, R.V., Kostin, V.V., Lupardin, A.I. 2000. Experimental study of young fish distribution and behavior under combined influence of baro-, photo-, and thermo-gradients. Journal of Fish Biology, vol. 57, 69-81

Perez, B.C., J.W. Day, L.J. Rouse, R.F. Shaw, and M. Wang. 2000. Influence of Atchafalaya Bay discharge and winter frontal passage on suspended sediment concentration and flux in Fourleague Bay, Louisiana. Estuarine Coastal and Shelf Science (2000) vol. 50 pp 271-290

Raynie, R. C., and S. K. Beasley 2000. Working to save our coastal wetlands. Public Information Brochure Louisiana Department of Natural Resources office of Coastal Restoration and Management. BR: LADNR, CRD 17pp

Rogers, B.D. and W.H. Herke. 1985. Temporal patterns and size characteristics of migrating juvenile fishes and crustaceans in a Louisiana Marsh. Research report no. 5, September 1985. School of forestry, wildlife and fisheries Louisiana agricultural experimental station

Rogers, Barton D., Shaw, Richard F., Herke, William H., R. Harry Blanchet. 1993 Recruitment of postlarval and juvenile brown shrimp (*Penaeus aztecus*) from offshore to estuarine waters of the Gulf of Mexico. Estuarine, Coastal and Shelf Science (1993) vol. 36: 377-394

Rottingen, I. 1976. On the relation between echo intensity and fish density. FiskDir. Skr. Havunders. vol.16, 301-314

Roundtree, R.A. and K.W. Able. 1992. Fauna of polyhaline subtidal marsh creeks in southern New Jersey: composition, abundance, and biomass. *Estuaries* 15(2): 171-185.

Salinas, C.M., Delaune, R.D. and W.H. Patrick, Jr. 1986. Changes occurring along a rapidly submerging coastal area: Louisiana, USA. Journal of Coastal Research vol. 2: 260-284

Shenker, J.M. and J.M. Dean. 1979. The utilization of an intertidal salt marsh creek by larval and juvenile fishes: abundance, diversity, and temporal variation. E*stuaries* 2:154-163.

Soule, M., Hampton, I., Barange, M. Potential improvements to current methods of recognizing single targets with a split-beam echo-sounder. ICES Journal of Marine Science 53, 1996

Stanley and Wilson, D.R. and C.A. Wilson. 1995. Effect of scuba divers on fish density and target strength estimates from stationary dual-beam hydroacoustics. *Trans. Am. Fish. Soc.* 124:946-949.

Subrahmanyam, C.B. and C.L. Coultas. 1980. Studies on the animal communities in two north Florida salt marshes. Part III. Seasonal fluctuations of fish and macroinvertebrates. *Bull. Mar. Sci.* 30(4):790-818.

Subrahmanyam, C.B. and S.H. Drake. 1975. Studies on the animal communities in two north Florida salt marshes. Part. I. Fish communities. *Bull. Mar. Sci.* 25(4): 445-465.

Thorne, R.E. 1979. Hydroacoustic estimates of adult sockeye salmon (*Onchorynchus nerka*) in Lake Washington 1972-75. *J. Fish. Res. Board Can.* 36:1145-1149.

Trexler, J.C. and J. Travis. 2001. Nontraditional regression analysis. Ecology. 74(6): 1629-1637.

Turner, R.E., 1990. Landscape development and coastal wetlands losses on the Northern Gulf of Mexico. American Zoology vol. 30: 84-105

Whittington, D., Cassidy, G., Amaral, D., McClelland, E., Wang, H., Paulos, C. 1994. The economic value of improving the environmental quality of Galveston Bay. The Galveston Bay National Estuary Program, Publication GBNEP-38, June 1994. pp 121-147

Wilson, Charles A., Pierce, A., Miller, M. Submitted 2001. Rigs and reefs: a comparison of the fish communities at two artificial reefs, a production platform, and a natural reef in the northern Gulf of Mexico. Final Report for MMS.

Yakupzack, Paul M., W. H. Herke, and W. Guthrie Perry. 1977. Emigration of juvenile Atlantic croakers, *Micropogon undulatus*, from a semi-impounded marsh in southwestern Louisiana. Transactions of the American Fisheries Society vol. 106, no. 6 November, 1977

Zakharchenko, A.B., Skorobogatov, M.A., Mikleev, V.N. 1997. Influence of variation in hydrostatic pressure on the amount of food consumed by the Roach, Rutilus rutilus and by the Guppy, Poecilia reticulata. Journal of Ichthyology vol. 37, no. 2 191-195

Zimmerman, R.J. and T.J. Minello. 1984. Densities of *Penaeus aztecus*, *Penaeus setiferus*, and other natant macrofauna in a Texas salt marsh. *Estuaries* 7(4a):421-433.

Appendix. Biological samples from 14 October-18 December 2000

Date	Common Name	Latin Name	Wing Mass	Otter Mass	Total Mass	Wing Abun	Otter Abun	Total Abun	Wing Avg TL	Otter Avg TL	Overall Avg TL
10/14	Atlantic Bumper	C. chrysurus	50		50	37		37	4.55		4.55
10/14	Atlantic Croaker	M. undulatus	37	390	427	3	9	12	10.6	15.3	14.13
10/14	Bay Anchovy	A. mitchilli	8527.5	18.5	8546	7048	22	7070	5.45	5.01	5.45
10/14	Blue Crab	C. sapidus	33	171.5	204.5	25	3	28	2.69	4.73	2.91
10/14	Bluntnose jack	H. amblyrhyncus	5.4		5.4	1		1	2.3		2.30
10/14	Gulf Menhaden	B. patens	250	40	290	18	3	21	11.5	11	11.43
10/14	Lookdown	S. vomer	19.3		19.3	4		4	5.6		5.60
10/14	Pinfish	L. rhomboides	310	472	782	9	15	24	13.2	13	13.05
10/14	Rough Silverside	M. martinica	36		36	16		16	7.16		7.16
10/14	Scaled Sardine	H. jaguana	3.5		3.5	1		1	6.8		6.80
10/14	Scrawled Cowfish	L. quadicornis	0.5		0.5	1		1	3		3.00
10/14	Sheepshead	A. probactocephalus		3.6	3.6		1	1		11.4	11.40
10/14	Shrimp	Paenaus spp.	952.54	1927.8	2880.3	179	422	601	7.6	9.53	8.96
10/14	Silver Perch	B. chrysoura		765.44	765.44		31	31		12.8	12.79
10/14	Southern Kingfish	M. littoralis		31	31		1	1		15	15.00
10/14	Southern Puffer	S. nephalus	3.75		3.75	3		3	4.07		4.07
10/14	Spanish Sardine	S. aurita	2.1		2.1	2		2	4.95		4.95
10/14	Speckled Trout	C. nebulosus		65	65		2	2		15.2	15.20
10/14	Spot	L. xanthurus		361.5	361.5		10	10		14.1	14.08
10/14	Squid	Loligo sp.	68.5	10.7	79.2	41	4	45	2.52	3.13	2.58
10/14	Striped Mullet	M. cephalus	57.5		57.5	4		4	11.7		11.65
10/14	White Trout	C. arenarius	28.8	427	455.8	7	12	19	8.31	12.7	11.08
11/10	Atlantic Bumper	C. chrysurus	0.5		0.5	1		1	3.7		3.70
11/10	Atlantic Stingray	D. sabina		110.5	110.5		1	1			0.00
11/10	Bay Anchovy	A. mitchilli	1190.7		1190.7	1156		1156	5.31		5.31
11/10	Black Drum	P. cromis		45.5	45.5		1	1		15	15.00
11/10	Blue Crab	C. sapidus	4	232	236	6	1	7	2.68	17.5	4.80
11/10	Lookdown	S. vomer	4		4	1		1	6.2		6.20
11/10	Mantis Shrimp	S. empusa		32	32		1	1		13.5	13.50
11/10	Pinfish	L. rhomboides		93.5	93.5		2	2		14.2	14.15
11/10	Rough Silverside	M. martinica	56		56	35		35	6.23		6.23
11/10	Shrimp	P. spp.	38.5	233	271.5	15	51	66	7.58	8.84	8.55
11/10	Silver Perch	B. chrysoura	31	1615.9	1646.9	1	63	64	14.7	13.1	13.17
11/10	Southern Puffer	S. nephalus	2		2	1		1	1.8		1.80
11/10	Spadefish	C. faber	95		95	1		1	12.3		12.30
11/10	Spot	L. xanthurus		77	77		2	2		14.4	14.40
11/10	Squid	Loligo sp.	5	10	15	1	1	2	4	5.2	4.60
11/10	White Trout	C. arenarius		90	90		2	2		18.1	18.10
11/14	Atlantic Croaker	M. undulatus		377.4	377.4		7	7		16.7	16.74
11/14	Atlantic Stingray	D. sabina		1871.1	1871.1		1	1			0.00
11/14	Bay Anchovy	A. mitchilli	4082.3		4082.3	3780		3780	5.59		5.59
11/14	Black Drum	P. cromis		39.3	39.3		1	1		14.6	14.60

11/14	Blue Crab	*C. sapidus*	325	566.99	891.99	7	3	10	2.29	15.6	6.28
11/14	Bluefish	*P. saltatrix*	4.2		4.2	2		2	6.6		6.60
11/14	Cutlass Fish	*T. lepturus*	22.7		22.7	1		1	36.4		36.40
11/14	Fringed Flounder	*E. crossotus*	1.3	26.3	27.6	1	4	5	5.1	8.95	8.18
11/14	Gulf Killifish	*F. grandis*	4.1		4.1	1		1	4.2		4.20
11/14	Gulf Menhaden	*B. patens*	41.1	18.6	59.7	3	1	4	2	12.2	4.55
11/14	Hardhead Catfish	*A. felis*		1020.6	1020.6		3	3		36.2	36.17
11/14	Lookdown	*S. vomer*	1.4		1.4	1		1	4.7		4.70
11/14	Mangrove Snapper	*L. griseus*		17.1	17.1		1	1			0.00
11/14	Pinfish	*L. rhomboides*		396.8	396.8		11	11		13.5	13.50
11/14	Rough Silverside	*M. martinica*	2976.7		2976.7	1567		1567	6.77		6.77
11/14	Scaled Sardine	*H. jaguana*	2.3		2.3	1		1	5.8		5.80
11/14	Scrawled Cowfish	*L. quadicornis*	1.5		1.5	2		2	3.9		3.90
11/14	Sheepshead	*A. probactocephalus*		35	35		1	1		12.8	12.80
11/14	Shrimp	*Paenaus spp.*	2749.9	142.5	2892.4	1573	58	1631	6.94	7.73	6.96
11/14	Silver Perch	*B. chrysoura*	29.1	143.5	172.6	2	8	10	10.4	11.7	11.47
11/14	Southern Kingfish	*M. littoralis*	7	78.7	85.7	1	1	2	9.7	19.4	14.55
11/14	Southern Puffer	*S. nephalus*	6.5		6.5	3		3	4.27		4.27
11/14	Speckled Trout	*C. nebulosus*	97.8	878.83	976.63	3	20	23	16	16.5	16.44
11/14	Spot	*L. xanthurus*		652.04	652.04		8	8		17.4	17.36
11/14	Squid	*Loligo sp.*	94.8		94.8	29		29	3.38		3.38
11/14	Striped Mullet	*M. cephalus*	652.04	68.9	720.94	31	2	33	12.6	15.1	12.72
11/14	White Trout	*C. arenarius*	28.8	27.6	56.4	7	2	9	7.37	11.6	8.30
11/16	Atlantic Bumper	*C. chrysurus*	2.1		2.1	3		3	3.77		3.77
11/16	Atlantic Croaker	*M. undulatus*		144	144		5	5		14.5	14.46
11/16	Bay Anchovy	*A. mitchilli*	108.5		108.5	82		82	5.62		5.62
11/16	Blue Crab	*C. sapidus*	0.5	2523.1	2523.6	1	14	15	2.6	14.3	13.54
11/16	Bluntnose jack	*H. amblyrhyncus*	3		3	4		4	3.73		3.73
11/16	Gulf Menhaden	*B. patens*		23.4	23.4		1	1		13	13.00
11/16	Jellyfish	*A. aurita*	4932.8	9185.2	14118			0			
11/16	Lookdown	*S. vomer*		1.1	1.1		1	1		6.5	6.50
11/16	Pinfish	*L. rhomboides*	40	122.2	162.2	1	4	5	12.7	12	12.16
11/16	Rough Silverside	*M. martinica*	62.1		62.1	32		32	6.48		6.48
11/16	Shrimp	*Paenaus spp.*	6.9	112.3	119.2	3	22	25	7.33	8.95	8.76
11/16	Speckled Trout	*C. nebulosus*		116.2	116.2		5	5		17.4	17.36
11/16	Spot	*L. xanthurus*		417.2	417.2		11	11		14.3	14.32
11/16	Squid	*Loligo sp.*	4.6		4.6	2		2	2.65		2.65
11/16	Striped Mullet	*M. cephalus*	20		20	1		1	14.4		14.40
11/16	White Trout	*C. arenarius*	5.2	163.3	168.5	1	1	2	9.5	16.6	13.05
11/17	Atlantic Bumper	*C. chrysurus*	73.8		73.8	56		56	4.91		4.91
11/17	Atlantic Croaker	*M. undulatus*		31.6	31.6		1	1			0.00
11/17	Atlantic Stingray	*D. sabina*		907.18	907.18		2	2		57.5	57.50
11/17	Bay Anchovy	*A. mitchilli*	652.04		652.04	617		617	5.44		5.44
11/17	Black Drum	*P. cromis*		90.2	90.2		1	1		18	18.00

11/17	Blue Crabs	*C. sapidus*		8249.7	8249.7		28	28		14.6	14.63
11/17	Bluefish	*P. saltatrix*	5.2		5.2	2		2	6.2		6.20
11/17	Bluntnose jack	*H. amblyrhyncus*	39.2		39.2	26		26	4.51		4.51
11/17	Jellyfish	*A. aurita*	850.49	1162.3	2012.8			0			
11/17	Pinfish	*L. rhomboides*	65		65	2		2	13.9		13.85
11/17	Rough Silverside	*M. martinica*	144.7		144.7	74		74	6.3		6.30
11/17	Sheepshead	*A. probactocephalus*		34.6	34.6		1	1		12.4	12.40
11/17	Shrimp	*Paenaus spp.*	49.3	86.3	135.6	20	18	38	7.19	8.48	7.80
11/17	Silver Perch	*B. chrysoura*		108.8	108.8		4	4		13	12.98
11/17	Southern Kingfish	*M. littoralis*		29.2	29.2		1	1		14.8	14.80
11/17	Spanish Sardine	*S. aurita*	4.9		4.9	1		1	7.7		7.70
11/17	Speckled Trout	*C. nebulosus*	8.5	388.5	397	1	10	11	9.8	16.5	15.85
11/17	Spot	*L. xanthurus*		680.39	680.39		17	17		14.2	14.25
11/17	Squid	*Loligo sp.*	35		35	8		8	3.64		3.64
11/17	Striped Mullet	*M. cephalus*	27.8		27.8	1		1	14.1		14.10
11/17	White Trout	*Cynoscion arenarius*		108	108		2	2		23.6	23.55
11/19	Atlantic Bumper	*C. chrysurus*	4.1		4.1	2		2	5.2		5.20
11/19	Atlantic Croaker	*M. undulatus*		953.28	953.28		29	29		15	14.99
11/19	Bay Anchovy	*A. mitchilli*	5925		5925	5207		5207	5.51		5.51
11/19	Black Drum	*P. cromis*		4337.5	4337.5		25	25		18.2	18.21
11/19	Blue Crab	*C. sapidus*		1559.2	1559.2		9	9		14.8	14.84
11/19	Bluefish	*P. saltatrix*	3.8		3.8	2		2	6.05		6.05
11/19	Bluntnose jack	*H. amblyrhyncus*	5.5	21.9	27.4	1	10	11	6.7	4.72	4.90
11/19	Clown Goby	*M. gulosus*	8.5		8.5	1		1	12.5		12.50
11/19	Fringed Flounder	*E. crossotus*	6		6	1		1	8		8.00
11/19	Gulf Menhaden	*B. patens*	57.1		57.1	4		4	11.2		11.23
11/19	Pinfish	*L. rhomboides*	425.24	1020.6	1445.8	20	39	59	12.7	12.4	12.49
11/19	Rough Silverside	*M. martinica*	510.29		510.29	264		264	6.65		6.65
11/19	Scrawled Cowfish	*L. quadicornis*	0.3	5.3	5.6	1	1	2	2.8	6	4.40
11/19	Sheepshead	*A. probactocephalus*	18.6	225.8	244.4	1	8	9	10	10.8	10.69
11/19	Shrimp	*Paenaus spp.*	3504	980.03	4484	2817	388	3204	6.49	7.72	6.64
11/19	Silver Perch	*B. chrysoura*	13.2	40	53.2	2	1	3	8.95	14.4	10.77
11/19	Southern Puffer	*S. nephalus*	0.2		0.2	1		1	2.5		2.50
11/19	Speckled Trout	*C. nebulosus*	47.2	896.58	943.78	4	30	34	11.3	16	15.43
11/19	Spot	*L. xanthurus*		5641.6	5641.6		114	114		15.3	15.30
11/19	Squid	*Loligo sp.*	234.8		234.8	25		25	3.67		3.67
11/19	Striped Mullet	*M. cephalus*	24.1		24.1	1		1	13.4		13.40
11/19	White Trout	*C. arenarius*	18.8	425.5	444.3	5	2	7	7.68	17.9	10.59
12/17	American Eel	*A. rostrata*		737.09	737.09		1	1		36	36.00
12/17	Atlantic Croaker	*M. undulatus*		283.5	283.5		7	7		36.2	36.23
12/17	Atlantic Stingray	*D. sabina*		6047.9	6047.9		8	8			0.00
12/17	Bay Anchovy	*A. mitchilli*	538.64		538.64	962		962	5.66		5.66
12/17	Blue Crab	*C. sapidus*		226.8	226.8		2	2		10.5	10.50

12/17	Fringed Flounder	*E. crossotus*		2.1	2.1		1	1		7.7	7.70
12/17	Grass Shrimp	*P. vulgaris*	1		1	3		3	4.9		4.90
12/17	Gulf Killifish	*F. grandis*	3		3	2		2	5.6		5.60
12/17	Gulf Menhaden	*B. patens*	14	10.5	24.5	2	1	3	3.63	11	6.09
12/17	Longnose Killifish	*F. similis*	42		42	22		22	5.75		5.75
12/17	Rough Silverside	*M. martinica*	7484.3		7484.3	4351		4351	6.57		6.57
12/17	Scrawled Cowfish	*L. quadicornis*		2.8	2.8		1	1		6	6.00
12/17	Sheepshead	*A. probactocephalus*	13.2		13.2	1		1	9.4		9.40
12/17	Sheepshead Minnow	*C. variegatus*	11.5		11.5	8		8	4.23		4.23
12/17	Shrimp	*Paenaus spp.*	11	126	137	8	41	49	6.98	8.44	8.20
12/17	Southern Puffer	*S. nephalus*		2.7	2.7		1	1		6.8	6.80
12/17	Speckled Trout	*C. nebulosus*		1304.1	1304.1		44	44		17.9	17.92
12/17	Spot	*L. xanthurus*		6690.5	6690.5		219	219		13.7	13.70
12/17	Squid	*Loligo sp.*	18		18	7		7	3.5		3.50
12/17	Striped Mullet	*M. cephalus*		566.99	566.99		16	16		15.5	15.52
12/17	White Trout	*C. arenarius*		126	126		2	2		17.7	17.65
12/18	Atlantic Croaker	*M. undulatus*		182	182		5	5		15.5	15.52
12/18	Atlantic Stingray	*D. sabina*		252.3	252.3		5	5			0.00
12/18	Bay Anchovy	*A. mitchilli*	42		42	66		66	4.77		4.77
12/18	Gulf Killifish	*F. grandis*	4		4	1		1	5.5		5.50
12/18	Gulf Menhaden	*B. patens*	51.2		51.2	94		94	3.86		3.86
12/18	Pinfish	*L. rhomboides*		94	94		3	3		13	12.97
12/18	Rough Silverside	*M. martinica*	1077.3		1077.3	579		579	6.69		6.69
12/18	Silver Perch	*B. chrysoura*		156.8	156.8		3	3		16	16.03
12/18	Spanish Sardine	*S. aurita*	13		13	1		1	6.4		6.40
12/18	Speckled Trout	*C. nebulosus*		765.44	765.44		19	19		16.7	16.70
12/18	Spot	*L. xanthurus*		623.69	623.69		21	21		13.4	13.38
12/18	Striped Mullet	*M. cephalus*		51.9	51.9		2	2		13.7	13.70

Vita

David J. Harmon was born during a blizzard on January 6, 1977 in New Albany, Indiana, where he lived until the age of 6. His family moved briefly to Lacombe, Louisiana, before settling in Sumter, South Carolina. David enjoyed many activities as a youth and played varsity baseball in high school. He attended and received a Bachelor of Science degree in marine science from the University of South Carolina in May of 1999. While in college, David was an active member of Kappa Sigma fraternity. His early experiences in research were under the tutelage of Drs. John Mark Dean and Marcel Reichert in the field of fisheries biology and management, particularly age and growth and reproductive studies.

David accepted a graduate assistantship under Dr. Charles A. Wilson at Louisiana State University in May of 1999, shortly after his graduation from South Carolina. While at Louisiana State, David has participated in many field trips involving hydroacoustics, both in the marsh and in blue water aboard research vessels and petroleum platforms. David's research under Dr. Wilson centered on the effects of cold front passages on nekton in a tidal creek, detailing the fall emigration of many species from Louisiana's marshes. David completed a course of study granting him a concentration in wetlands science and management from the Department of Oceanography and Coastal Sciences and Institute for Environmental Studies.

David is currently attending the University of South Carolina School of Law. He plans to apply his background toward environmental law. Personal interests include the outdoors, sports, environmental conservation, and of course, fishing.